LIDAR AS A DIAGNOSTIC OF SMOKE/OBSCURANTS: OVERVIEW AND ASSESSMENT OF THE DEVELOPMENT WITH RECOMMENDATIONS

Ronald H. Kohl
3 October 1984

Final Report on Contract DAAD05-83-M-M106
prepared for

Project Manager
Smoke/Obscurants
Attn: DRCPM-SMK-T
Aberdeen Proving Ground, MD 21005

RHK&A
RONALD H. KOHL & ASSOCIATES
Tullahoma, Tennessee 37388

LIDAR AS A DIAGNOSTIC OF SMOKE/OBSCURANTS: OVERVIEW AND ASSESSMENT OF THE DEVELOPMENT WITH RECOMMENDATIONS

Ronald H. Kohl
3 October 1984

Final Report on Contract DAAD05-83-M-M106
prepared for

Project Manager
Smoke/Obscurants
Attn: DRCPM-SMK-T
Aberdeen Proving Ground, MD 21005

RHK&A

RONALD H. KOHL & ASSOCIATES
Tullahoma, Tennessee 37388

PREFACE

This report is the result of inputs from the author's knowledge and his own continuous literature survey, from informed technical contact with a number of investigators working in this area, and from a smoke/obscurants lidar survey (conducted under contract DAAD05-82-M-E270). The analysis and assessments made, unless attributed to others, are the author's own and he is responsible for them. The author has tried to make assessments that are as fair, objective and useful as possible. He would be pleased to receive comments, particularly regarding assessments which fail to meet these criteria or regarding important points which have been inadvertently omitted.

ACKNOWLEDGEMENTS

The author would like to thank those who took the time to answer the numerous questions associated with the work reported here. He would particularly like to thank Major Dan Adams of OPM Smoke/Obscurants, who served as COTR during the course of this effort, and his back-up Mr. John Green for their clear-headed and timely assistance on administrative matters and for their continuous encouragement and support. Finally, he would like to thank Gary Nelson, formerly with OPM Smoke/Obscurants, for recognizing the need for this overview and assessment.

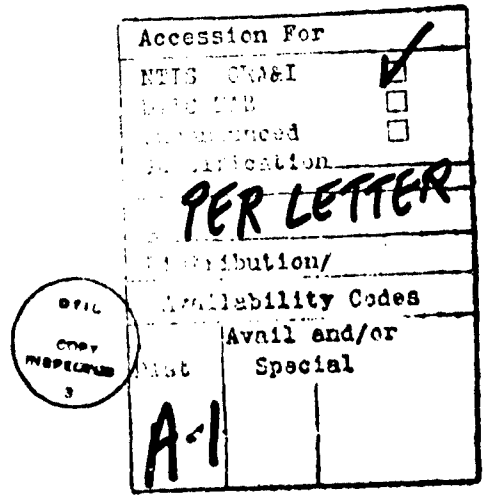

TABLE OF CONTENTS

I. STRUCTURE OF THE REPORT

This report is divided into two main parts. The first (Part II) is an overview and assessment of the development of lidar as a diagnostic of smoke/obscurants, beginning with an introduction to lidar and the potential payoff in its quantitative use, through a discussion of lidar principles, to consideration, in individual sections, of each of the problem areas lying along the various paths of smoke/obscurant diagnostic-lidar development. At the end of each of the latter sections the recommendations are made which are pertinent to the problem which is the topic of that section. The recommendations regarding specific problem areas are therefore placed where the reason for them is evident from what is discussed immediately before.

However, these specific recommendations are also gathered together and put in a hierarchy in the second main part (Part III) titled "Recommendations". Here they serve as a more ready reference and as a summary. General recommendations, not specifically related to particular problem areas, have been put in Part III before the specific recommendations.

II. OVERVIEW AND ASSESSMENT (WITH RECOMMENDATIONS)

A. INTRODUCTION

LIDAR

A lidar is a device which emits radiation from a laser out into the atmosphere and then detects the radiation which returns to it as a result. The acronym LIDAR, which is now commonly used as a word: lidar, stood for "light detection and ranging". Lately, the name "lidar" is being used more specifically to denote those systems used to determine properties of the atmosphere or an atmospheric aerosol, and the name "laser radar" is used to denote systems designed for the detection of solid objects. We will conform to this use, though the differentiation of the words "lidar" and "laser radar" described here is not universal. The vast majority of lidar work, at least until recently, has been civilian funded and directed, while the majority of laser radar work has been militarily funded and directed toward military use.

QUALITATIVE USE OF LIDAR WITH SMOKE/OBSCURANT CLOUDS

The type of image that can be obtained with a lidar scan is shown in Figure 1. This is a cross section of a forest fire plume above the haze layer. (The plume is relatively thin compared to typical smoke/obscurant clouds at the same wavelength.) The lidar was looking vertically downward and was flown above the plume in an aircraft. The limits of the smoke cloud are well defined, especially on the side of the cloud toward the lidar. It can be seen that such a qualitative display of a cloud cross section makes a nice complement to point measurements or line-of-sight measurements. The qualitative uses of relatively unprocessed lidar return signals in smoke/obscurant field tests include the determination of cloud location and the detection of unsuspected foreign clouds on the instrumented line of sight. For an example, see the Smoke Week III report (Farmer et al, 1981) where previously unsuspected dust clouds, due to target

vehicle movement and mortar firings, were detected on the line of sight on the opposite side of the cloud from the observers.

PAYOFF OF POTENTIAL QUANTITATIVE USE OF LIDAR

USE OF LIDAR WITH SMOKE/OBSCURANT CLOUDS. Variations in lidar signal level are not particularly apparent in Figure 1. Such variations are more apparent in Figure 2. It is only natural to ask if such variations in lidar signal cannot be quantitatively related to smoke-cloud properties. Further, by rapidly scanning the cloud in numerous cross-sectional planes, such quantitative data could be obtained throughout the cloud as the cloud develops.

As shown below the most likely quantity obtainable by lidar throughout a smoke/obscurant cloud is the attenuation coefficient. (The attenuation coefficient is a fundamental quantity which is defined later, but many will be familia with it as the product of the extinction coefficient times the concentration, αC.) Knowledge of the attenuation coefficient throughout the cloud means that the transmittance throughout the cloud on any line of sight will be known, and this means that transmittance contours in the cloud can be drawn from any viewpoint, not just from the viewpoint of the lidar. This is illustrated in Figure 3.

To understand how this may be brought about, and what problems lie in the way, we must consider lidar principles and what goes into making up the lidar signal. This is done below.

USE OF LIDAR WITH TRACER CLOUDS. We intervene to note that for reasons (discussed below) having to do with low transmittance in smoke/obscurant clouds and the varying relationship of backscatter to attenuation in aerosols, difficulties must be overcome to obtain the attenuation coefficient (and from it other cloud properties) using lidar as a diagnostic of actual smoke/obscurant clouds. A possible alternative is the use of a tracer cloud, whereby one gets around the two problems just alluded to.

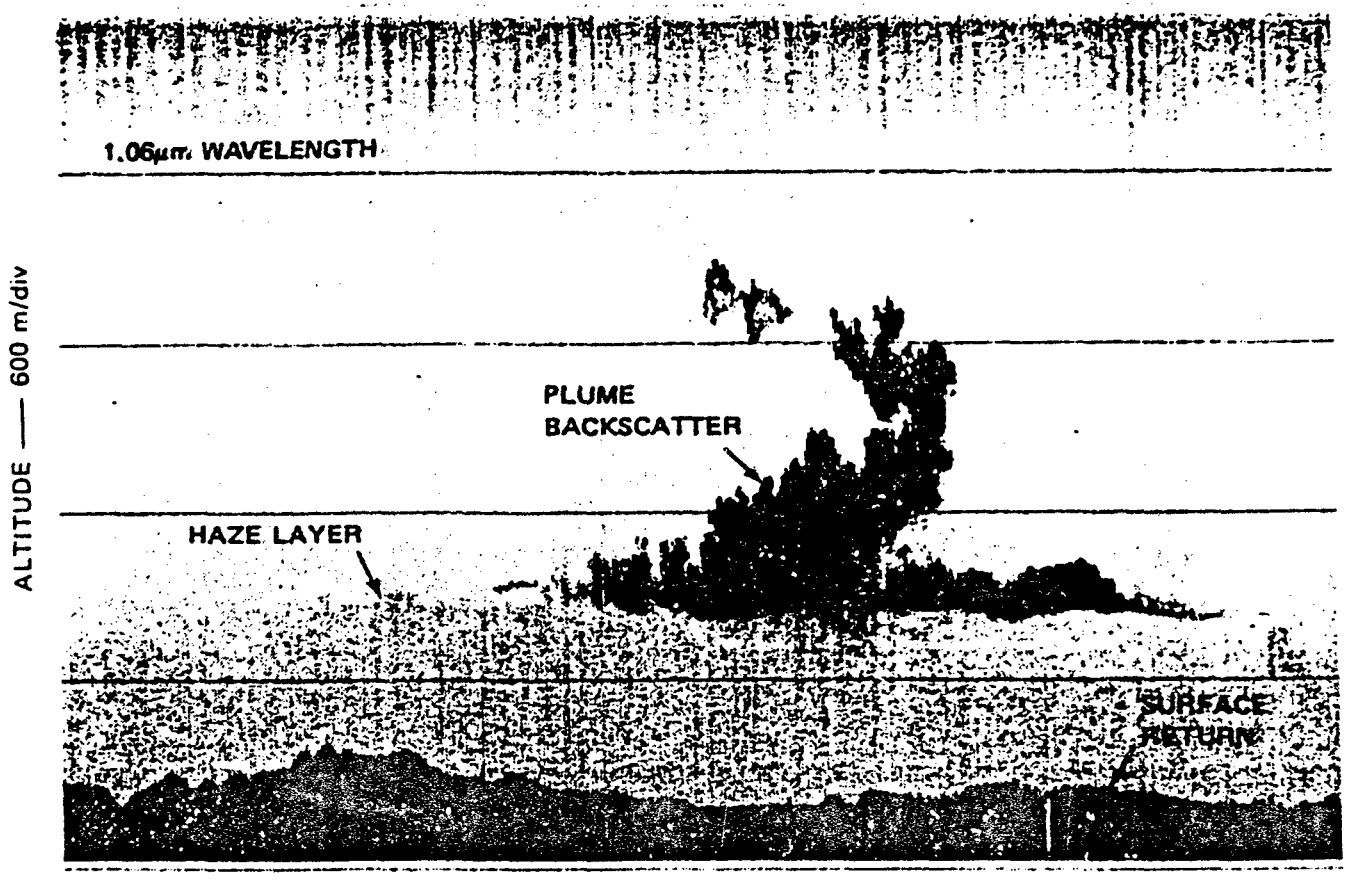

FROM UTHE, SRI

Figure 1. Lidar scan of a forest fire plume. The lidar was directed downward from an aircraft in overflight across the plume.

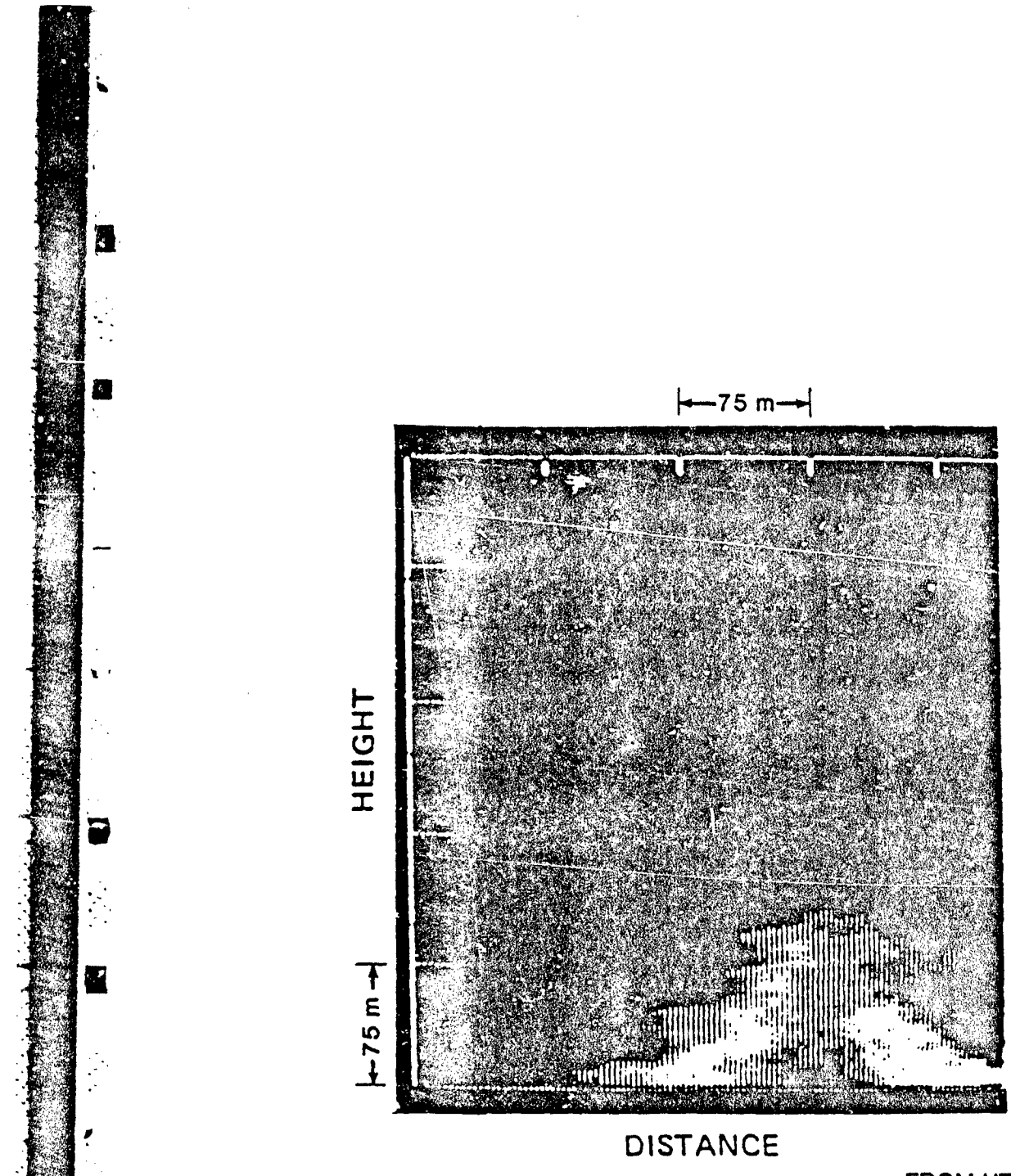

FROM UTHE, SRI
(ADAPTED)

Figure 2. Lidar scan of a plume. The lidar was to the left on the ground which forms the base plane of the plume.

If a smoke/obscurant is a passive additive to the atmosphere, and if, once the properties of a smoke/obscurant cloud are known at some initial time, its properties at some later time are the result of the transport and diffusion caused by the atmosphere, the use of a tracer cloud, in place of the smoke/obscurant cloud, to determine the effects of this atmospheric transport and diffusion will lead to the determination of the desired smoke/obscurant cloud properties for any smoke/obscurant cloud with the same relative initial conditions as the tracer cloud. While the use of a tracer cloud in the place of an actual smoke/obscurant cloud gives rise to its own problems, from the lidar developer's point of view the use of a tracer may well make his problems much less severe. All this is discussed further below.

SMOKE/OBSCURANTS LIDAR SURVEY

Prior to the effort reported here, a survey was conducted (under contract DAAD05-83-M-E270 with the US Army Project Manager, Smoke/Obscurants) in both the US and the free world of those in government, industry and academia who are knowledgeable (whether as users, developers or analyzers) concerning the use or potential use of lidar as a diagnostic of smoke/obscurant clouds or as a diagnostic of tracer substitutes for smoke/obscurant clouds. Specific, knowledgeable, technical questions were asked to elicit strengths and weaknesses as seen from the viewpoint of the user. The survey consisted of a 10-page questionnaire preceded by two pages of description. A copy of the survey with the descriptive pages sent to US groups will be found in Appendix A.

Seventeen US responses were received describing 23 lidar systems and one Doppler radar system. Eleven foreign responses were received describing 15 lidar systems. Thus, in all, 38 lidar systems and one Doppler radar system were described in the survey responses. Some of these lidar systems are dual

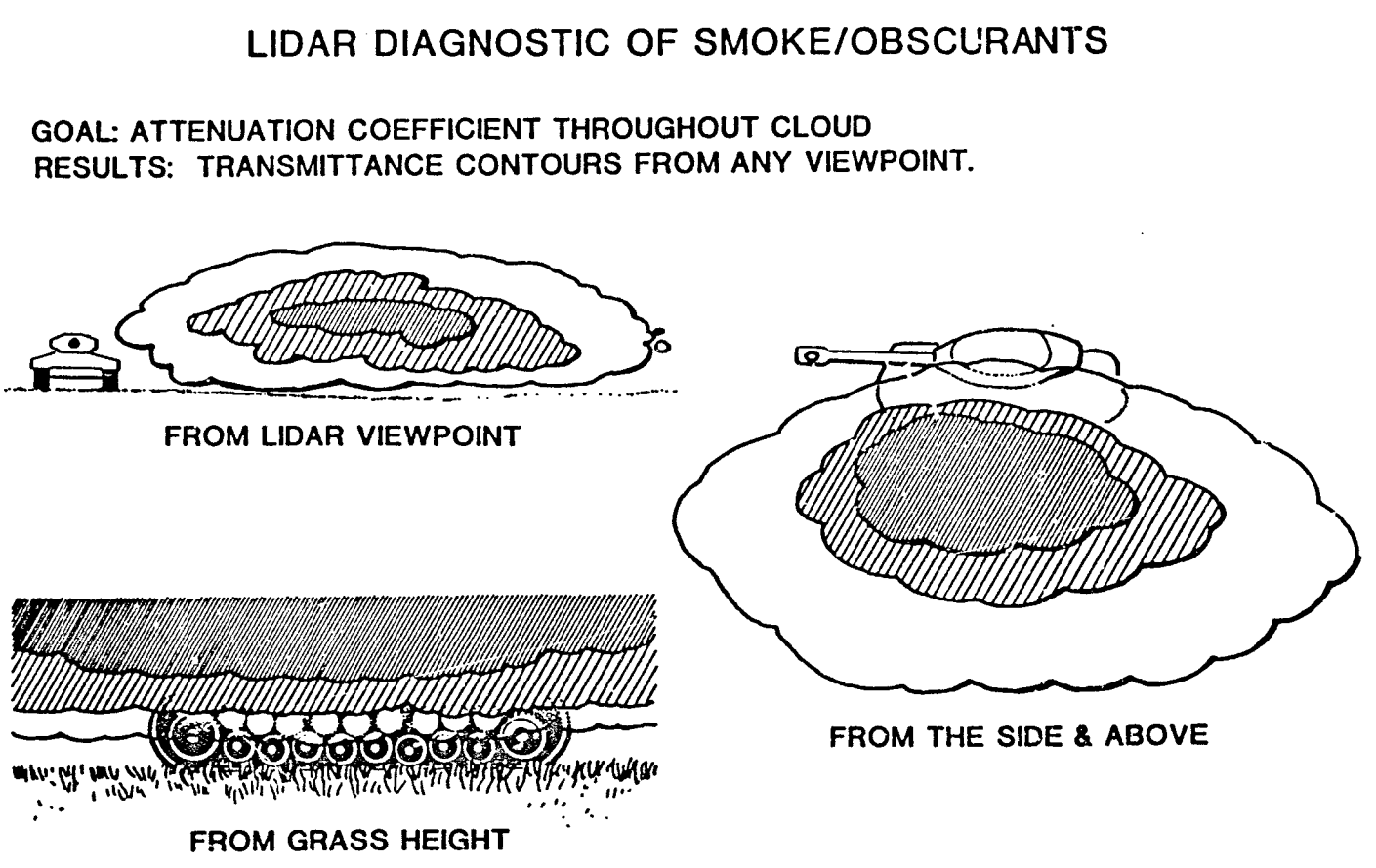

Figure 3. A payoff of a successful lidar technique development. From (Kohl, 1984)

wavelength systems. The total of the survey response material received ran over 1,140 pages. This material was reviewed for the effort reported here. From time to time references to particular survey responses will be made.

BRIEF DISCUSSION

A brief discussion, but of only some of the points made here, will be found as paper A-20 of the Proceedings of the Smoke/Obscurants Symposium VIII (Kohl, 1984).

B. LIDAR BASICS

THE LIDAR EQUATION AND ITS PARAMETERS

THE LIDAR EQUATION. A lidar interacting with a smoke or obscurant cloud sends out radiation in a forward beam and observes the radiation backscattered to it from the smoke cloud. The part of the lidar signal corresponding to a given distance from the lidar is known. For the common, incoherent type of lidar, this is because the lidar emits a very short pulse and one can observe, on a fast display or by rapid sampling, the return signal as a function of time as the backscattered radiation returns to the lidar from deeper and deeper in the cloud. The coherent, continuous type of lidar obtains its signal from its focus which can be put at various depths within the cloud.

With the distance from the lidar out along the lidar beam indicated by L, the lidar return signal associated with distance L, R(L), can be expressed as

$$R(L) = C_1 \, G(L) \, \beta(L) \, T^2(L) \, . \qquad (1)$$

(If the lidar is a coherent lidar, then Equation (1) describes the processed return signal rather than the raw return signal.)

THE QUANTITY C_1. The quantity C_1 is composed of lidar parameters. It depends, in both coherent and incoherent lidars, on the lidar transmitter power and the receiver sensitivity. With any quantitative use of lidar, the quantity C_1 must be shown to be constant, or, if it varies, then this variation must be compensated. (C_1 need not be known directly, as we shall see.) Testing of the constancy of the compensated, or uncompensated C_1 can be done by observing an appropriate surface (or, in some cases, a specially prepared test aerosol) with the lidar.

The time period over which C_1 must remain constant varies with the method of lidar signal interpretation, in some cases it is the length of the smoke trial. Any variation of C_1 over this time period contributes error to the lidar-derived results. Compensation of variation in C_1 is done by measuring the relative changes in those lidar parameters whose variation causes C_1 to vary and then, in the digital processing of the lidar signal, adjusting C_1, or its equivalent, for the variation of each such parameter according to the role played by that parameter in C_1. For example, a 10% increase in pulse energy in an incoherent lidar system would require a 10% increase in C_1, but a 10% increase in the power output of a continuous, or CW (continuous wave), coherent lidar requires a 21% increase in C_1 (or its equivalent) as C_1 is proportional to the square of the power output by such a lidar.

THE BEAM GEOMETRY FACTOR G(L). The quantity G(L) in Equation (1) is a beam geometry factor. In the common, incoherent lidar this is composed of the factor L^{-2} multiplied by the lidar transmitter-beam/receiver-field-of-view overlap function (Kohl, 1978). This overlap function starts at zero at L=0. This is because the transmitter aperture and receiver aperture are separated and shielded from each other so that the close-in scattering of the transmitted radiation by the transmitter optics and supports will not devastate the functioning of the sensitive receiver.

The overlap function very rapidly climbs from zero with increasing L as the transmitter beam and receiver field of view start to overlap, causing the quantity G(L) to also climb rapidly from zero despite the factor L^{-2}.

In the region from L=0 to a distance where a fair degree of overlap is achieved, no useful data can be collected. This distance is 10 m, 30 m, 50 m or 100 m in front of the lidar, depending on the system--these values being examples.

After climbing rapidly from zero with increasing L, the overlap function then begins to approach an asymptotic value in the usual parallel beam/field-of-view situation. (The overlap function can oscillate some as it approaches its asymptotic value due to hot spots or cold spots (shadows) in the beam and/or field of view.) As the overlap function transitions from rapid growth to more asymptotic behavior, the L^{-2} factor in G(L) begins to dominate, causing G(L) to go from rapid growth from zero, through a maximum and then transition to asymptotically decreasing as L^{-2}.

In the continuous, coherent lidar G(L) is 1 (Zalay, Kohl and Coffey, 1979) where L is the distance from the lidar to the focal point of the lidar optics. (The coherent lidar is sensitive to the scattered lidar radiation from the focal point.) There is a limitation at short L for this system also, however, in that, in the currently used configuartion at least, bringing the focal length in close to the lidar requires excessively long travel of the optics element involved (when considered from a rapid scanning point of view). Currently no data is collected at distances closer than 30 meters.

The dependence of the quantity G(L) on L must be either known or determined in order to interpret the lidar signals from any type of lidar. Furthermore, any variation of this dependence on L contributes to error. The determination/verification of the dependence of G(L) on L can be done by using a large standard, diffuse surface at various distances from the lidar (being aware of the opposition effect, see Montgomery and Kohl, 1980), or by averaging multiple returns from clear air (if the lidar is sensitive enough to pick up returns from the background aerosol). In the latter case the assumed, time-averaged uniformity of the background aerosol in clear air at the lidar site can be verified by running the test with two different lidar beam directions with respect to the wind.

THE BACKSCATTER COEFFICIENT $\beta(L)$ AND THE TRANSMITTANCE $T(L)$. The last two parameters in Equation (1) are cloud properties. The first, $\beta(L)$, is the backscatter coefficient at distance L. The backscatter coefficient is the fraction of the radiation incident at L which is backscattered per unit length of propagation along L, per unit solid angle about the backwards direction.

The second cloud property parameter, T(L), is the transmittance from the lidar to the distance L. This is the fraction of the radiation reaching distance L from the lidar which has traveled directly from the lidar, not having been scattered or absorbed along the way. The square of T(L) appears because the radiation detected as coming from L has had to travel from the lidar to L, be backscattered, and then travel from L back to the lidar.

THE ATTENUATION COEFFICIENT σ. The transmittance to L, T(L) is the result of the multiple effect of the local attenuation encountered from the lidar at L=0 out to distance L. The local attenuation is described by the attenuation coefficient, σ, which is the relative fraction lost from radiation which is propagating in a given direction, per unit length of propagation in that direction. The loss of radiation propagating in one direction may be due to absorption or to scattering out of the direction of propagation. At wavelengths that propagate unabsorbed in the atmosphere, the attenuation coefficient will be essentially zero outside of smoke or other man-made or natural obscurants.

The transmittance, T(L), from the lidar at distance $L'=0$ out the lidar beam to distance $L'=L$ is the result of contributions from the attenuation coefficient from $L'=0$ to $L'=L$, namely,

$$T(L) = e^{-\int_0^L \sigma(L')\, dL'} \qquad (2)$$

where (L') is the attenuation coefficient in the lidar beam at distance L'.

INSTANTANEOUS SENSITIVE VOLUME OF THE LIDAR: LENGTH EFFECTS. The quantity $\beta(L)$ in Equation (1) is actually an average of β over the length of the instantaneous sensitive volume of the lidar, ΔL. For incoherent lidars, the length interval ΔL is the temporal pulse length of the lidar output pulse times the speed of light, c, divided by 2. (A convenient and accurate relationship is that half the pulse length in nanoseconds gives ΔL in feet. For example, a lidar output pulse length of 40 nanoseconds gives a ΔL of 20 feet or a little over 6 meters.) For coherent lidars ΔL is the effective length of the focal volume. The spatial resolution required in the determination of local optical properties such as β are discussed below.

The quantities $G(L)$ and $T^2(L)$ are also effective average values (with distance resolution ΔL) which are treated as samples of the actual functions at distance L. Linear variation of the actual functions with L causes no error due to ΔL being nonzero, but non-linear variation does. In attenuating media, at the distances from which data is collected, it is the non-linear behavior of T^2 which usually dominates the non-linear behavior of $G(L)$. One can see from Equation (2) that extending L to $L + \Delta L$ where ΔL is small compared to the value of σ^{-1} in the region near L will cause $T(L + \Delta L)$ to be close to $T(L)$. (The quantity σ^{-1}, called the attenuation length, is a handy length scale with which to compare a distance interval to determine whether or not attenuation will be significant over the distance interval.) How large ΔL can be in terms of σ^{-1} before the non-linear variation of $T^2(L)$ over ΔL causes significant error in Equation (1) is the question before us.

Surprisingly, unlike an earlier publication (Zalay, Kohl and Coffee, 1979) where ΔL was arbitrarily set at $0.1\ \sigma^{-1}$, ΔL can be as large as $0.55\ \sigma^{-1}$ (over which $T^2(L)$ drops by 1/3) before the relative systematic error in $R(L)$ [the

R(L) obtained is too high] reaches 5%. Using values of significance as shown later, if ΔL = 1 m, the maximum σ for 5% error is 0.55 m^{-1} corresponding to a cross-cloud transmittance of 10^{-12} in a uniform cloud 50 meters across (i.e., this effect is of no concern), but, if ΔL = 6 m, the maximum σ is 9.2 x 10^{-2} m^{-1} corresponding to a cross-cloud transmittance of 1.02 x 10^{-2} in a uniform cloud 50 m across. Relaxing the systematic error limit in R(L) to 10%, allows ΔL as large as 0.77 σ^{-1} or, at ΔL = 6 m, allows a maximum σ of 0.13 m^{-1}, corresponding to a cross-cloud transmittance of 1.63 x 10^{-3} in a uniform cloud 50 m across. Thus this limitation on ΔL can be significant in smoke/obscurants for ΔL up near 6 meters.

INSTANTANEOUS SENSITIVE VOLUME OF THE LIDAR: CROSS-SECTIONAL EFFECTS. The quantities $\beta(L)$ and $T^2(L)$ are also averages over the lidar transmitter beam cross-section at L or the effective cross-section of the focal volume depending on the lidar type. [G(L) is a cross-sectional average by its definition.] Small cross-sectional variations in T^2 will be twice the cross-sectional variations in T. Cross-sectional variation in local optical properties, such as β, and in T are treated later, in the section on spatial resolution. For the cross-sectional dimensions involved here they are shown to be no problem except perhaps for the larger transmitter beam divergences (5 mr) of some incoherent lidars when operated from the ground beyond 200 m range (vertical dimension gets above about 1 m).

THE LIDAR EQUATION REVISITED. The quantity G(L) in Equation (1) is either known or it, or its equivalent, can be determined as discussed above. Then, defining I(L) by

$$I(L) = R(L)/G(L), \qquad (3)$$

and dividing Equation (1) by G(L), one has

$$I(L) = C_1 \beta(L) T^2(L) \qquad (4)$$

where the left-hand side of Equation (4) is known.

COMMON, INCOHERENT LIDAR

ADDITIONAL DESCRIPTION. Many of the principles of the common incoherent lidar are laid out above. A pulsed laser is the source of the transmitter beam which issues from transmitter optics with low (½ mr to 5 mr) beam divergence. The transmitter beam volume is observed using a receiver with a field of view which includes the entire transmitter beam cross-section (beyond overlap) but no additional field of view beyond what is needed to keep the lidar response constant in the face of the normal, small mechanical vibrations and displacements of the field of view direction relative to the transmitter beam direction. The small transmitter-beam/field-of-view size allows for low solar-induced background signal levels (in the visible and near-IR) relative to the lidar signal, good spatial resolution and reduced multiple scattering effects.

Large receiver collection optics are used to collect the backscattered radiation to get the lidar signal well above non-solar-induced noise. The collection and secondary receiver optics focus the collected backscattered radiation onto a fast detector where the backscattered radiation flux (power) is detected as a function of time. The time from last pulse emission, t, is related to the distance L out the lidar beam from which scattering is being observed at time t by $L = ct/2$.

Such lidars are called incoherent because the detection process is incoherent; the scattered flux is detected and the phase of the scattered wavefronts

do not play a role in the detection process. The illumination, being from a laser, is coherent, however, and the backscattered radiation collected by the receiver exhibits speckle.

SPECKLE. Speckle is the large spatial variation, or spotty, grainy nature of the reflected radiation flux observed when a laser beam is directed upon a diffuse surface or aerosol. (It can be observed by shining a HeNe laser beam on a white piece of paper and observing the diffuse reflection on another white piece of paper, taking pains to shield the second piece from stray radiation coming directly from the laser or another light source.)

Speckle arises from interference between the scattered fields (wavefronts) from the many, randomly distributed individual scatterers. A different random distribution of the same scatterers with the same mean number of scatterers per unit volume will give rise to a different speckle pattern. The average scattered radiation flux observed at a point as the scatterers are distributed in a great many such random distributions is the incoherent scattered radiation flux, the scattered flux observed when an incoherent source of the same wavelength is used. Typically, as one collects the coherent scattered flux falling on a larger and larger area (increases the receiver aperture) the difference between the actual flux collected and the flux that would be collected if the scattered radiation was incoherent diminishes.

NECESSITY FOR AND ACHIEVEMENT OF SMALL SPECKLE EFFECT. The backscatter coefficient (or any other volumetric scattering coefficient) is an incoherent scattering parameter, it arises from the total of the scattered fluxes from each scatterer (incoherent scattering) not from the actual flux which is the total of the scatterer fluxes plus an interference contribution (coherent scattering). The interference contribution is positive (bright speckle spot)

and negative (dark speckle spot) over an area intercepting the scattered coherent radiation. As described above, the average of the interference contribution over such an area tends to zero as the size of the area increases. As we need to observe incoherent scattering effects, we need a small interference contribution, and the usual way to get this is to increase the size of the receiver aperture (the area over which the scattered radiation is collected). Roughly speaking, the mean total radiation (the total radiation if the scattered radiation were incoherent) which is collected by a receiver aperture is proportional to the number of speckles (speckle spots, or grains) N, falling on the aperture and the typical variation from the mean due to interference (coherent) effects is proportional to $\sqrt{N}$, so the relative error in any one instance due to observing coherent scattering rather than incoherent scattering is about $1/\sqrt{N}$.

The size of the speckles at the lidar receiver aperture which arise from the backscattering taking place at distance L is the full-diffraction angle, $\lambda/D_B(L)$, based on the transmitter-beam cross-section size at L, $D_B(L)$, times L, or $L\lambda/D_B(L)$ where λ is the lidar wavelength. An estimate of the number of speckles, N, in the receiver aperture is the ratio of the area of the receiver aperture (of diameter D_R) to the typical area of a speckle ($L\lambda/D_B(L)$ That is, the relative error in I(L) due to observing coherent rather than incoherent scattering (a random relative error) is about

$$\frac{1}{\sqrt{N}} = \frac{\lambda}{D_R\ \theta_T} \qquad (5$$

where θ_T is the full transmitter-beam divergence angle. Two other, equivalen expressions for N are, first, the ratio of the transmitter beam cross-section

area at L to the area of the receiver (diffractional) resolution element at L and, second, the ratio of the square of the full transmitter-beam divergence angle to the square of the full receiver aperture diffraction angle. Note that the variations whose relative size is estimated by Equation (5) are random and the variations from different instantaneous sensitive volumes of a lidar are completely uncorrelated.

Values of the relative error in I(L) (see Equation (4)) due to speckle as estimated by Equation (5) are shown in Table I where parameter values were used which are typical of those found in application to smoke/obscurants. (The author's experience in using Equation (5) was with 10.6 μm in reflection from solid surfaces. He found the speckle effects to be somewhat greater than estimated.)

TABLE I. ESTIMATES OF THE RELATIVE ERROR IN THE LIDAR SIGNAL DUE TO SPECKLE IN INCOHERENT LIDARS

LIDAR EXAMPLE	WAVELENGTH λ (μm)	RECEIVER DIAMETER D_R (cm)	TRANSMITTER BEAM DIVERGENCE θ_T (mr)	APPROX. RELATIVE ER IN LIDAR SIGNAL DUE TO SPECKLE $1/\sqrt{N}$
SRI Alpha-1	1.06*	36	2	0.15%
Optech-DREV/Cloud Mapper	1.06	12.5	1.2*	0.71%
ASL CO_2	10.6	30.5	1.2	2.9%

* Largest of two, therefore worst error case.

* Smallest, therefore worst error case.

Table I shows that speckle effects are not significant for typical incoherent lidars except at 10.6 μm.

[Indeed, Ed Measure of ASL confirmed that fluctuations in the return of their CO_2 lidar, which were definitely not due to output pulse energy changes

and were attributed to speckle, were about 7%, which agrees very much with the author's experience with Equation (5).] The speckle effect with focused coherent CW lidar is very different.

COHERENT CW FOCUSED LIDAR

DESCRIPTION. Some basic ideas are given here. A more detailed development is to be found in (Zalay, Kohl and Coffey, 1979) which is fairly complete though a little outdated. The development of focused, CW (i.e., continuous--continuous wave) coherent lidar is very much more in a state of flux relative to that of incoherent lidar. The coherent lidar and its use is roughly 15 years younger than the incoherent lidar. It has some definite advantages for use in smoke/obscurants but it is a uniquely different type of system with complications all its own. There are quite possibly better ways to be developed to process its signal and there may be advantages and problem areas found which are not currently fully appreciated.

The coherent focused lidar operates continuously. There is a laser source and a detector, but there is not a separate transmitter and receiver. Much of the optics of the lidar handle both outgoing and incoming waves.

The lidar optics output a converging spherical wavefront from the large, primary mirror. The radius of curvature of this wavefront is the desired distance L from the lidar, so that the wavefront is focused at L.

The wavefronts backscattered by the individual, small particles in a smoke/obscurant cloud are spherical for any incident wavefront. Each spherical, backscattered wavefront has the scatterer from which it originated at its center of curvature and so the radius of curvature of each spherical scattered wavefront at the lidar is the distance of the scatterer from the lidar. Therefore

only the scattered wavefronts from scatterers at distance L and on the lidar optical axis can be superimposed on the outgoing wavefront all across the primary mirror.

(Some of the outgoing wavefront is split off by the lidar optics before it reaches the primary mirror and is directed onto the detector. An incoming, scattered-wave wavefront is directed back through the optical train and onto the detector in a way that, if the incoming wavefront superimposes with the outgoing wavefront all across the primary mirror, then the incoming wavefront will superimpose on the split-off part of the outgoing wavefront all across the detector aperture. The interference of the two wavefronts at the detector can be obtained by observing the interference of the two wavefronts across the primary mirror, instead of having to consider the details of the changing of the wavefronts as they propagate along the lidar optical train to the detector.)

The outgoing wavefront and any scattered wavefront coming from distance L on the lidar optical axis will superimpose and so will interfere constructively all across the primary mirror aperture. The interference of the outgoing wavefront and a scattered wavefront arising from a scatterer not at distance L and/or not on the lidar optical axis will be destructive. In the latter case, over some regions of the primary aperture the interference of the two waves will be positive and over other regions it will be negative, giving an overall cancellation effect. Thus the coherent focused lidar is sensitive to those scatterers at distance L on the optic axis but is not sensitive to scatterers located elsewhere. (The sensitive volume of the coherent lidar is discussed below.)

The disturbance by the atmosphere of the wavefronts propagating out to, and back from the distance L is believed to be not important over the distances of concern (see below) as the primary effect is to randomly steer the wavefront

(tilt). This results in the focal point being slightly displaced laterally, but there is no net effect on lidar performance due to tilt because the tilt experienced by the outgoing wave is exactly reversed on the incoming wave causing there to be no effect at the lidar aperture.

Because the coherent lidar operates by interference across a wavefront, random disturbances across the wavefront that distort the wavefront by distances approaching $\lambda/2$ cannot be allowed. This is much easier to accomplish with a wavelength of 10 micrometers than with a wavelength of 1 micrometer, and therefore such lidars are based on the CO_2 laser rather than visible or near-IR lasers.

It is the detection process that gives rise to the name "coherent lidar" as the phase of the scattered waves plays a dominant role in that process.

With E_o representing the electric field at the detector of the wave which comes directly from the laser oscillator and with E_s representing the electric field at the detector which is the total of the scattered fields, the total electric field incident on the detector is $E_o + E_s$. The detector is the normal type of detector which detects the square of this field, the flux incident on it. That is, the output of the detector (the raw signal) is proportional to

$$(E_o + E_s)^2 = E_o^2 + 2E_oE_s + E_s^2 . \qquad (6)$$

The radiation incident on the detector from the laser oscillator is much stronger than the scattered radiation incident on the detector, so E_o is much greater than E_s, thus the third term on the right-hand side of Equation (6) can be neglected compared to the second term. The first term is in turn much larger than the second term, but it is a DC term, whereas the second term--due

to the Doppler shift in the scattered field E_s which occurs because of the wind velocity--is an AC term and may be detected separately from the first term. Note that the coherent lidar system, as described, requires a wind component along the lidar beam to separate the desired second term on the right in Equation (6) from the much more dominant first term. Other approaches involve using a separate laser oscillator (local oscillator), separate from the laser transmitter, to generate a frequency offset in E_o, or involve producing a frequency offset in E_s.

The second term in Equation (6), the raw lidar signal, contains terms at every frequency corresponding to a scatterer velocity in the lidar sensitive volume. This signal is sampled and the integrated power spectrum over these frequencies gives R(L) of Equation (1) or, what for coherent lidars is the same thing, I(L) of Equation (4).

Many of the advantages of the coherent lidar arise from the fact that the raw lidar signal is proportional to the scattered field, E_s, rather than the scattered flux. This causes the raw lidar signal to decrease proportionally with T and not with T^2 as with common incoherent lidars. This lessened raw signal dynamic range also makes raw signal sampling easier.

The distribution of the sensitivity in the lidar sensitive volume (the focal volume) is Lorentzian along the lidar optical axis, with its peak centered at distance L and with a width along the lidar optical axis proportional to L^2/D_R^2, where D_R is the primary mirror diameter. This width dependence limits the useful range of the coherent lidar to several hundred meters, so in application of this lidar, the lidar head will not be back in a van with its operating personnel, but will be located separately out in the vicinity of the

smoke cloud. This is also advantageous with respect to atmospheric wave propagation effects. The width of the cross section of the lidar sensitive volume is about 1 cm or less.

SPECKLE. The total scattered field, E_s, is a sum of the scattered field components from each scatterer. In obtaining the integrated power spectrum or its equivalent, E_s is essentially squared and the individual components give rise to cross product or interference terms which are equivalent to the speckle phenomenon discussed earlier. As discussed earlier, what is desired is the flux contribution from each scatterer with little contribution from interference terms.

With the coherent lidar the instantaneous speckle can be expected to be especially severe. Consider the estimate of the number of speckles, N, as the ratio of the transmitter-beam cross-sectional area at L to the area of the receiver (diffractional) resolution element at L. (See the speckle discussion above.) Since the transmitter optics and the receiver optics are the same and since these optics are focused at distance L, the "transmitter-beam cross-sectional area" and the "area of the receiver resolution element" are the same and one speckle fills the aperture of the coherent lidar!

Speckle averaging is therefore, very much needed. It is accomplished by, first, time averaging, letting the random motions of the scatterers set up new phase relations as they move distance $\lambda/2$ with respect to one another within the lidar sensitive volume every fraction of a microsecond and, second, perhaps, by spatial averaging, inadvertant and advertant sampling of different regions by the sensitive (focal) volume of the lidar.

Speckle averaging with a coherent focused lidar is further discussed in the section on scanning and data rates.

DEPENDENCE ON BACKSCATTER AND ATTENUATION

AMBIGUITY IN BACKSCATTER AND ATTENUATION EFFECTS. Note from Equation (4),

$$I(L) = C_1 \beta(L) T^2(L), \tag{4}$$

that the lidar signal depends on the product βT^2; that is, it depends on both the backscatter properties and the attenuating properties of the atmosphere through which the lidar beam is traveling. Note that there is no lidar parameter that can be changed to make the lidar signal any more or less dependent on β compared to T^2; that is, from Equation (4) there is no way to tell how much of the lidar signal is due to β and how much is due to T^2.

This is illustrated in Figure 4. Altitude is plotted vertically and horizontal distance, horizontally. The stronger the lidar signal, the darker the image. The lidar was above the cloud looking downward as it made a traverse of the cloud.

Consider the lidar-signal image on the left of Figure 4. In the central part of the cloud, we see that there is no signal from the lower part. Is this due to the fact that there is no cloud there, and so there is nothing there to backscatter the lidar radiation; i.e., is β equal to 0 there? Or is the transmittance from the lidar to this portion of the cloud so low that the small amount of radiation being backscattered from this portion of the cloud is again reduced so much in traveling back to the lidar that it is too small to be detected; i.e., is T^2 in Equation (4) too small to give a significant lidar return signal?

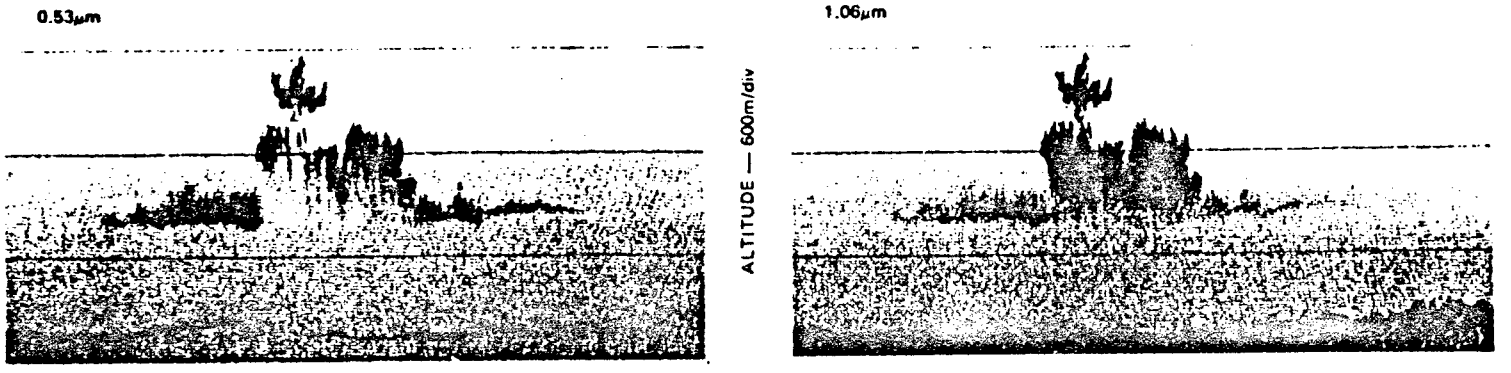

FROM UTHE, SRI

Figure 4. Illustration of lidar signal dependence on βT^2. From (Uthe, 1983)

The right-hand side of Figure 4 is a lidar-signal image taken at the same time as the lidar-signal image on the left but at a different wavelength. We see that there is a cloud in the lower part of the central portion, and that, for the lidar signal on the left, the lack of signal is due to small T^2 and not due to small β.

Note that this same βT^2 ambiguity exists in trying to interpret the lidar signals on the right in Figure 4: How much of the lidar signal on the right is due to β and how much to T^2?

Generally speaking Equation (4) applies to any beaming of a lidar into the atmosphere, whether the lidar is directed into a smoke/obscurant cloud or not (aside from non-ideal instrument effects and multiple-scattering effects to be discussed later), and, in general, the backscatter coefficient, $\beta(L)$, in Equation (4) and the transmittance, $T(L)$, in Equation (4) are both made up of atmospheric gas contributions and aerosol particle contributions.

To remove the ambiguity between the effect of $\beta(L)$ and the effect of $T^2(L)$ on the lidar signal (and thereby be able to recover either the backscatter or the attenuation properties from the lidar signal) either the spatial dependence of $\beta(L)$ or $T^2(L)$ must be known or some relationship must be known to exist between the backscatter and attenuation properties affecting the lidar signal. We shall consider all such possibilities in this report, some in later sections.

RELATIONSHIP OF BACKSCATTER TO ATTENUATION IN SMOKE/OBSCURANT CLOUDS. In clouds, for the wavelengths of interest (UV wavelengths and longer) the backscatter contribution from the cloud particles is orders of magnitude greater than the contribution to the backscattering from both the atmospheric gases and the naturally occurring haze aerosols. Thus at the wavelength of the lidar

transmitter the backscatter coefficient of Equation (4) in a smoke/obscurant cloud is due to the cloud itself. (We shall discuss, below, backscattering from the atmospheric gases in a cloud.)

The attenuation due to the cloud particles is much higher than that due to the atmospheric gases or the naturally occurring haze aerosols at the window wavelengths that readily transmit through the atmosphere. More to the point in Equation (4), the transmittance factor arising from the natural atmosphere is either essentially 1 or is close enough that a readily-obtained correction factor (a function of L) can be applied to I(L) so that, with the corrected I(L), the transmittance T(L) in Equation (4) can be ascribed solely to the cloud effects.

In this sense, in smoke/obscurant clouds, both $\beta(L)$ and $T^2(L)$ of Equation (4), and the related $\sigma(L)$ of Equation (2) are considered cloud properties in this section.

As mentioned above, either $\beta(L)$ must be known, $T^2(L)$ must be known, or a relationship between the backscatter and attenuation properties must exist in order to interpret the lidar signal (i.e., to recover the backscatter or attenuation properties contributing to the signal). In a smoke/obscurant cloud neither $\beta(L)$ due to the cloud nor $T^2(L)$ is known. Thus we must consider whether a relationship exists between the backscatter and the attenuation properties of the cloud.

The backscatter coefficient, $\beta(L)$, is a local property of the cloud; it depends on the cloud properties at distance L on the lidar beam, while T(L) is an effect of the cloud properties all along the beam from the lidar to distance L. Therefore any relationship between $\beta(L)$ and the cloud attenuation properties must be between $\beta(L)$ and $\sigma(L)$, the latter being the local attenuation property. We start with the equation

$$\beta(L) = C_0(L)\, \sigma(L) \ . \qquad (7)$$

Equation (7), as it stands, is completely general and applicable because $C_0(L)$ is still arbitrary and can take on the value $\beta(L)/\sigma(L)$ at each L and make Equation (7) an identity at each L.

We note in Equation (7) that both $\beta(L)$ and $\sigma(L)$ are proportional to the number of cloud particles per unit volume at L (the particle number density at L). Therefore $C_0(L)$ cannot depend on the particle number density at L. It can depend on the particle size distribution, the particle shape distribution and the particle composition distribution, and if these vary in the cloud or along L then $C_0(L)$ will vary. These latter distributions will vary much less than the number of cloud particles per unit volume, however. This will vary greatly throughout the cloud, from very high values in eddy volumes injected with cloud particles at the smoke source to very low values in eddy volumes of clear air which have been folded into the cloud by turbulent mixing. Thus $C_0(L)$ in Equation (7) will vary relatively little with respect to the two quantities it relates, $\beta(L)$ and $\sigma(L)$, and in this sense (and in this sense only) the relationship

$$\beta(L) = C_0\, \sigma(L), \tag{8}$$

with C_0 a constant, holds, although from what has been developed here, order of equality ($\sim$) rather than absolute equality ($=$) would be more appropriate.

We shall discuss the variation of C_0 and its effects on lidar interpretation in a later section.

A variation of the form of Equation (8) with $\sigma(L)$ raised to the k ($k \neq 1$) power is dismissed in Appendix B.

RECOMMENDATIONS

The recommendation regarding the type of lidar and lidar hardware to be developed is given here as the two generic lidar types were discussed in this section. However, the recommendation made is based on material not yet presented, indeed very few of the lidar principles and problem areas have been discussed yet.

Satisfactory answers in other problem areas need to be found with higher priority than the determination of one lidar type over another. Indeed, these solutions, or their lack, should play a major role in determining the final desirable lidar type.

In light of the above, fastening on a single lidar type at this time is too premature, instead, with the higher priority problems mentioned in the sections below being satisfactorily addressed, remaining resources should be directed to efforts within each lidar type to obtain solutions to those problems limiting the application of that type, particularly in smoke obscurants. For incoherent lidars this means attacking or finding a way around the dynamic-range(T^2)/time-of-flight problem. In addition, for incoherent visible and near-IR lidars it means seeing if improvements are feasible regarding the multiple-scattering problem. For incoherent lidars at 10 μm it means seeing if appropriate speckle-averaging techniques might be developed. For coherent lidars, whose development is newer, this means obtaining performance closer to design, probing performance limits including speckle averaging, seeing if signal processing can be improved and, finally, scanning velocities increased.

The major emphasis on lidar hardware should be on using it to obtain those answers which impact the use of lidars as smoke/obscurant diagnostic instruments, as a whole, in the various wavelength regions. An idea of the

variation of the backscatter to attenuation coefficient ratio, C_π, needs to be determined in the many different smoke/obscurants at the several lidar wavelengths. This variation, coupled with the sensitivity of lidar interpretation schemes to this variation, will determine to what extent backscattering from the smoke/obscurant particles themselves can be used and whether the development of the use of tracers needs to be looked at. Incoherent lidars, being better developed than the coherent, need to be used to address the questions of desired spatial and temporal resolution raised in a later section (they can do this with partial cloud scans), though the coherent lidar, with improved speckle averaging, might be able to assist some in this area also. While experience can be gathered and methods developed for handling the large data flows and amounts resulting from lidar use on smoke/obscurants and on tracer clouds, this is a situation that will tend to improve with time, by itself, as better equipment becomes available, so that as a current objective for its own sake it should be given a rather low priority.

All the problem areas mentioned in this recommendation which were not mentioned in the preceding sections are discussed in the sections that follow.

C. LIDAR SIGNAL INTERPRETATION IN SMOKE/OBSCURANTS

EXPRESSIONS FOR $\sigma(L)$

DERIVATION OF A BASIC FORM. All lidar signal interpretation techniques used where the scattering medium is the attenuating medium--the techniques currently used in smoke/obscurants--utilize Equation (8) invoking C_o as a constant. [Klett's solution (Klett, 1981) is stated with σ raised to the k power (see Equation (B-1) in Appendix B), but in application k=1 is always used as it should be.)

If we define C_2 as

$$C_2 = C_1 C_o / 2 \tag{9}$$

then Equations (2), (4) and (8) allow us to write the reduced lidar signal as

$$I(L) = -C_2 \frac{d}{dL} T^2(L) \ . \tag{10}$$

The integral of Equation (10) with a boundary condition, when combined wit Equations (4) and (8) allows us to solve for $\sigma(L)$ all along the lidar beam. There are several forms for the resulting solution for σ and several ways to determine the boundary condition. We will derive and discuss these here. These derivations are built on the work of Hitschfeld and Bordon (1954); Barrett and Ben-Dov (1967); Davis (1969); Collis, Viezee, Uthe and Oblanas (197 Fernald, Herman and Reagan (1972); Klett (1981); Evans, Cerny and Gagné (1983) and the work of this author, but the form of the derivations here is more appropriate for an overview.

Integrating Equation (10) gives

$$\int_{L_1}^{L_2} I(L')dL' = -C_2[T^2(L_2) - T^2(L_1)] \tag{11}$$

where L_1 and L_2 are two distances out the lidar beam, between which I(L) is known. (Therefore L_1 and L_2 are both greater than L_o which is the distance at which useful overlap of the transmitter beam and receiver field of view occurs. At any L less than L_o, I(L) is not known.) Note that the left-hand side of Equation (11) is known.

We turn more directly to the matter at hand and use Equations (8) and (9) in Equation (4) and solve for $\sigma(L)$, obtaining

$$\sigma(L) = \frac{I(L)}{2C_2T^2(L)} . \tag{12}$$

The numerator in Equation (12) is known, the denominator--as it requires T(L) fo every L of interest--is not, but one can substitute for the denominator from Equation (11) with $L_2 = L$ to get

$$\sigma(L) = \frac{I(L)}{2C_2T^2(L_1) - 2\int_{L_1}^{L} I(L')dL'} . \tag{13}$$

The quantity $2C_2T^2(L_1)$ in Equation (13), or its equivalent, is a boundary-condition/calibration value. In the form given in Equation (13), $T^2(L_1)$ is the boundary condition (evaluated at L_1) and C_2 is the calibration factor. The bou condition/calibration value, in its several forms, can be determined in several

ways as shown shortly, but for now consider the relationship of L_1 to the distances L, the latter being the distances at which $\sigma(L)$ is desired.

BOUNDARY CONDITION ON THE NEAR SIDE OF THE CLOUD. If the boundary condition distance L_1 is less than the L values of interest, that is, the boundary condition is determined on the lidar side of the cloud, the integral on the right-hand side of the denominator of Equation (13), the second term in the denominator, is positive and subtracts from the boundary condition/calibration term, the first term in the denominator.

To see the effects of this as L increases away from L_1, one can substitute for the second term from Equation (11) to get

$$\text{Denominator of Equation (13)} \propto T^2(L_1) + [T^2(L) - T^2(L_1)] , \qquad (14)$$

where the first term is proportional to the first term of the denominator in Equation (13), the boundary-condition/calibration term, and the second term, in square brackets, is proportional to the second term of the denominator in Equation (13). Here L_1 is on the near side of the cloud and so $T(L_1)$ is about 1.

With L starting at L_1 and then increasing away from L_1, $T^2(L)$ will start at $T^2(L_1)$ and then decrease with respect to $T^2(L_1)$ so the square-bracket term of Equation (14) will start at 0 at $L = L_1$ and go toward $-T^2(L_1)$ as L goes optically deeper into an optically thick cloud and $T^2(L)$ goes toward zero. Thus the right-hand side of Equation (14) and the denominator of Equation (13) will go toward zero and the determination of $\sigma(L)$ will become highly unstable, $\sigma(L)$ blowing up toward positive infinity. Where this instability occurs depends on the experimental error in the two terms of the denominator of Equation (13).

If the random, uncorrelated relative experimental error in each term is 5%, the denominator of $\sigma(L)$ will typically be about 100% in error for L such that the transmittance from L_1 to L is only about 0.27 (about 1.3 optical depths). This is an unacceptably shallow penetration in smoke/obscurant clouds, though it is no problem in tracer clouds where the optical depth is not that great. (As pointed out by Klett (1981); Collis, Viezee, Uthe and Oblanas (1970) may have been the first to notice a lidar-determined $\sigma(L)$ becoming too large due to this effect. It was not explained at the time; multiple scattering contributions (which would also make the determined $\sigma(L)$ too large) were calculated as too small to cause the problem.)

Both Uthe of SRI and Evans of DREV have indicated to the author that they have been able to interpret to greater optical depths than one would expect from the existence of the instability. Whether this is due to lower-than-expected experimental errors in the denominator terms (if there is no cloud at L less than L_1, $T^2(L_1) = 1$ will be close to exact and all the error will be in C_2 or its equivalent) or whether this is due to correlated experimental errors in these terms, this needs to be investigated.

As the instability sets in when the second term in the denominator of Equation (13) approaches the first in size, at shorter L or in optically thin clouds where the instability does not play a role and good values of $\sigma(L)$ are being obtained, the denominator of Equation (13) is very much determined by the value of the boundary-condition/calibration term, the first term in the denominator, and this value cannot be guessed but must be determined to a relative error which is approximately the same as or less than that desired in σ .

BOUNDARY CONDITION ON THE FAR SIDE OF THE CLOUD. If the boundary condition distance L_1 is greater than the L values of interest, that is, the boundary

condition is determined on the opposite side of the cloud from the lidar, the integral itself in Equation (13) will be negative. Rewriting Equation (13) in terms of a positive integral we have

$$\sigma(L) = \frac{I(L)}{2C_2T^2(L_1) + 2\int_L^{L_1} I(L')dL'} \qquad (15)$$

where, to repeat, as L_1 is greater than L, the integral is positive. The denominator of Equation (15) (and Equation (13)--as they are the same) is the sum of two positive terms and does not go to zero, that is, $\sigma(L)$ does not become unstable because L is less than L_1. (Klett (1981) was probably the first to recognize the importance of this, though others may have observed it and discarded it due to the requirement for a boundary condition on the far side of the cloud. [We will discuss this aspect below.])

The denominator of Equation (15) (equivalent to Equation (13)) is also proportional to the right-hand side of Equation (14). As here L is less than or equal to L_1, $T^2(L)$ is greater than or equal to $T^2(L_1)$ and the two terms on the right-hand side of Equation (14), as just stated, are positive. For L near L_1 (i.e., on the far side of the cloud) such that $T^2(L)$ is approximately equal to $T^2(L_1)$, the denominator of Equation (15) is very much determined by its first term, the boundary-condition/calibration term.

As L_1 is on the far side of the cloud, $T^2(L_1)$ will typically be very small (10^{-2} to 10^{-6}) in smoke/obscurant clouds, so that as L reduces from L_1 on the far side of the cloud and comes back toward the lidar, $T^2(L)$ grows back toward 1, its value on the near side of the cloud. The quantity $T^2(L)$ need

not progress far toward 1 before it is much greater than $T^2(L_1)$ where, as can be seen in Equation (14), the second (integral) term in the denominator of Equation (15) dominates the boundary-condition/calibration term, i.e., in the near part of the cloud and to some unknown but fair-sized extent into the cloud the determined $\sigma(L)$ does not depend much on the boundary condition or the calibration.

VARIOUS FORMS OF THE EQUATION FOR $\sigma(L)$. Before discussion of the evaluation of the boundary-condition/calibration term, let us consider the various forms it can take and the resulting forms of Equation (13) or (15).

The first form requires knowledge of a single parameter, σ, at one point in a cloud on the lidar beam beyond the overlap position. This mathematically more direct form of boundary condition eliminates need of a calibration factor. Using Equations (4), (8) and (9) we find

$$I(L)\sigma^{-1}(L) = 2C_2T^2(L) \ . \tag{16}$$

Evaluating Equation (16) at $L = L_1$, substituting for the boundary-condition/calibration term, $2C_2T^2(L_1)$, in Equation (13) and then dividing numerator and denominator by $I(L_1)$ gives

$$\sigma(L) = \frac{I(L)/I(L_1)}{\sigma^{-1}(L_1) - 2\int_{L_1}^{L} [I(L')/I(L_1)]\, dL'} \ . \tag{17}$$

With the quantity S(L) defined as

$$S(L) = \ln I(L) \ , \tag{18}$$

Equation (17) can be put in the form

$$\sigma(L) = \frac{e^{[S(L) - S(L_1)]}}{\sigma^{-1}(L_1) - 2\int_{L_1}^{L} e^{[S(L') - S(L_1)]}\, dL'} \quad . \tag{19}$$

This is the form discussed by Klett (1981) although the particular emphasis of Klett was on L_1 greater than L (far-side boundary condition) for which, with the integral of Equation (19) written so as to be positive, Equation (19) takes the form

$$\sigma(L) = \frac{e^{[S(L) - S(L_1)]}}{\sigma^{-1}(L_1) + 2\int_{L}^{L_1} e^{[S(L') - S(L_1)]}\, dL'} \quad . \tag{20}$$

Note that G(L) must be applied to R(L) to get I(L) via Equation (3) for use in Equations (17) through (20) and that G(L) may differ significantly from L^{-2}, especially for short L, unlike the assumption used in Klett's original paper (Klett, 1981).

As a means of not having to explicitly determine G(L) (or the correction for the ambient atmospheric transmittance $T_c(L)$--as mentioned above Equation (7)) Evans (1983) takes the ratio of the lidar signal in the smoke/obscurant cloud R(L) to the lidar signal at the same L obtained before and/or after a smoke trial in the ambient atmosphere, $R_c(L)$, with a uniform, though unknown, background-aerosol backscatter coefficient, β_c. (With Evans' system the lidar signal from the natural or background aerosol can be readily obtained). Using Equations (1) and (3) this ratio is found to be

$$\frac{R(L)}{R_c(L)} = \frac{I(L)}{C_1^c \beta_c} \tag{21}$$

where C_1^c is the constant value of C_1 when $R_c(L)$ is obtained, and where T(L) in I(L) [see Equation (4)] is now automatically corrected to be the transmittance due to the smoke/obscurant cloud. Note that C_1 need not remain constant between obtaining R(L) and $R_c(L)$.

Dividing the numerator and denominator of the right-hand side of Equation (13) by $C_1^c \beta_c$ therefore gives

$$\sigma(L) = \frac{R(L)/R_c(L)}{\frac{2 C_2}{C_1^c \beta_c} T^2(L_1) - 2\int_{L_1}^{L} [R(L')/R_c(L')]\, dL'} \cdot \tag{22}$$

The quantity $2C_2/C_1^c\beta_c$, which is σ_c^{-1} if C_1 is constant and C_0 (for smoke) is the same as β_c/σ_c for the ambient atmosphere, is a form of calibration constant called $\tilde{\sigma}_c^{-1}$ by Evans.

Note that, as with the previous equations for $\sigma(L)$, Equation (22) has the usual, stable form for $L < L_1$ with the sum in the denominator.

Finally, note that although Equations (21) and (22) arise from relationships where R(L)=0 is assumed for L in the ambient atmosphere on the near side of the smoke/obscurant cloud rather than $R(L) \approx R_c(L)$ there, for $\tilde{\sigma}_c^{-1}$ much greater than the distance to the smoke/obscurant cloud and $\tilde{\sigma}_c$ negligible compared to σ in the cloud, no real problem will arise.

EVALUATION OF THE BOUNDARY-CONDITION/CALIBRATION (B-C/C)TERM

Equations (13) and (15), and (22), are forms which have the boundary-condition/calibration term made up of a calibration factor [e.g., C_2 itself in Equation (15)] and a separate boundary condition factor [e.g., $T^2(L_1)$ in Equation (15)]. The calibration factor, under the assumption of constant C_2 in a cloud [constant C_0 and constant or compensated C_1--see Equation (9)], should apply to all lidar beam paths at all times in a cloud. The boundary condition factor, usually $T^2(L_1)$, must be supplied on each lidar-beam path whose length is scanned, whether scanned with a pulse moving at the speed of light or with a moving focal volume.

Equations (19) and (20) on the other hand have only a boundary condition factor in the boundary-condition/calibration term. This is because the more direct form of the boundary condition to be supplied requires no dependence on C_2 so long as C_2 is constant. This can be seen by substituting for $I(L)/I(L_1)$ in the numerator and the denominator of Equation (17) using Equation (12) or (16) and noting that the C_2 dependence cancels out, leaving only dependence on cloud attenuation properties.

In what follows we reverse the above order and look at the evaluation of the boundary condition $\sigma^{-1}(L_1)$ and then at the evaluation of the transmittance and the calibration factor. Finally we discuss the ways of obtaining evaluations which allow whole-cloud scanning.

In every case we do not consider boundary condition evaluation with substantial cloud optical depth beyond the boundary-condition application distance L_1 because of the instability discussed above.

EVALUATION OF $\sigma^{-1}(L_1)$

Evaluation of $\sigma(L_1)$ [Equations (17), (19) and (20)] must take place in the cloud where $\sigma(L_1)$ is non-zero and also where $I(L_1)$ can be determined (for example, $I(L_1)$ cannot be buried in the noise or L_1 cannot be less than the receiver-field-of-view/transmitter-beam overlap distance L_o) as $I(L_1)$ is required along with the application of $\sigma^{-1}(L_1)$--see Equation (17) and, via Equation (18), Equations (19) and (20).

MEASUREMENT OF $\sigma(L_1)$. Any measurement of $\sigma(L_1)$ applies to a localized volume according to the definition and use of the attenuation coefficient, σ. The maximum size of the localized volume is limited to the larger of the correlation volume of the attenuation coefficient (perhaps as large as 6 m by 6 m by 1 m vertically--see the section on spatial resolution) and the instantaneous sensitive volume of the lidar.

In order to scan a full cloud, with each measured $\sigma(L_1)$ applicable to this maximum volume size, it would be impractical, in terms of the number of measurement devices required, to make the measurements at any distance from the lidar on the numerous lidar-beam paths involved. Thus geometry requires that any measurements of $\sigma(L_1)$ would have to be made essentially at the lidar aperture, but the measurement could only be made there if the lidar were immersed in the cloud, if the measurement could be made so as not to interfere with the lidar beam, if the overlap distance could be brought back to the lidar aperture (see the subsection on G(L)) and, even then, only if the cloud were a smoke/obscurant cloud or a tracer cloud of relatively low optical depth (because of the instability in the determination of $\sigma(L)$).

To scan a fixed vertical cross-section with the lidar on the ground, the number of $\sigma(L_1)$ measurements required to get the necessary one measurement every

meter, vertically, would not be too great at the far side of the cloud, but since the measurement has to take place in the cloud (and, in smoke/obscurants, without much optical depth beyond the measurement) this would require the impracticality of large numbers of measurement devices distributed throughout a spatial cross-section plane in order to obtain useful far-side measurements of $\sigma(L_1)$ wherever the cloud might appear in this plane. This leaves only the limited approach of the previous paragraph.

An additional consideration is that use of measured $\sigma(L_1)$ as the boundary condition implies basing the determination of $\sigma(L)$ on the rest of the lidar-beam path on a point measurement at L_1 where (looking ahead) C_2 may deviate compared to its typical value over the rest of the lidar-beam path or where the associated lidar return signal at L_1, $I(L_1)$, may from time to time contain a noise spike. Thus an aberration at the one point of measurement will affect the determination of $\sigma(L)$ at all points along the lidar-beam path.

<u>"ESTIMATING" $\sigma(L_1)$ (OR ANY OTHER B-C/C TERM) WITH $L < L_1$</u>. In optically thick smoke/obscurant clouds with $L < L_1$ the relative lack of dependence of the determined $\sigma(L)$ on the boundary-condition/calibration (B-C/C) term, once the integral term has become much larger, gives rise to the idea of estimating the B-C/C term, here represented by $\sigma^{-1}(L_1)$. See, for example, the reports by Lentz (1982) and Measure, Lindberg and Lentz (1983).

(It should be noted that when the B-C/C term represented by $\sigma^{-1}(L_1)$ is unimportant, the B-C/C term in any of the other forms for $\sigma(L)$ above is equally unimportant, as the ratio of the B-C/C term in the denominator to the integral term in the denominator is the same in all the expressions for $\sigma(L)$.)

The ambiguity in lidar return signals was discussed in Section B. This ambiguity implies, even under the conditions of the discussion in this section,

that for any given lidar signal there is an infinite number of curves, $\sigma(L)$, which can give rise to that signal. On the curves giving rise to any particular lidar signal, the values of σ at the far-side boundary-value distance L_1--the possible values of $\sigma(L_1)$--range from 0 to ∞ ! See (Kohl, 1978). So one cannot tell from the lidar signal alone whether L_1 is located in a hole in the cloud or in a most dense region of the cloud. One cannot tell anything about $\sigma(L_1)$ by observing the lidar signal! (In fact it is the independent furnishing of $\sigma(L_1)$ (or any other B-C/C term) that picks out the one curve, $\sigma(L)$, from the infinite number allowed by the lidar signal.)

USE OF OPTICAL DEPTH IN INTERPRETATION WITH AN UNKNOWN FAR-SIDE BOUNDARY CONDITION. Without any lidar-independent determination of $\sigma(L_1)$, it turns out that one is not really using an estimate of $\sigma(L_1)$ to get $\sigma(L)$ at some distances, L, less than L_1, but one is using the knowledge or expectation that the square of the transmittance from such L to L_1, is small compared to 1. This can be seen by considering Equation (14), defining $T(L, L_1)$ to be the transmittance from distance L out to distance L_1, using the fact that

$$T^2(L_1) = T^2(L)T^2(L, L_1), \tag{23}$$

and putting Equation (14) in the form

$$\text{Denominator of } \sigma(L) \propto T^2(L)\{T^2(L, L_1) + [1 - T^2(L, L_1)]\} . \tag{24}$$

Here it can be seen that the B-C/C term [the first term in curly brackets in Equation (24)], the term which differs between curves allowed by the lidar

signal, is insignificant compared to the integral term (the square-bracket term), the term which is the same for all curves allowed by a given lidar signal, when $T^2(L, l \quad << 1$.

All the curves for σ allowed by the lidar signal and compatible with the condition $T^2(L^*, L_1) << 1$ (even the one with $\sigma(L_1) = \infty$!) converge to the same value of σ at $L = L^*$, $\sigma(L^*)$. This can be seen by noting in Equation (15), (20) or (22) that the numerators are the same for all curves at $L=L^*$ and the denominators are also the same for all the compatible curves according to the condition $T^2(L^*, L_1) << 1$ and Equation (24). Further, of course, these curves stay together at L smaller than L^*.

There are curves for σ as a function of L which are allowed by the lidar signal [they start from smaller values of $\sigma(L_1)$] which do not converge to the value formed by the previous curves at $L=L^*$. These necessarily have $T^2(L^*, L_1) \not< 1$ (otherwise by Equation (24) their value of σ would not be different at $L=L^*$) and, without an independent determination of $\sigma(L_1)$, they can only be ruled out because of the determination or expectation that $T^2(L^*, L_1)$ is small compared to 1. (They cannot be ruled out by considering the lidar signal!)

Figures 5 and 6 illustrate the aspects of multiple (infinite) possible solution curves from a given lidar signal and the convergence of possible solutions when $T^2(L^*, L_1)$ begins to be small compared to 1 on each of the possible solution curves which are converged at $L=L^*$. (Note the boundary value is really not being estimated in Figures 5 and 6. The range of boundary values used is 10^3.) In Figure 6 the solid curve cannot be eliminated as a solution at lower altitudes compared to the converged curves unless it is known independentiy that $T^2(L, L_1)$ is indeed small compared to 1 for L

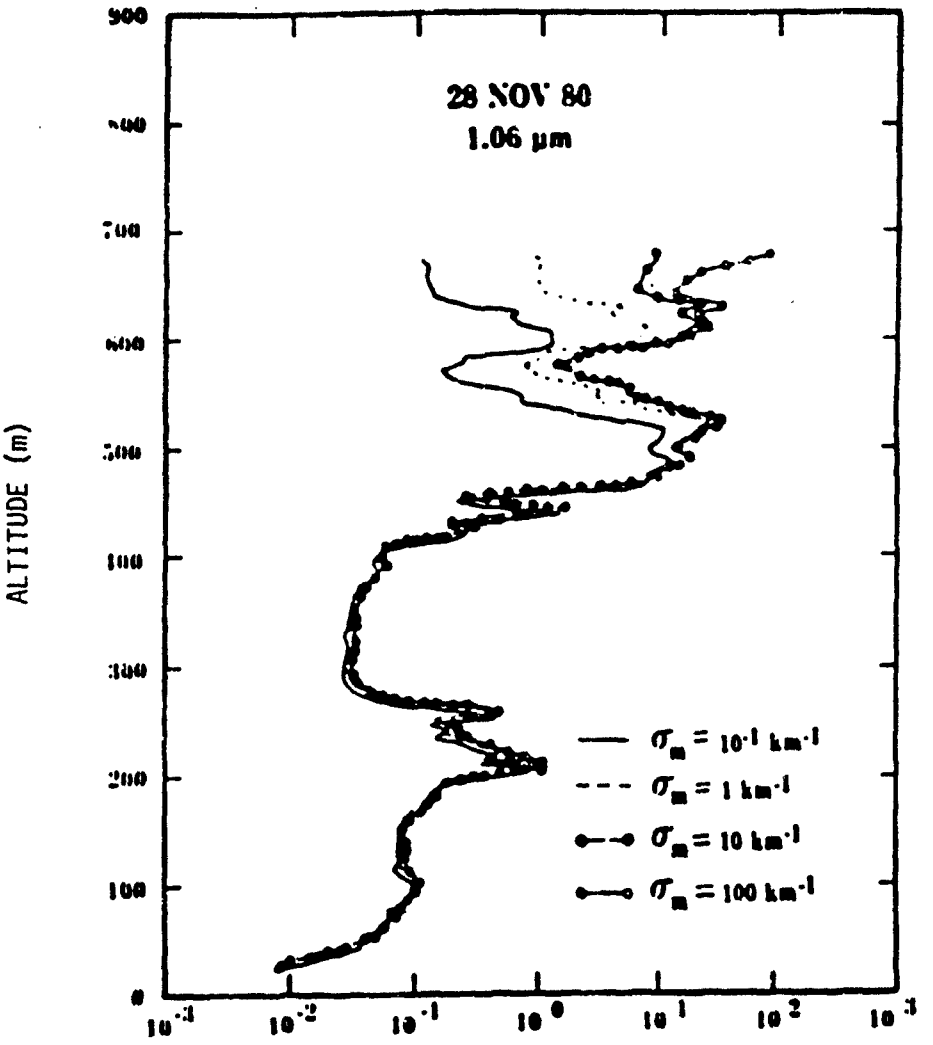

from Measure et al, ASL

Figure 5. Lidar-determined attenuation coefficient profiles for four different boundary value estimates at 1.06 μm. The quantity σ_m is our $\sigma(L_1)$. Here L_1 = 700 m. (The lidar beam is vertically upwards in fog and cloud at Meppen, West Germany.) In this case $T^2(L, L_1)$ on the solid curve does get sufficiently small compared to 1 that the solid curve converges to the other curves of higher $\sigma(L_1)$ for which this condition is also met. (Compare the solid curve to a vertical line at 10^1 km^{-1}.) From (Measure et al, 1983).

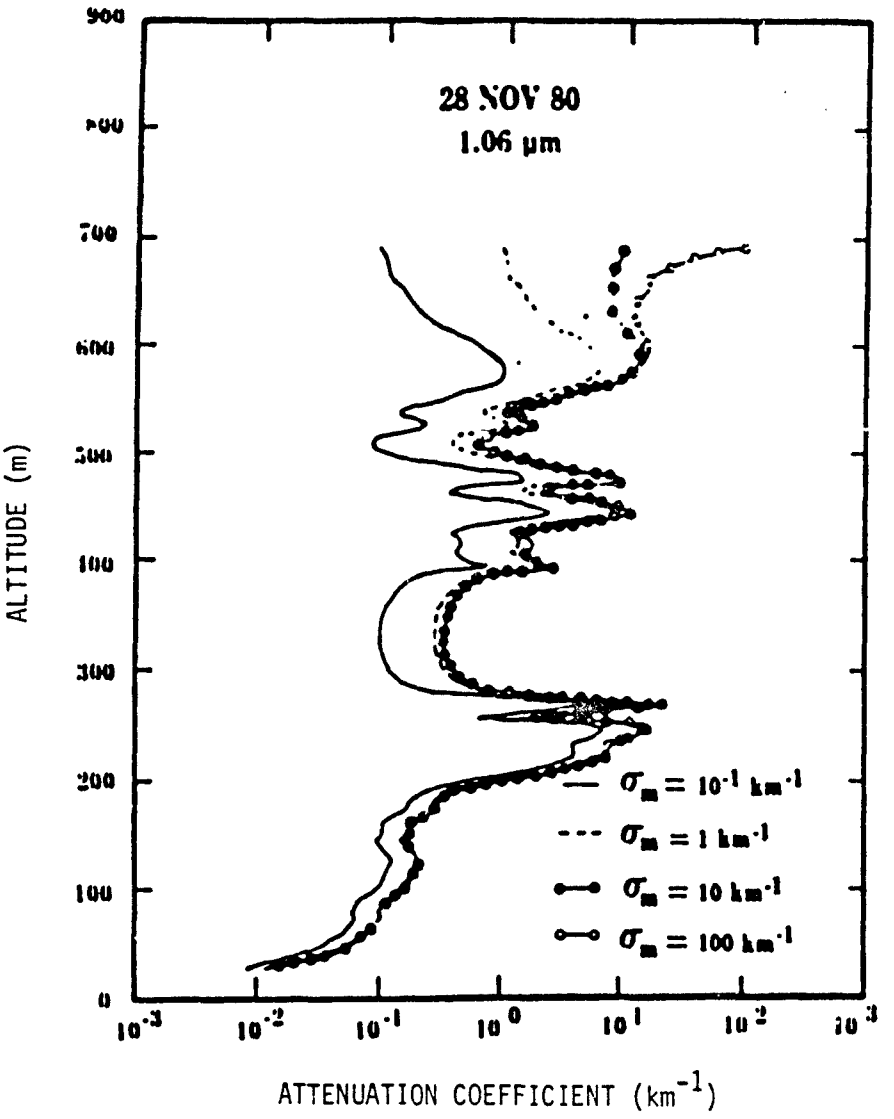

from Measure et al, ASL

Figure 6. Lidar-determined attenuation coefficient profiles for four different boundary value estimates at 1.06 μm. The quantity σ_m is our $\sigma(L_1)$. Here L_1 = 700 m. (The lidar beam is vertically upwards in fog and cloud at Meppen, West Germany.) In this case $T^2(L, L_1)$ on the solid curve never gets sufficiently small compared to 1 that the solid curve converges to the other curves of higher $\sigma(L_1)$ for which this condition is met. (Compare the solid curve to a vertical line at 10^1 km^{-1}.) From (Measure et al, 1983)

of lower altitude. (Such knowledge is the basis of the author's interpretation scheme discussed below.) If $T^2(L, L_1)$ was known not to be small compared to 1, the solid curve or one of the other curves (unplotted) of lower $\sigma(L_1)$ value would be possible solutions. Selecting which such curve was indeed the solution would depend on knowing a boundary condition such as $\sigma(L_1)$ or $T(L, L_1)$.

Thus in order for the lidar signal in the "estimated $\sigma(L_1)$" approach to yield a unique solution for some distances L less than some further distance L_1 from which useful lidar signals are still received, it must be known that $T^2(L, L_1)$ is small compared to 1. In fact, this last is the actual boundary condition used. So if lidar-determined $\sigma(L)$ values obtained using this method are to compare favorably with non-lidar determined $\sigma(L)$ values, the cloud or dispersion in which the estimated boundary condition method is used must be somewhat optically thick beyond the region in which the comparison is made, such as in Figure 7. (As discussed below, C_o is expected to have little variation over a lidar beam path for 1.06 μm radiation in water cloud and fog.)

ANOTHER $\sigma(L_1)$ ESTIMATION SCHEME. The scheme of Ferguson and Stephens (1983) which iterates between estimations of $\sigma(L_1)$ at $L_1 < L$ and $L_1 > L$ is based on a fallacy in that a $\sigma(L)$ curve which reproduces the lidar signal is not unique (see the discussion above). It appears that iteration is required in their scheme only because an approximation does not allow the $\sigma(L)$ curve resulting from the first iteration to reproduce the lidar signal.

USE OF $\sigma(L_1)$ AS THE BOUNDARY CONDITION IN SMOKE/OBSCURANTS. No doubt for the reasons discussed above, none of the lidar development efforts working with smoke/obscurants use $\sigma(L_1)$ as the actual boundary condition. They have all, apparently independently, arrived at the use of transmittance as a boundary condition.

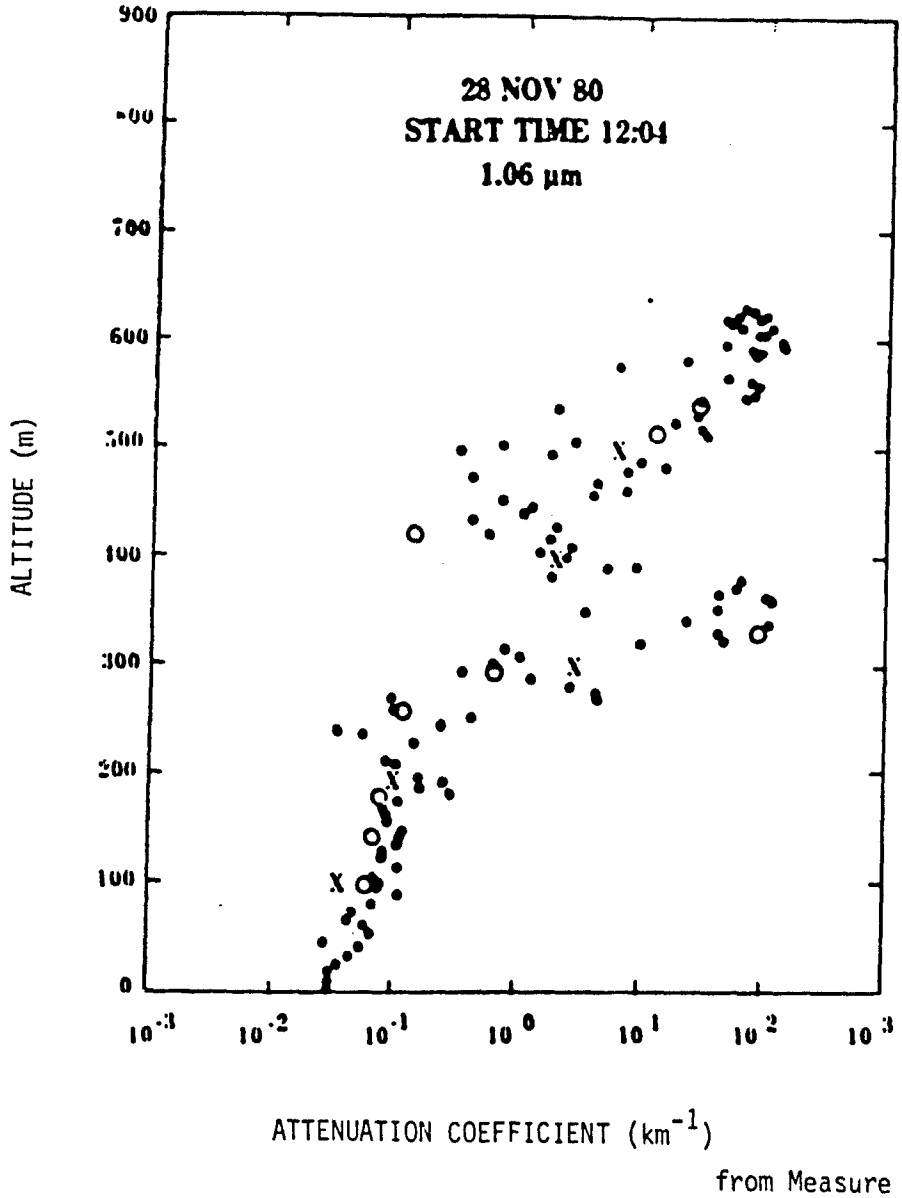

from Measure et al, ASL

Figure 7. Comparison of attenuation coefficient values obtained from 1.06 µm lidars (x's and o's) with attenuation coefficient values obtained by calculation from particle size data obtained from tethered-balloon-borne particle spectrometers in fog and cloud at Meppen, West Germany. (From Measure et al, 1983).

(It should be mentioned also, that use of $\sigma(L_1)$ as the boundary condition in a development effort would mean that C_2 would not be determined, and no data would be obtained on the amount of variation of this important parameter either with time on a fixed lidar beam-path, or from one lidar-beam path to another.)

EVALUATION OF $T(L_i)$

In this subsection L_i may be a distance at which a boundary condition is to be applied or a distance at which $T(L_i)$ is to be obtained in order for it to be used to evaluate C_2 or its equivalent.

Note that unlike $\sigma(L_i)$, L_i for $T(L_i)$ need not be in the smoke/obscurant cloud. However, $I(L_i)$ must be observable (L_i must be greater than L_o, the overlap distance, and $I(L_i)$ must not be buried in the noise) if such observation would show $I(L_i)$ to be non-zero, or else there must exist some adequate compensating or approximating theory in its place.

MEASUREMENT OF $T(L_i)$ BY SEPARATE TRANSMISSOMETER. One method of measuring $T(L_i)$ is by a separate transmissometer system operating at the lidar wavelength with source at the lidar and receiver at L_i. This has not been used in smoke/obscurant lidar development work probably because it requires an additional system. However, use of an independent system does not put constraints on the variation of the lidar C_1 parameter over the course of the trial.

MEASUREMENT OF $T(L_i)$ USING THE LIDAR. The method of measuring $T(L_i)$ that has been used in the current development work involves using the lidar as the source and, by most groups, as the receiver also, comparing certain signals in the presence of the smoke/obscurant cloud to the same sort of signals obtained in the clear air before and/or after the trial. This requires that C_1 be sufficiently constant or adequately compensated over more than the entire time period of the trial.

WITH SURFACES. Diffuse surface (target) panels are used by ASL (Rubio, Measure and Knauss, 1983) and DREV (Evans, Cerny and Gagné, 1983) to get an incoherent lidar return signal from the far side of the cloud. The ratio of the lidar surface signal in the presence of the cloud to the lidar surface signal in the absence of the cloud recovers T^2. In scanning operations, hitting the panels fully with the lidar beam (the panels must be bigger than the beam cross section) presents some difficulties.

Ed Uthe of SRI is investigating the use of the underlying terrain surface as the transmittance-determining surface in observing a smoke/obscurant cloud with an incoherent lidar system from above. In such an approach one must overcome non-uniform surface reflectance and one must guard against lack of spatial resolution (caused by the pulse width or trailing edges on the pulse) causing interference of the terrain signal with the cloud backscatter signal up to significant heights above the terrain.

Due to speckle effects, obtaining T^2 from a surface return signal with a coherent lidar is not as simple as with an incoherent lidar. Speckle averaging requires transverse surface motion so that a number of completely independent surface-area regions are illuminated by the coherent lidar while the lidar focal volume intersects the surface. For example, for speckle-induced fluctuation of 5%, 400 surface regions are required. With a minimal beam cross section on the far side of the cloud of 1 mm this requires 40 linear centimeters of unrepeated surface to move through the focal volume while it intersects the surface. Belt sanders are often used.

There is a possibility of developing a speckle-free "surface" for coherent lidars, but this has not been investigated.

WITH A SEPARATE RECEIVER. Instead of a surface on the far side of the cloud a receiver may be used there collecting radiation from the lidar beam. Use of a receiver on the far side gives the transmittance, T, directly. This approach is used in the DPG-Lockheed coherent lidar development work. The rapid motion of the coherent lidar focus along the lidar-beam optical axis causes the divergent flux density at the receiver aperture on the far side to vary, giving an AC signal whose relative amplitude is a measure of T.

SCANNING AND CURRENT $T(L_i)$ MEASUREMENT METHODS. With current methods to obtain lidar-signal interpretation over a lidar-beam path in optically thick smoke/obscurant clouds an instrument or surface must be on the other end of the path from the lidar.

Using the coarsest correlation distances for correlation of transmittance over transverse path displacements (see the section on spatial resolution), taken as 6 m horizontally and 1 m vertically, a whole-cloud, transverse lidar beam scan covering, for example, a far-end area 100 m horizontally by 10 m vertically would require 170 such surfaces or instruments or, where a large, fixed surface will do, a strong, 100 m by 10 m wall is required with an optically uniform surface that withstands weathering. This is not a pleasing prospect, and this is probably a minimal requirement as such surfaces, instruments or wall would be fixed with respect to the ground, not moving along with the cloud.

For vertical, cross-wind cloud cross-sectional scans, something like 10 such surfaces or instruments would be required in a vertical, linear array (or a single 10 m by 1 m surface would be required). This is much more feasible.

Means of obtaining far-side boundary conditions without the presence of an instrument or surface on the far-side end of interpreted lidar-beam paths are discussed below.

ESTIMATING $T(L_i)$ WITH L_i ON THE NEAR SIDE. The transmittance $T(L_i)$ on the near side of the cloud is required in evaluating C_2 or its equivalent. It may be used as the boundary condition factor only in smoke/obscurant clouds of relatively low optical density or in tracer clouds of purposefully low optical density. If it is known that there is no cloud at all between L=0 and $L=L_i$ then the transmittance $T(L_i)$ can be taken to be identically 1.

Note that L_i must be beyond the transmitter-beam/receiver-field-of-view overlap distance L_o and that cloud coming between the lidar and this distance will deteriorate or ruin the ability of lidar signals to be interpreted when the required near-side transmittance is obtained in this way--and it is required (due to use of a calibration factor) and it is obtained in this way in all the current, useful interpretation techniques.

ESTIMATING $T(L_i)$ WITH L_i IN THE CLOUD OR ON THE FAR SIDE. The estimation of $T(L_i)$ with L_i in the cloud or on the far side when $T(L_i)$ is to be used as a boundary condition is dismissed above. [See the discussion on the near-side and far-side boundary conditions and on estimating $\sigma(L_i)$.]

With L_i known to be optically deep within the cloud and L_i used as L_2 in determining C_2 (or its equivalent) from Equation (11), the condition $T^2(L_i) << 1$ is all that is required to evaluate C_2 with $T(L_1)$ known to be 1.

EVALUATION OF THE CALIBRATION FACTOR (C_2 OR A RELATED QUANTITY)

Use of a transmittance for a boundary value is not as direct, mathematically, as use of a value of the attenuation coefficient, σ, itself, and requires determination of a calibration factor (C_2 or a related quantity) in the B-C/C term. (See Equations (13), (15) and (22).)

Note that with C_o and C_1 constant, C_2 (or its equivalent) can be determined once in a trial (see Equation (9)), or updated from time to time if C_o and/or

C_1 change systematically. The boundary condition must be determined on each longitudinal scan of a lidar-beam path.

EVALUATION OF C_2. The DPG-Lockheed effort uses Equation (15). Evaluation of C_2 is done using Equation (11). The transmittance at the far-side distance L_2 in Equation (11) is measured as described above. The near-side distance L_1 is the distance of closest approach of the focus to the lidar (and is equivalent to L_o in effect) and, as with all other current lidar schemes, no cloud is allowable at closer distances than L_1 when C_2 is determined because $T(L_1)$ is used as equal to 1.

EVALUATION OF δ_c^{-1}. The calibration factor used by Evans of DREV is δ_c^{-1} (see the discussion below Equation (22)). How it can be and is evaluated can be seen by dividing Equation (11) by $C_1^c\beta_c/2$ to get

$$\delta_c^{-1} \equiv \frac{2C_2}{C_1^c\beta_c} = \frac{\int_{L_1}^{L_2} [R(L')/R_c(L')]\, dL'}{T^2(L_1) - T^2(L_2)} \qquad (25)$$

where the symbols used are those of Equation (22). The transmittance to the near-side distance L_1 in Equation (25) is used as 1 and the transmittance at the far-side distance L_2 is determined from a surface panel as described above.

EVALUATION OF THE ASL B-C/C TERM. In smoke/obscurants, ASL reports (Rubio, Measure and Knauss, 1983) evaluating the whole B-B/C term essentially every lidar pulse. Equation (20) was used, but the far-side transmittance was measured, and that value of $\sigma^{-1}(L_1)$ (with L_1--here and in Equation (20)--the distance to the far edge of the cloud) was solved for and used which causes the resultant, lidar-determined $\sigma(L)$ to give the measured transmittance.

From Equation (16) it can be seen that this value of $\sigma^{-1}(L_1)$ is

$$\sigma^{-1}(L_1) = 2C_2 \frac{T^2(L_1)}{I(L_1)} \quad . \tag{26}$$

The transmittance to the far edge of the cloud, $T(L_1)$, and the measured transmittance to a point beyond that are the same as no cloud intervenes, thus $T^2(L_1)$ is known. The quantity $2C_2/I(L_1)$ of Equation (26) can be determined from Equation (11) with L_1 of Equation (11) being a near-side distance at which T=1 (the near edge of the cloud was used) and with L_2 of Equation (11) being the distance to the far edge of the cloud, the L_1 of Equation (26).

One of the apparent problems encountered was in picking the signal from the far edge of the cloud, $I(L_1)$, out of the often small, and therefore noisy signal I(L) near that far edge. The presence of noise, or the burying of the signal $I(L_1)$ deep inside unrecognized noise, was recognized (Rubio, Measure and Knauss, 1983) as causing the apparent $I(L_1)$ to be too large and, therefore, $\sigma^{-1}(L_1)$ to be too small ($\sigma(L_1)$ too large)--as can be seen from Equation (26). With the benefits of hindsight it can be seen (by substituting Equation (26) in Equation (20) with the latter put in a form like Equation (17) [$L < L_1$]) that use of such overlarge $\sigma(L_1)$ causes no problem because the determined $\sigma(L)$ along the lidar-beam path is--with no numerical error--completely independent of $I(L_1)$ no matter how much noise is in that quantity. The lidar determined $\sigma(L)$ will be in error for L near L_1 due to the noise in I there, but this comes from I(L) in the numerator of Equation (17) [$L < L_1$].

INTERPRETATION APPROACHES ALLOWING WHOLE-CLOUD SCANNING IN TYPICAL (OPTICALLY THICK) SMOKE/OBSCURANTS

As discussed above, use of the current approaches involving the use of transmittance for the far-side boundary condition apparently allows interpreted scanning of typical smoke/obscurant clouds or plumes in a fixed (with respect to the ground) vertical cross section, but becomes unwieldy for whole-cloud (three dimensional) scanning of operational, optically thick smoke/obscurant clouds. Approaches allowing such whole-cloud scanning are discussed here.

(Note that whole-cloud scanning of clouds whose optical depth is small enough to allow near-side boundary conditions to be used--relatively thin smoke/obscurant clouds and tracer clouds--can, and is, done now.)

VARIATIONS ON CURRENT APPROACHES. The problem with current approaches is that large numbers of surfaces or instruments (boundary condition devices) would be required to cover the horizontal and vertical area on the far side of the cloud across which the lidar beam would play as it was scanned transversely, horizontally and vertically, to interrogate all volume elements of the cloud. The numbers of such boundary condition devices are set by the extent of the region to be transversely scanned (already on the small side in the example used) and the separation distances between the boundary condition devices, which are the electro-optically significant, horizontal and vertical, attenuation-coefficient and transmittance correlation lengths (see the section on spatial resolution). The largest the latter lengths might be is about 6 meters horizontally and 1 meter vertically.

The only variation that might allow whole-cloud scanning with current approaches is to increase the separation distances of the boundary condition devices beyond the correlation lengths. The resulting data would have much

reduced utility as this would mean giving up interpolated values of σ between point to point (volume element to volume element) measurements of σ as electro-optically accurate determinations. The best one could obtain with some relation to reality would be running spatial averages of σ over volumes of the size of several of the (larger) separation distances, with the distribution of lidar-determined σ's about the running mean giving some indication of the variation of σ about the mean. Essentially all the spatial frequency information so important to the prediction and understanding of imaging and of interaction with a dynamic or rapidly responding E-O system would be lost--even low spatial frequency information would be lost due to aliasing.

Still, the attenuation coefficient information obtained would be more than is obtained in smoke trials now.

A NEW APPROACH. A new approach which does not require a far-side boundary condition device, as such, for each lidar-beam path interpreted in optically thick clouds, which is useable with coherent and incoherent lidar, which does not require constant C_1 over the entire time period of the trial, and which allows clouds to penetrate to the lidar, inside any minimum interpretation distance L_o, has been devised by the author.

Mathematically this approach uses an approximate boundary condition with a known maximum error. Operationally it requires a back-up plume or cloud behind the cloud under diagnosis to intercept any interpreted lidar-beam path. Thus geometry requires the back-up plume or cloud to be bigger, with possible use of multiple generating sources, some perhaps elevated. The back-up plume need not be too thick optically. With the same type of aerosol in both the back-up plume and the cloud under test, a back-up plume transmittance at or below 0.2 allows less than 5% error in interpretation. There are no transmittance conditions on the test cloud. The approach is being developed with internal support. It is unpublished but an early manuscript has been circulated.

It is more evident with such an approach, perhaps because of the use of two separate plumes or clouds, that unknown or uncompensated variation of C_0, the ratio of backscattering to attenuation, along the lidar-beam path--here, in particular, from one plume to another--will affect the answer obtained, but the reader should now be in a position, based on the above discussions, to see that all the interpretation techniques discussed above rely on the constancy of C_0. After stating our recommendations therefore, we take up the question of the constancy of C_0 and its effect on lidar interpretation.

SUMMARY AND RECOMMENDATIONS

All current interpretation schemes assume and require that the ratio of the backscatter to attenuation coefficient ratio, C_0, be constant.

A boundary condition/calibration term is required in addition to the lidar data in order to interpret the lidar signal where the backscattering and attenuation both are due to the cloud under test--the usual situation.

Application of a boundary condition on the near side of the cloud gives rise to a solution that is unstable with increasing distance into a dense cloud and is apparently limited to transmittances at and above 0.1 (though Uthe and Evans report more stability than expected).

Application of a boundary condition on the far side of the cloud gives rise to a stable solution, but current methods require a surface or instrument on the end of every lidar-beam path through the cloud. (The author has devised a new approach that eliminates this restriction.)

Use of the solution form with an attenuation coefficient as a boundary condition, while more direct mathematically, has too many disadvantages for use in smoke/obscurants.

All four lidar groups working at recovering quantitative data by lidar from smoke/obscurants have independently arrived at use of far-side transmittance as the boundary condition factor. Use of transmittance, because it is less mathematically direct, requires evaluation of a calibration factor. This evaluation does not allow the cloud to approach the lidar aperture. Use of transmittance, as practiced, requires the lidar performance parameter either to remain constant (C_1 to remain constant) or to be compensated for variation throughout the length of a trial, because before and after comparisons have to be made. (The author's new approach also eliminates these restrictions.)

Recommendations are made in the next section regarding the effects of the variation of C_o (the ratio of the backscatter coefficient to attenuation coefficient) on lidar signal interpretation. Aside from these, which are of primary importance, the development of the author's interpretation scheme, because of its many advantages, needs to be completed and the independent observations of both Uthe and Evans, that interpretation from a near-side boundary condition remains stable at greater depths than one would expect, should be investigated. Finally, the development of any new interpretation scheme should include an investigation of its sensitivity to variation in C_o.

D. THE VARIATION OF C_2 AND THE VARIATION OF C_o AND ITS EFFECT

VARIATION OF C_2

The theory of all the interpretation techniques discussed in Section C, whether near-side or far-side boundary condition techniques, whether used in optically thick or optically thin smoke/obscurants or tracer clouds, is based on the assumption that the parameter C_2 is constant on a lidar-beam path within a cloud or plume. The quantity C_2 is defined by Equation (9) as

$$C_2 = C_1 C_o / 2 \tag{9}$$

where C_1 contains all the lidar performance parameters and C_o is the ratio of the backscatter coefficient at a point in the cloud to the attenuation coefficient at the same point.

When the constancy of C_2 is used with Equation (10)

$$I(L) = -C_2 \frac{d}{dL} T^2(L) \ , \tag{10}$$

an integration of the lidar signal I(L) from the closest distance (L_o) at which a useful signal is obtained, along the lidar beam path to the other side of the cloud gives

$$\int I(L)\, dL = C_2(1 - T^2) \tag{27}$$

where $T(L_o) = 1$ (no cloud at distance L less than L_o) and T is the transmittance through the cloud. The data we will use is given in terms of the

optical depth τ where

$$\tau = -\ln T \quad , \qquad (\text{illegible})$$

so the form of Equation (27) we will use is

$$\int I(L)\, dL = C_2(1 - e^{-2\tau}) \quad . \qquad (\text{illegible})$$

In the data we will use, the optical depth τ arises from the measurement of the transmission T obtained by observing the lidar signal from a surface on the other side of the cloud. The lidar was directed at the surface throughout the test. The parameter C_2 is unknown and we will allow ourselves to adjust it to obtain the best fit of Equation (29) to the data. The data we will use was obtained by [illegible] from SRI (Uthe, 1983).

Comparison of theory and data are shown in Figures 8 and 9. Where non-zero mean optical depth [illegible] with the simultaneous occurrence of integral lidar signals of [illegible] we have not hesitated to shift the optical depth origin, the maximum shift [illegible] equivalent to about 90% transmittance or a drift of [illegible] in the combined laser output power and receiver sensitivity between the clear air calibration and smoke/obscurant data collection. Since we expect multiple scattering to set in at the higher optical depths, we have given greater weight to the fit at the smaller optical depths.

The approximately best fits of Equation (29) to the data of Figures 8 and 9 are indicated by the solid curves in those figures.

Some indication of multiple scattering effects may be present (consider the plot on the right in Figure 9). Multiple scattering effects will show u

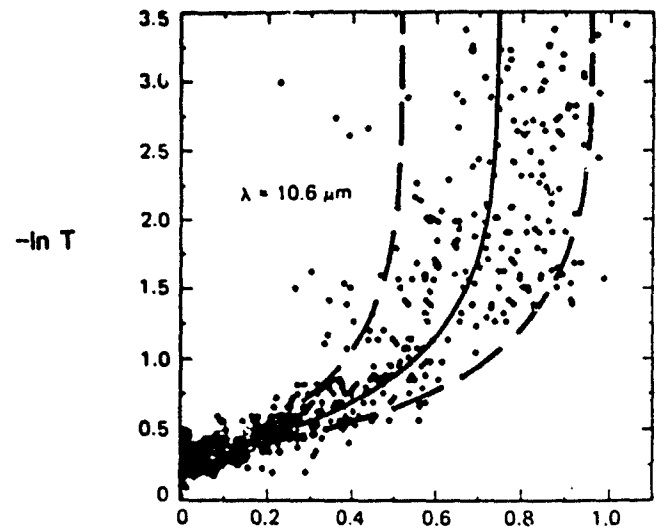

FROM UTHE, SRI
(ADAPTED)

FIGURE 8. Lidar data and theory comparison for a phosphorus smoke clou

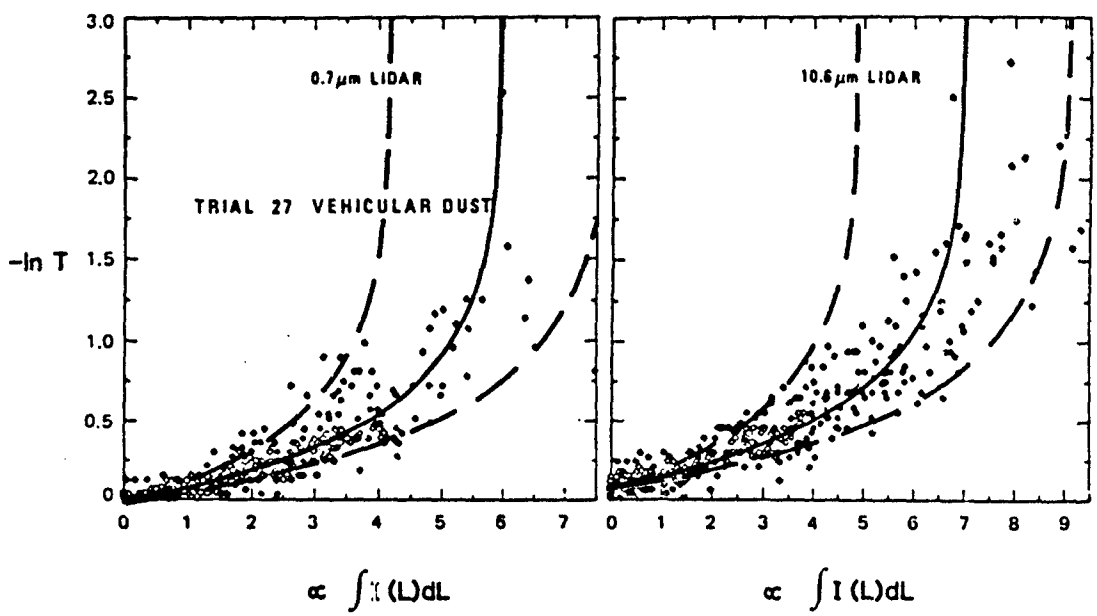

FROM UTHE, SRI
(ADAPTED)

FIGURE 9. Lidar data and theory comparison for a vehicular dust cloud

as an increase, at higher optical densities (higher -ln T), of the mean of the integrated-lidar-signal data beyond the value given by the solid-line fit. (The solid-line fit is a single-scattering fit as the data at lower optical densities were heavily weighted in obtaining it. The multiply-scattered radiation adds to the singly-scattered radiation and causes an increase in the integrated lidar signal, $\int I(L)dL$, beyond that due to single scattering alone. Multiple scattering is discussed in a later section.)

The major feature of the comparisons of theory and data in Figures 8 and 9, however, is the scatter in the data. Plotted as dashed curves, for purposes of comparison, are the theoretical relationships [Equation (29)] with C_2 varied by ±30%. Except for the relatively small amount of scatter which shows up in the lower left portion of the curves (which may be due to errors in measuring T), the data scatter is well fit by fluctuations in C_2.

Similar C_2 variation is observed with other lidar systems.

How much of the variation in C_2 is a lidar instrument effect (variation in C_1), and how much of the variation is a smoke/obscurant effect (variation in C_o) is not known. If the variation is a lidar effect, it can be corrected or compensated, but if a substantial amount of the large amount of scatter around the single curve obtained from theory seen in Figures 8 and 9 is due to variation of C_o during a trial, serious trouble may well be indicated. If the value of C_o obtained over a fixed lidar-beam path varies during a trial, C_o almost certainly varies spatially, causing C_o to generally vary along individual lidar-beam paths through the cloud and thereby causing C_2 to vary along these paths also, even if an ideal lidar is used, in contradiction to the basic assumption of the theory on which the interpretation of the lidar signal is based. Furthermore, if the large amount of scatter in Figures 8 and 9 is due substantially to variation in C_o, and unsystematic variation in C_o, the variation in C_o along lidar-beam paths might well be large enough to have serious consequences.

VARIATION IN C_o AND ITS EFFECT

Two aspects need to be known. Namely, how large is the variation in C_o along lidar-beam paths in the different smoke/obscurants at lidar wavelengths, and what is the effect of such variations (as minimum variations in C_2) on the interpretation of the lidar signal and its usefulness?

VARIATION IN C_o. Current data does not begin to answer the question of how large the variation of C_o is along potential beam paths at different wavelengths in the various smoke/obscurants and smoke/obscurant candidates. See Appendix C. There is a good indication that in natural water clouds there will be a much greater tendancy to have C_o variation along a path with 10.6 μm radiation than with visible or near-IR radiation. There is some data on C_o at 0.9 μm obtained by Sztankay's group at HDL in a few obscurants at Smoke Week III (see Appendix C), but there is no indication as to how much of the variation observed is instrument effect and how much is C_o variation.

The use of current lidars can be very valuable in collecting the much needed information on C_o variation. This can be done by demonstrating that a low maximum variation in C_1 can be expected for a lidar during a trial (immediate pre-trial and post-trial demonstrations would be ideal) and then obtaining the variation of C_2 with time in the smoke/obscurant cloud during that trial, as in Figures 8 and 9. Wind velocity relative to the lidar beam direction will then help give some idea of the spatial variability of C_o in that cloud.

EFFECT OF VARIATION IN C_o. No one has published any information on the effects of the spatial variation of C_o on the ability to obtain quantitative data by lidar using the current interpretation techniques. Kohl (1978) has

indicated that a very small change in C_o could have very disastrous effects, but the author has also seen cases where the effect does not appear to be too large.

The author has begun an investigation of the effect of spatial variation of C_o on the various, current interpretation techniques, under the sponsorship of ASL. Hopefully, he will be able to investigate the effects of a varying C_o on his new interpretation approach also. It is understood that Jim Klett is investigating the same subject, but from a different point of view (Measure, 1984).

Between these efforts it can be hoped that a good idea of the effects of varying C_o on the various lidar signal interpretation techniques will be obtained and that this will spur on the answering of the other half of the question--how much variation of C_o in smoke/obscurants is there?

RECOMMENDATIONS

If theoretical efforts yield understanding of the sensitivity of current and developing lidar interpretation techniques to variation in the ratio of the backscatter coefficient to the attenuation coefficient, C_o, then all effort should be put forth in using the current lidars, particularly those at each wavelength shown to be suitable, to obtain an idea of the variation of C_o at different wavelengths in different obscurants and obscurant candidates. There are indications that such information will make or break the application of the current (and developing) lidar signal interpretation techniques of the type described in Section C.

Finally, the research community (i.e., Stuebing) should be approached to see if an understanding of the potential for variation of the backscatter to attenuation coefficient ratio [and other property relationships] exists or can be obtained at various lidar wavelengths for smoke/obscurants and smoke/obscurant candidates as a function of the particle composition, particle shape and shape distribution, and particle size distribution, building on the work of Pinnick et al (1983) and others cited in Appendix C.

E. ON THE POSSIBILITY OF USING SCATTERING BY THE ATMOSPHERIC GASES IN SMOKE/OBSCURANT CLOUDS

IF THE C_o OF A SMOKE VARIES TOO MUCH, WHAT THEN?

Should variation of the ratio of the backscatter coefficient to the attenuation coefficient in some or all smoke/obscurants not allow adequate quantitative use of lidar radiation which is both attenuated and backscattered by the smoke/obscurant cloud, the use of other possibilities needs to be explored. One of these is to replace the smoke/obscurant cloud with a substitute more amenable to use with a lidar. This is described in the section on tracers below. But there are other possibilities which might not require the replacement of the smoke/obscurant cloud as normally generated in the field. These are discussed here.

Reconsider the completely general single-scattering form of the lidar equation with any beam geometry, G(L), effects compensated via Equation (3),

$$I(L) = C_1 \beta(L) T^2(L) \qquad (4)$$

where β describes the (local) backscattering properties and T describes the (path-length) attenuating properties of the atmosphere through which the lidar radiation is traveling.

As discussed toward the end of Section B, to remove the ambiguity between the effect of $\beta(L)$ and the effect of $T^2(L)$ on the lidar signal (and thereby to be able to recover either the backscatter or the attenuation properties from the lidar signal) the spatial dependence of either $\beta(L)$ or $T^2(L)$ must be

known, or some relationship must be known to exist between the backscatter and attenuation properties affecting the lidar signal. If too large a spatial variability is found to exist in C_o, the latter possibility is destroyed. This leaves only the possibilities of knowing the spatial dependence of $T(L)$ or $\beta(L)$.

CONSIDERATION OF THE TRANSMITTANCE. The only way known to the author to know the spatial dependence of $T(L)$ in the presence of a cloud is to have $T(L) \cong 1$ for all L, or, more to the point for Equation (4) above, $T^2(L) \cong 1$ for all L. (This is the basis for one type of tracer approach.) For a particular type of smoke/obscurant, it may be possible to find a wavelength that is essentially unattenuated and thus obtain $T^2=1$. But, it cannot be stated as generally possible due to the general effect of volumetric absorption by the particulate material at long wavelengths where scattering tends to be decreased, and the effect of the finite cross section of the particles themselves at all other wavelengths. So, keeping the smoke/obscurant itself unaltered, it is very unlikely that use of $T^2=1$ can be generally applied.

CONSIDERATION OF BACKSCATTERING. Besides scattering from the particles of a smoke/obscurant cloud, the only other scattering taking place in such a cloud is the scattering from the ambient or non-cloud aerosol particles and the scattering from the gases of the atmosphere. Such scattering which takes place with a wavelength shift (Doppler shift or Raman shift) relative to the wavelength scattered from the smoke/obscurant cloud itself has properties which might allow it to be detected. (These are discussed below.)

BACKSCATTERING FROM NON-CLOUD AEROSOLS. The spatial dependence of the backscattering coefficient for scattering from any non-cloud aerosol particles will not be a known quantity in the smoke/obscurant cloud as one cannot count

on it being an instantaneously uniform quantity (a constant in L) during a trial, particularly with the activities that accompany some obscurant generation.

Further, the velocities of non-cloud particles would be the same (i.e., wind) velocities of the cloud particles, and Doppler-shift wavelength discrimination could not work. The nature of the ambient aerosol certainly could not be relied on where this nature might be utilized for wavelength shifting by Raman scattering, and the generation of a uniform (well-mixed), special, Raman scattering aerosol upwind of the trial location, so as to engulf and permeate the smoke/obscurant cloud, would not appear to be feasible even if voids in such an aerosol caused by the smoke/obscurant generation could be neglected.

It appears, therefore, that it is not feasible to use ambient or introduced aerosols in order to obtain a wavelength-shifted lidar signal arising from a backscatter coefficient of known or constant spatial distribution.

BACKSCATTERING FROM ATMOSPHERIC GASES. The major constituent atmospheric gases, in particular the major component, nitrogen, are well-mixed and uniform in the field and their backscatter exhibits both Doppler-shifted and Raman-shifted wavelengths relative to the wavelengths obtained from backscattering by particles or droplets. The difficulty in their use is that their backscatter coefficients are orders of magnitude smaller than those of aerosols. Put a little imprecisely, one will be using the blue-of-the-sky scattering (and less) from the midst of the smoke cloud.

LIDAR EQUATION USING SCATTERING BY ATMOSPHERIC GASES

The single-scattering lidar equation, Equation (4), when backscattering by the atmospheric gas is used under the conditions of smoke trials takes the form

$$I(L) = C_1 \beta_g T^2(L) . \qquad (30)$$

In Equation (30) C_1 refers to the emission of the laser wavelength and the detection of the scattering-shifted wavelength.

The quantity β_g is the backscatter coefficient for the process being considered. It is proportional to the density of the atmospheric gas and so is proportional to the ratio of pressure to absolute temperature. Pressure correction will be negligible over altitudes several times those typical of smoke clouds. An estimated temperature correction within a cloud may be required in the very early stages of a smoke/obscurant cloud formed explosively or exothermically as a temperature rise of 15° C implies an error of 5%.

The quantity $T^2(L)$ in Equation (30) is actually the product of the laser wavelength transmittance on the way out to the scattering point and the scattered wavelength transmittance on the way back. (The attenuation coefficient recovered at each point is the average of these two attenuation coefficients at that point.)

Before considering (to a limited extent) the possibilities of using the Doppler-shifted and Raman scattering processes, there are some experimental error aspects that need to be considered in recovering attenuation coefficient information from an equation of the form of Equation (30).

RECOVERING $\sigma(L)$ FROM A LIDAR EQUATION OF THE FORM
$I(L) = C_3 T^2(L)$

A lidar signal arising from an equation of the form of Equation (4) with Equation (8) and (9) substituted and with constant C_2 (i.e., the lidar signal of Section C), namely,

$$I(L) = 2C_2 \sigma(L) T^2(L) , \tag{31}$$

is a signal which is determined by the local attenuation coefficient value at distance L, modified by the transmittance from the lidar to L. A lidar signal arising from an equation of the form of Equation (30), that is, arising from the form

$$I(L) = C_3 T^2(L) , \tag{32}$$

is a signal which, though it comes from distance L does not depend on the attenuation coefficient value there but depends only on the transmittance from the lidar to L, so that the effect of the attenuation coefficient at a distance L is only seen in a parameter (T^2) in which the effects of the attenuation coefficient values from all other positions along the lidar beam path are also seen simultaneously. (While this is somewhat of a disadvantage, use of Equation (32) does not require a boundary condition, and never requires determining a calibration factor or having a cloud free region in the lidar beam.)

Use of Equation (32) to recover $\sigma(L)$, therefore, requires some different considerations compared to using Equation (31).

SOLUTION FOR σ. Let $\bar{\sigma}(L, L + \Delta L)$ be the average value of $\sigma(L)$ from distance L to $L + \Delta L$ out the lidar-beam path, that is,

$$\bar{\sigma}(L, L + \Delta L) = \frac{1}{\Delta L} \int_{L}^{L+\Delta L} \sigma(L') \, dL' \quad . \tag{33}$$

Note that as ΔL goes toward zero, $\bar{\sigma}$ goes to $\sigma(L)$, but, as we shall see from experimental error considerations, we will generally not want ΔL to be too small and ΔL at this point in our development can be any length, it is not differentially small.

Using $T(L, L + \Delta L)$ to denote, as in Section C, the transmittance from L to $L + \Delta L$, that is,

$$T(L, L + \Delta L) = e^{-\int_{L}^{L+\Delta L} \sigma(L') \, dL'} \tag{34}$$

[so $T(L) \equiv T(0, L)$], we have

$$\int_{L}^{L+\Delta L} \sigma(L') \, dL' = - \ln T(L, L + \Delta L) = - \ln \frac{T(L + \Delta L)}{T(L)} = - \ln \left[\frac{I(L + \Delta L)}{I(L)} \right]^{\frac{1}{2}} \tag{35}$$

where the last equality uses Equation (32). Therefore, $\bar{\sigma}$ of Equation (33) can be written in terms of the lidar signal of Equation (32) as

$$\bar{\sigma}(L, L + \Delta L) = - \frac{1}{2\Delta L} \ln \frac{I(L + \Delta L)}{I(L)} \quad . \tag{36}$$

RELATIVE EXPERIMENTAL ERROR IN $\bar{\sigma}$. Define the measured lidar signal as

$$I^m(L) = I(L) + \Delta I(L) \ , \tag{37}$$

where $I(L)$ is the ideal signal without error and $\Delta I(L)$ is the experimental error in $I^m(L)$. Define the relative experimental error in $\bar{\sigma}(L, L + \Delta L)$ as

$$\text{Rel. Error in } \bar{\sigma} \ = \ \frac{\bar{\sigma}^m - \bar{\sigma}}{\bar{\sigma}} \ , \tag{38}$$

where $\bar{\sigma}^m$ is $\bar{\sigma}$ calculated with measured lidar signals, I^m, and $\bar{\sigma}$ is calculated with the ideal lidar signals, I. From Equations (37) and (38) the relative experimental error in $\bar{\sigma}$ can be expressed as

$$\text{Rel. Error in } \bar{\sigma} \ \approx \ \frac{1}{2\bar{\sigma}\Delta L} \ \frac{[-\Delta I(L+\Delta L)\, e^{2\bar{\sigma}\Delta L} + \Delta I(L)]}{I(L)} \ , \tag{39}$$

where Equations (32), (33), (34) and (36) and $|\Delta I(L)/I(L)| << 1$ were used in the derivation.

Exactly how the expected relative error in $\bar{\sigma}$ (the typical relative error) depends on the expected relative error in the lidar signal, $\Delta I(L)/I(L)$, depends on the type of experimental (non-ideal) error that is dominant in the lidar signal--whether it is systematic and independent of I and L, random and independent of I and L, photon signal noise or speckle noise--but one can see from Equation (39) some general trends.

At small ΔL (in particular small ΔL compared to the attenuation length or small $\Delta L/\bar{\sigma}^{-1}$), the magnitude of the relative error in $\bar{\sigma}$ will diverge to

infinity relative to the error in the lidar signal as ΔL gets smaller. This is due to the first factor on the right in Equation (39). This may well have severe consequences as $\bar{\sigma}^{-1}$ is a physical scale length over which the transmittance changes appreciably and it may be that, in order to be useful, knowledge of the spatial dependence of σ may be required on a scale small compared to $\bar{\sigma}^{-1}$. Only if the dominant error in the lidar signal at small ΔL is a constant systematic error, independent of I and L, will the relative error in $\bar{\sigma}$ not blow up as ΔL is made smaller.

At large ΔL, that is $\Delta L/\bar{\sigma}^{-1}$ larger than 1, the relative error in $\bar{\sigma}$ may also diverge as ΔL gets larger due to the first term in square brackets in Equation (39) if ΔI is not very dependent on L. (This arises because $I(L + \Delta L)$ gets significantly smaller than $I(L)$ under such conditions.) This should not be much of a problem as, as we remarked above, our interest will be in knowing σ on a spatial scale (ΔL) of about $\bar{\sigma}^{-1}$ or smaller.

AN EXAMPLE OF THE REQUIREMENTS ON THE EXPERIMENTAL ERROR IN THE LIDAR SIGNAL AS A FUNCTION OF THE DESIRED SPATIAL RESOLUTION. To illustrate the potential problems related to spatial resolution and arising from experimental error in the lidar signal in recovering $\bar{\sigma}$ from a lidar equation of the form of Equation (32), we give an example. As Equation (32) should most often arise in situations where the backscattering is not strong (in this section, Section F, scattering from the atmospheric gas is being considered), we take the dominant error to be one appropriate to this situation and consider the dominant error to be due to photon noise in the signal (applicable to a case below). This noise occurs with very low radiation levels and is due to the randomness of the arrival of the photons in a radiation stream.

The required maximum relative experimental error in the lidar signal, where this error is dominated by photon noise, is shown in Table II for

two possible values of required spatial resolution, ΔL = 6 meters and ΔL = 1 meter (obtained in the section on spatial resolution below), for a desired 5% error in the obtained value of $\bar{\sigma}$ (the average of the attenuation coefficient, σ, over ΔL) [see the section on the desired accuracy in σ]. The required maximum lidar signal error is proportional to the error in $\bar{\sigma}$ desired and so the values of Table II can be readily converted to any other desired error in $\bar{\sigma}$. Other than where the dominant experimental error in the lidar signal at the indicated ΔL is a constant systematic error, independent of the lidar signal and distance L, the requirements for all types of lidar signal error will be the same as those of Table II for $\bar{\sigma}\Delta L$ less than 1.

The first column of Table II is meant to put the $\bar{\sigma}$ values used in the table in the rough perspective of transmittance across a somewhat typical cloud size.

TABLE II. REQUIREMENTS ON THE EXPERIMENTAL ERROR IN A LIDAR SIGNAL PROPORTIONAL TO T^2 (ONLY)

TRANSMITTANCE ACROSS A UNIFORM CLOUD 50 METERS WIDE WITH $\sigma = \bar{\sigma}$	AVERAGE ATTENUATION COEFFICIENT ($\bar{\sigma}$) OVER DISTANCE ΔL (in m^{-1})	SPATIAL RESOLUTION (ΔL) OF 6 METERS:		SPATIAL RESOLUTION (ΔL) OF 1 METER:	
		$\bar{\sigma}\,\Delta L$	REQUIRED MAXIMUM ERROR IN THE LIDAR SIGNAL*	$\bar{\sigma}\,\Delta L$	REQUIRED MAXIMUM ERROR IN THE LIDAR SIGNAL*
0.5	1.39×10^{-2}	8.3×10^{-2}	0.56%	1.39×10^{-2}	0.097%
10^{-1}	4.61×10^{-2}	2.8×10^{-2}	1.7%	4.61×10^{-2}	0.32%
10^{-2}	9.21×10^{-2}	0.55	2.8%	9.21×10^{-2}	0.62%
10^{-3}	1.38×10^{-1}	0.83	3.3%	0.14	0.91%
10^{-4}	1.84×10^{-1}	1.11 **	3.5% **	0.18	1.2 %
10^{-5}	2.30×10^{-1}	1.38	3.4%	0.23	1.4 %

*For 5% error desired in the lidar-determined attenuation coefficient. The lidar signal error is proportional to the desired error.

**Large $\bar{\sigma}\Delta L$ effects begin to dominate.

From Table II it can be seen that if the required spatial resolution is 6 meters the situation does not look too bad at all, the required experimental error on the lidar signal is only slightly reduced from the desired error on the lidar-determined attenuation coefficient value, much as with the lidar signals of Section C. If the spatial resolution required is 1 meter, however, the situation appears bleak.

Depending on the situation, the lower transmittance values of Table II may not be reached before other limitations are encountered. These are discussed in Sections F and G below.

ON THE USE OF DOPPLER-SHIFTED (CABANNES) SCATTERING FROM THE ATMOSPHERIC GAS

The largest amount of scattering per molecule of atmospheric gas is found in the elastic or Cabannes scattering [and until lately also called Rayleigh scattering (Young, 1980 & 1982)] where the wavelength of the radiation backscattered to the lidar by a molecule is simply Doppler shifted by the velocity of the molecule. The velocity distribution of the molecules gives rise to the spectrum of this backscattered radiation. The mean is shifted by the wind velocity, the mean vector velocity of the molecules, but the width, with perfectly monochromatic radiation incident, arises from the much higher thermal velocities of the molecules, approximately characterized by the speed of sound, about 300 meters per second. The spectrum of the Doppler-shifted radiation backscattered by the aerosol particles has its mean also shifted by the wind velocity but its width, with perfectly monochromatic radiation incident, arises from the spread of the wind turbulence velocities within the instantaneous sensitive volume of the lidar, a spread of the order of 1 meter per second.

The problem with using the Cabannes scattering from the atmospheric gas within a smoke/obscurant cloud is that the scattering by the aerosol in a volume element in a cloud will be several factors of 10 larger than the Cabannes scattering from the same volume element and will be situated in the middle of and very close, spectrally, to all significant amounts of Cabannes scattering in comparison to the spectral width of typical lidar sources and receivers.

The spectrum of backscattered radiation in clear air, with about the same amount of aerosol scattering as molecular scattering, is shown in Figure 10 as observed with a recent, specially built high spectral resolution lidar (Shipley, Tracy, Eloranta, Trauger, Sroga, Roesler and Weinman, 1983 and Sroga, Eloranta, Shipley, Roesler and Tryon, 1983). The contributions of the central, aerosol backscattering spike and the broader bandwidth molecular backscattering can be seen in Figure 10. The width on the aerosol spike in Figure 10 is entirely due to the combined spectral widths of the lidar source and receiver, as the width due to the aerosol itself would not be discernable on the scale of Figure 10, being more on the order of 10^{-2} m^{-1}. (The instrument spectral width also makes a good-sized contribution to the Cabannes-scattering spectral width.)

It is spectral rejection by the instrumentation that is important in order to be able to observe the Cabannes scattering from the atmospheric gas within a smoke/obscurant cloud. With the lidar receiver slaved to observe the Cabannes-scattered radiation, say, 5 mA° away from the incident wavelength of the laser transmitter, the receiver must have a responsivity down several orders of magnitude only 5 mA° away from its detected wavelength so as to block the much larger amount of radiation scattered by the cloud aerosol. Further, the lidar transmitter must not emit radiation only 5 mA off of its central frequency in

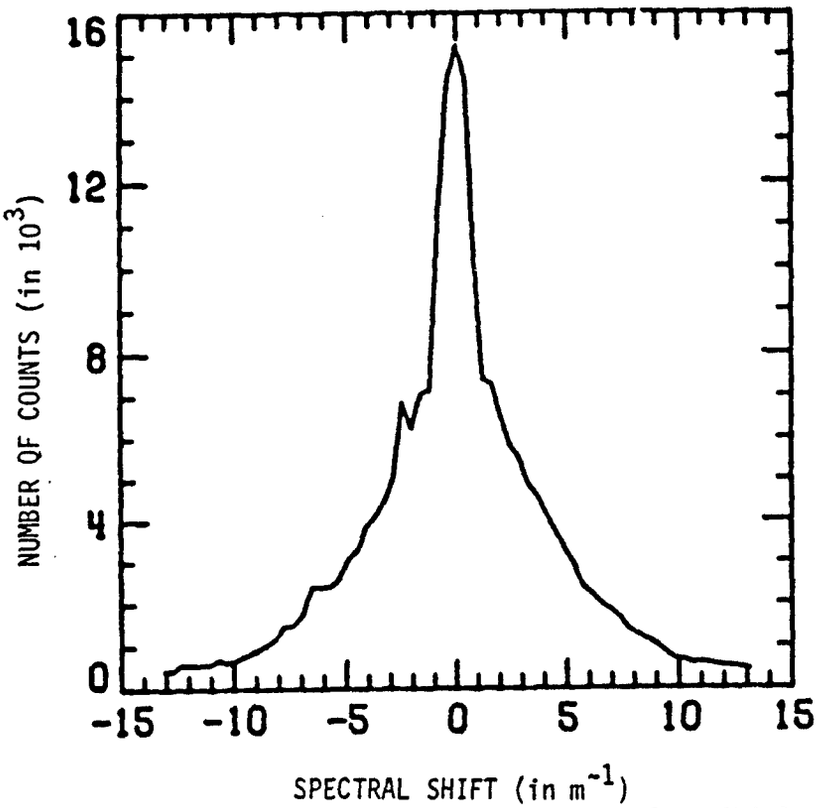

from Shipley et al,
U. of Wisconsin

Figure 10. Spectrum of light backscattered from a clear atmosphere near 467.8 nm (4678 A°, 2.14 x 10^6 m^{-1} or 6.41 x 10^{14} Hz) as observed by a high spectral resolution lidar. A spectral shift of 10 m^{-1} corresponds here to 22 mA°, 0.0022 nm or 3 GHz. From (Shipley et al, 1983).

the direction of the receiver's spectrally sensitive region to avoid mixing an aerosol backscattering signal with the Cabannes backscattering signal.

Such severe spectral requirements tend not to be consistent with high laser output powers, and, for example, the spectrum of Figure 10, despite being a clear-air spectrum, was obtained using photon counting for 2.5 seconds at each abscissa point with the photons returning from a 600 meter range increment of clear atmosphere.

(If one can develop an appropriate two-channel lidar, one channel to observe the aerosol scattering and one to observe the Cabannes scattering, and then obtain and maintain the calibrations required, the measured ratio of the aerosol to Cabannes backscattering coefficients along with the knowledge of the Cabannes backscattering coefficient from pressure and temperature measurements can give the backscatter coefficient of the aerosol (Shipley et al, 1983). For use in smoke/obscurants, however, such an approach would probably be less desirable than using that of Equation (36), which requires only one channel, no calibration beyond knowledge of G(L) and which produces a more useful smoke/obscurant property, the attenuation coefficient.)

No feasibility study has been attempted here. The basis for the use of the Cabannes or elastic [Rayleigh] scattering is given along with indications of where difficulties will be found to lie. Note that the limiting difficulties appear to be in the instrumentation, not in the principles involved, though the difficulties appear to be considerable.

ON THE USE OF RAMAN SCATTERING

In addition to elastic or Cabannes backscattered radiation from the molecules of the atmospheric gas, which leaves the molecules in the same

internal energy state as before, there is some backscattered radiation which leaves some energy behind, called Raman scattering. Here, at first, we will consider the Raman scattering which leaves energy behind in the form of increased vibrational energy in the predominant (78%) nitrogen gas molecules of the atmosphere. (There is typically, roughly 10^{-3} less of this type of scattering compared to Cabannes scattering.) The photons of the radiation so backscattered have each lost energy and so have their frequency decreased (by 2,331 cm^{-1}) or their wavelength increased (about 1,340 A° with ruby laser radiation incident at 6,943 A°). The resultant spectral separation of the radiation thus backscattered by the atmospheric nitrogen and the radiation backscattered by a smoke/obscurant cloud make a lidar operating on Raman-scattered radiation easier to build, currently, than one operating on the Cabannes scattered radiation, despite the relatively reduced amount of the former type of scattering in the typical, non-resonant case.

Despite the decreased spectral constraints, the problem of having a scarcity of photons will have to be dealt with in trying to utilize Raman scattering to get desirable smoke/obscurant attenuation coefficient results. For purposes of the illustration of this point, we use the results of a previous feasibility study (Lamberts and Dekker, 1975) and push the capabilities cited there even further. Lamberts and Dekker considered a ruby-laser lidar detecting the majority of the vibrational Raman backscattering from nitrogen (N_2), the backscattering due to the vibrational Raman transition in N_2 with no change in N_2 rotational state (Q branch or $\Delta v=1$, $\Delta J=0$).

We first note that the major, inherent noise contribution in approaching desirable performance will be signal-photon fluctuation noise rather than

background-photon fluctuation noise. Using the Lamberts and Dekker (1975) value of about 120 background photons from a sunlit natural water cloud (worst case) detected by a pulsed lidar of 50 feet spatial resolution, but going to 6 meters spatial resolution, gives about 47 background photons, N_B, per lidar spatial resolution element. However, with no more than a 3.5% error allowed in the lidar signal (see Table II above), the minimum average number of detected signal photons (the minimum N_T) required is determined by taking the ratio of the typical photon number fluctuation to the average or expected number of signal photons, which ratio is $\sqrt{N_T+N_B}/N_T$, and setting that ratio equal to 0.035, from which the minimum value of $N_T \cong 850$ is obtained. Thus we can ignore the background photon contribution to the photon fluctuation or uncertainty per spatial resolution element (even though we must subtract off the average background photon flux from the total flux detected, which is the background flux plus the signal flux).

We will use below, Lamberts and Dekker's number of N=9,000 detected photons obtainable in backscatter from 300 m range in clear air using a 15 J ruby-laser pulse but assume this can be obtained in a smaller pulse width of 6 meters spatial resolution. Further, without investigating the current feasibility, we assume we can get the same number of photons output by a lidar transmitter operating at half the wavelength (a 30 J per pulse lidar!) in order to take advantage of the $1/\lambda^4$ efficiency factor in Raman non-resonant scattering, increasing N by 16 times. (The number of background photons from a sunlit cloud at the new [near UV] wavelength is essentially the same.)

We then calculate the minimum transmittance allowed by photon scarcity considerations as follows: the inherent minimum number of detected signal photons, N_T, per spatial resolution element required by a given value of

the required maximum relative error in the lidar signal (Table II) is found by setting the relative error in the lidar signal, $\sqrt{N_T}/N_T$, to that value. The ratio of this N_T to the clear air value of N then gives the square of the minimum transmittance, T, which the Raman-lidar radiation may encounter between the lidar and a scattering position without having the number of photons detected drop below N_T.

The discouraging results are shown in Table III. The boxed values indicate where the minimum transmittance is already above the cross-cloud transmittance of a 50 meter cloud of the same, uniform attenuation coefficient as that which gives rise to the lidar error requirement. Even with 50% error in the lidar-determined attenuation coefficient (10 times the value used in Table III) and with 6 meters spatial resolution the cross-cloud transmittance cannot be much below about 10^{-2}.

TABLE III. MINIMUM CLOUD TRANSMITTANCE VALUES FOR A NEAR-UV RAMAN LIDAR USING THE VIBRATIONAL TRANSITION ($\Delta v=1$, $\Delta J=0$) IN THE NITROGEN OF THE ATMOSPHERIC GAS

TRANSMITTANCE ACROSS A UNIFORM CLOUD 50 METERS WIDE WITH $\sigma = \delta$	AVERAGE ATTENUATION COEFFICIENT (δ) OVER DISTANCE ΔL (in m^{-1})	SPATIAL RESOLUTION (ΔL) OF 6 METERS: REQUIRED MAXIMUM ERROR IN THE LIDAR SIGNAL*	SPATIAL RESOLUTION (ΔL) OF 6 METERS: RESULTANT MINIMUM TRANSMITTANCE**	SPATIAL RESOLUTION (ΔL) OF 1 METER: REQUIRED MAXIMUM ERROR IN THE LIDAR SIGNAL*	SPATIAL RESOLUTION (ΔL) OF 1 METER: RESULTANT MINIMUM TRANSMITTANCE**
0.5	1.39×10^{-2}	0.56%	.47	0.097%	***
10^{-1}	4.61×10^{-2}	1.7%	1.6×10^{-1}	0.32%	.82
10^{-2}	9.21×10^{-2}	2.8%	9.4×10^{-2}	0.52%	.43
10^{-3}	1.38×10^{-1}	3.3%	8.0×10^{-2}	0.91%	.29
10^{-4}	1.84×10^{-1}	3.5%	7.5×10^{-2}	1.2 %	.22
10^{-5}	2.30×10^{-1}	3.4%	7.8×10^{-2}	1.4 %	.19

*From Table II, for 5% error desired in the lidar-determined attenuation coefficient. The lidar signal error is proportional to the desired error.

**The minimum transmittance is inversely proportional to the maximum lidar signal error.

***Cannot be met even at a transmittance of 1.

Adapting the above near-UV lidar to use the purely rotational Raman transitions in the nitrogen of the atmosphere [which produce about 50 times more scattering than the vibrational Raman transition (Melfi, 1970)] gives the results shown in Table IV. These are a bit more encouraging. However, the spectral region which must be observed comes within a few Angstroms of the scattering from the cloud and rejection of the large amount of scattering from the cloud must be achieved, though it would not be as difficult as it would be in trying to observe Cabannes [Rayleigh] scattering. (The lidar-observed spectral width would have to be increased to observe the purely rotational Raman scattering, but neglecting background photon fluctuations still only introduces an error in the minimum transmittance which is 12% at its worst in Table IV.)

There are other approaches that can be tried.

TABLE IV. MINIMUM CLOUD TRANSMITTANCE VALUES FOR A NEAR-UV RAMAN LIDAR USING THE ROTATIONAL TRANSITIONS ($\Delta v=0$, $\Delta J=\pm 2$) IN THE NITROGEN OF THE ATMOSPHERIC GAS

TRANSMITTANCE ACROSS A UNIFORM CLOUD 50 METERS WIDE WITH $\sigma = \bar{\sigma}$	AVERAGE ATTENUATION COEFFICIENT ($\bar{\sigma}$) OVER DISTANCE L (in m^{-1})	SPATIAL RESOLUTION (ΔL) OF 6 METERS: REQUIRED MAXIMUM ERROR IN THE LIDAR SIGNAL*	SPATIAL RESOLUTION (ΔL) OF 6 METERS: RESULTANT MINIMUM TRANSMITTANCE**	SPATIAL RESOLUTION (ΔL) OF 1 METER: REQUIRED MAXIMUM ERROR IN THE LIDAR SIGNAL*	SPATIAL RESOLUTION (ΔL) OF 1 METER: RESULTANT MINIMUM TRANSMITTANCE**
0.5	1.39×10^{-2}	0.56%	6.7×10^{-2}	0.097%	.38
10^{-1}	4.61×10^{-2}	1.7%	2.2×10^{-2}	0.32%	1.2×10^{-1}
10^{-2}	9.21×10^{-2}	2.9%	1.3×10^{-2}	0.62%	6.0×10^{-2}
10^{-3}	1.38×10^{-1}	3.3%	1.1×10^{-2}	0.91%	4.1×10^{-2}
10^{-4}	1.84×10^{-1}	3.5%	1.1×10^{-2}	1.2 %	3.1×10^{-2}
10^{-5}	2.30×10^{-1}	3.4%	1.1×10^{-2}	1.4 %	2.7×10^{-2}

*From Table II, for 5% error desired in the lidar-determined attenuation coefficient. The lidar signal error is proportional to the desired error.

**The minimum transmittance is inversely proportional to the maximum lidar signal.

SUMMARY AND RECOMMENDATIONS

If an insufficient relationship should be found to exist between the backscatter and attenuation properties of a smoke/obscurant, so that adequate interpretation of lidar radiation which has been both backscattered and attenuated by the smoke/obscurant cannot be achieved, investigation of the means of obtaining lidar measurements of a local optical property of the smoke/obscurant leads, apparently solely, to consideration of the use of scattering by the atmospheric gas.

The reasonable form of the lidar equation for use with scattering from the atmospheric gases implies the need, if the desirable 5% error in the lidar-determined attenuation coefficient is to be achieved, for experimental error limits which are extremely stringent if 1 meter resolution along the lidar beam is required, but are not too bad if 6 meter resolution is required, as shown in Table II. (See the section on desired data accuracy and spatial resolution.) Note that this is another reason for knowing what spatial resolution is required.

The two types of scattering from the atmospheric gas that occur are elastic, where the scattered photon leaves the internal energy of the gas molecule unchanged (Cabannes [Rayleigh] scattering), and inelastic, where the photon changes the internal energy of the molecule (Raman scattering). In Cabannes scattering the principle problem is the elimination of the interference by the radiation scattered by the smoke/obscurant. In Raman scattering, in the approaches outlined, the problem is the scarcity of photons, causing insufficient accuracy at typical smoke/obscurant cloud transmittance values. (In both types of scattering, there will be a tendency to utilize shorter wavelengths, λ, to take advantage of the $1/\lambda^4$ dependence of non-resonant scattering, but the shorter wavelengths are also those at which multiple scattering effects are worse (see Section G).)

If the relationship between backscatter and attenuation should be found to be inadquate in some smoke/obscurants, these two types of scattering are apparently the only alternatives short of replacing the smoke/obscurant with a simulant (a tracer) which makes the lidar-determined optical properties at least once removed (and probably several times removed) from the desired optical properties of the smoke/obscurant. (Use of tracers is treated below.) In such a situation, further investigation would be warranted into use of these two forms of scattering by the atmospheric gas, but, as innovation and improvement in the state of the art is required, lidar hardware should not be built for its own sake unless there is a reasonable chance of success--rather, feasibility studies should be made based on existing knowledge or, if progress-preventing gaps exist in that knowledge, these gaps should be filled.

Note alsc that the effects discussed in both sections F and G, the T^2 effects and multiple-scattering effects, will apply to the use of lidars in smoke/obscurants whether scattering from the cloud or scattering from the atmospheric gases is observed.

F. THE T^2 PROBLEM AND THE MEANS OF OVERCOMING IT

For a lidar to obtain information from a point in a smoke cloud, the lidar must send radiation out to that point and then must detect the scattered radiation from that point that arrives back at the lidar site. If the point in question is on the far side of the cloud where the transmittance from the lidar site to that point is $T = 10^{-3}$, then the radiation flux returning to the lidar has undergone a total transmittance from the lidar to the scattering point and back to the lidar of $T^2 = 10^{-6}$. Radiation returning to the lidar from a scattering point on the near side of the smoke cloud, however, undergoes a round-trip transmittance near 1. Thus, from the near side of the cloud to the far side of the cloud, the desirable returning lidar radiation undergoes a relative decrease of T^2, or 10^{-6} in our example, where T is the transmittance through the cloud at the lidar wavelength. This fundamental problem is called the T^2 problem. See Figure 11.

The effects of this problem on data rates are discussed in that section.

Currently, at least, one cannot get around this problem by having lidar radiation which is scattered on the far side of the cloud observed by a receiver also on the far side of the cloud. The latter set-up with transmitter and receiver at two different locations is called a bistatic (two-site) lidar as opposed to the normal configuration where both receiver and transmitter are at the same site, the monostatic lidar. There is not a mathematical inversion technique for bistatic lidar (at least, known to the author) which would be applicable to the completely inhomogeneous situation of a smoke/obscurant cloud. Any such technique conceivable, using scattering from the cloud, would

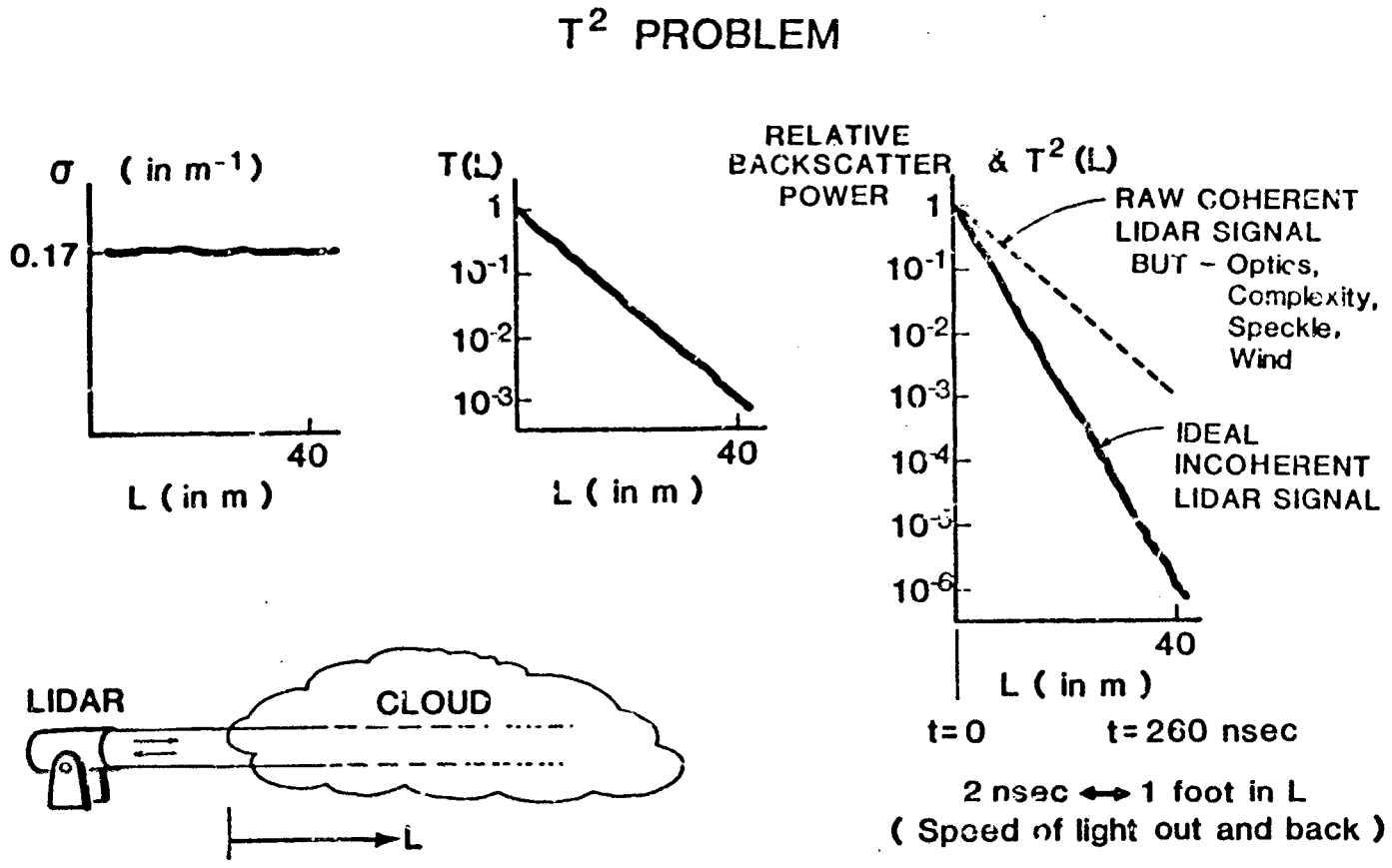

Figure 11. Illustration of the T^2 problem. In this figure L is measured from the near edge of the cloud.

require a scattering coefficient proportional to the attenuation coefficient and a known relative scattering function (phase function) throughout the cloud. See Appendix D.

INCOHERENT LIDAR

The common incoherent lidar, that is, lidar where the detector detects the energy of the scattered radiation, uses a detector with sufficient dynamic range to handle the variation of the signal by T^2 and follows it with a logarithmic amplifier whose output is a logarithm of the input. The dynamic range of the resulting output analog signal is therefore much reduced, enabling the analog-to-digital conversion to be done on this signal so that digital processing of the signal can be done. In the visible and near-IR, silicon avalanche photodiode detectors are used followed by logarithmic amplifiers of dynamic range typically between 10^6 and 10^8. In incoherent lidars operating at 10.6 μm the HgCdTe detector is similarly followed by a logarithmic amplifier before the signal is converted to digital form.

The problem that arises in using incoherent lidars in smoke/obscurant clouds of low transmittance is that the lidar-beam path is interrogated by such pulsed lidars at half the speed of light (the radiation travels at the speed of light out and back). Thus both the signal at the detector output and the signal at the logarithmic amplifier output must sweep through their respective dynamic ranges in a very short time. This is illustrated by the solid line in the plot on the right in Figure 10 for the detector output signal.

With such a rapid, and relatively very large backscattered radiation decrease as undergone by the returning incoherent lidar radiation as it first comes from the near side of a dense cloud and then comes from the far side, there occurs, along with the low, far-side backscattered radiation incident on the detector, the effect of some remaining charge carriers left behind in the semiconductor components of the detector and amplifier(s) from the high, near-side signal. These diffuse out of these components and give rise to a low-level output signal from the detector/logarithmic-amplifier combination which, though it is very, very low compared to the near-side cloud signal, is enough to limit performance at the cloud far-side when smaller, denser cloud regions are present. Nothing has been published yet on these performance limits and not much is yet known, in general, about them. The performance limits are very detector/amplifier system dependent. The decay or recovery times have been observed to be greater with systems detecting 10.6 μm radiation (Uthe, 1984). The performance limitations can not be described by specified component fall times or response times as these are defined as the time for a relative signal decrease of about 0.1 (or $T^2 = 0.1$) while the effect mentioned lasts longer at smaller signal levels.

The manufacturer of the commonly used logarithmic amplifier has found the performance, in this regard, of a silicon avalanche photodetector followed by a logarithmic amplifier to very much limited by the detector (Crawford, 1984).

Data on logarithmic amplifiers alone was available only with input step-downs of about 10^{-3} to 10^{-4} due to the difficulty of obtaining such data. The decay of the logarithmic output of the appropriate amplifier (recovery time is inversely proportional to bandwidth) was found to be approximately

exponential with decay to an output equivalent to a 10^{-3} input change being reached about 30 nanoseconds after a 10^{-4} step-down (Crawford, 1984). Extending such a decay curve to an output of 1.05×10^{-4} (5% error), finds this value being reached at a time corresponding to 17.6 m beyond the step-down of 10^{-4}. A transmittance of 1.05×10^{-4} in 17.6 m would require quite a high average attenuation coefficient, 0.52 m^{-1}, a value which, over a 40 meter cloud such as in Figure 11, would give rise to a cross-cloud transmittance of 10^{-9}. Matching the decay curve at shorter times would require even larger attenuation coefficient values. Thus the logarithmic amplifier performance limitation, itself, would not seem to be very severe.

No data could be obtained from silicon avalanche or HgCdTe detector manufacturers. This is not too strange as the effect would be rarely encountered except in using lidar in optically dense clouds. [Not all manufacturers were questioned.]

In fact, use of a lidar viewing a relatively dense cloud is apparently one of the best ways to observe and measure the phenomenon, as it is difficult to generate the fast, very large signal decrease in other ways. This suggestion arises from observations with the DREV Cloud-Mapper lidar. This lidar is currently undergoing upgrading in hardware and signal processing. In this lidar's earlier form, this signal-level decay phenomenon could be observed as the lidar beam was scanned horizontally across a cloud of high albedo at 1.06 μm which contained a relatively dense region in its interior (Evans, 1984). As the dense region was encountered, if it was dense enough (so as to drop the transmittance to around 0.15 or less), the lidar signal could be seen to continue on into the region behind the cloud, as determined from the apparent back edges of the cloud as seen in the lidar signals

to each side of the direction of the dense region. Therefore, use of a small dense cloud from a nozzle, having a well defined, known, back-edge position, may well be the way to observe, check or measure this effect.

Even photomultipliers contain effects that lead to T^2 type problems as shown in Figure 12.

Use of a lidar well above a smoke cloud, looking down on it, improves the T^2 problem considerably. The uniform 40 meter wide cloud of Figure 11, with transmittance across the cloud of $T = 10^{-3}$ ($T^2 = 10^{-6}$), if 10 meters high has a vertical cross-cloud transsmittance of only $T = .18$ ($T^2 = 3.2 \times 10^{-2}$).

COHERENT LIDAR

In the coherent lidar, the scattered electromagnetic fields are detected rather than the scattered radiation energy or photon flux. Seen from the point of view of the scattering of the electromagnetic field, the incoherent lidar detects the square of the scattered electromagnetic field, E_s^2, which is proportional to the radiation energy, while the coherent lidar detects the scattered electromagnetic field, E_s. Thus, as E_s^2 is proportional to T^2, so E_s is proportional to T, with the result that the dynamic range in the coherent lidar signal from the detector is much reduced (10^{-3} versus 10^{-6} in the example--see the dashed line on the right in Figure 11). Furthermore, the detector signal dynamic range is not covered at half the speed of light, but at the rate at which the focal volume of the coherent lidar is scanned along the lidar-beam path. Analog-to-digital conversion is applied to the coherent lidar detector signal of decreased dynamic range. The digitally obtained, speckle-averaged, DC component of the square of this signal is

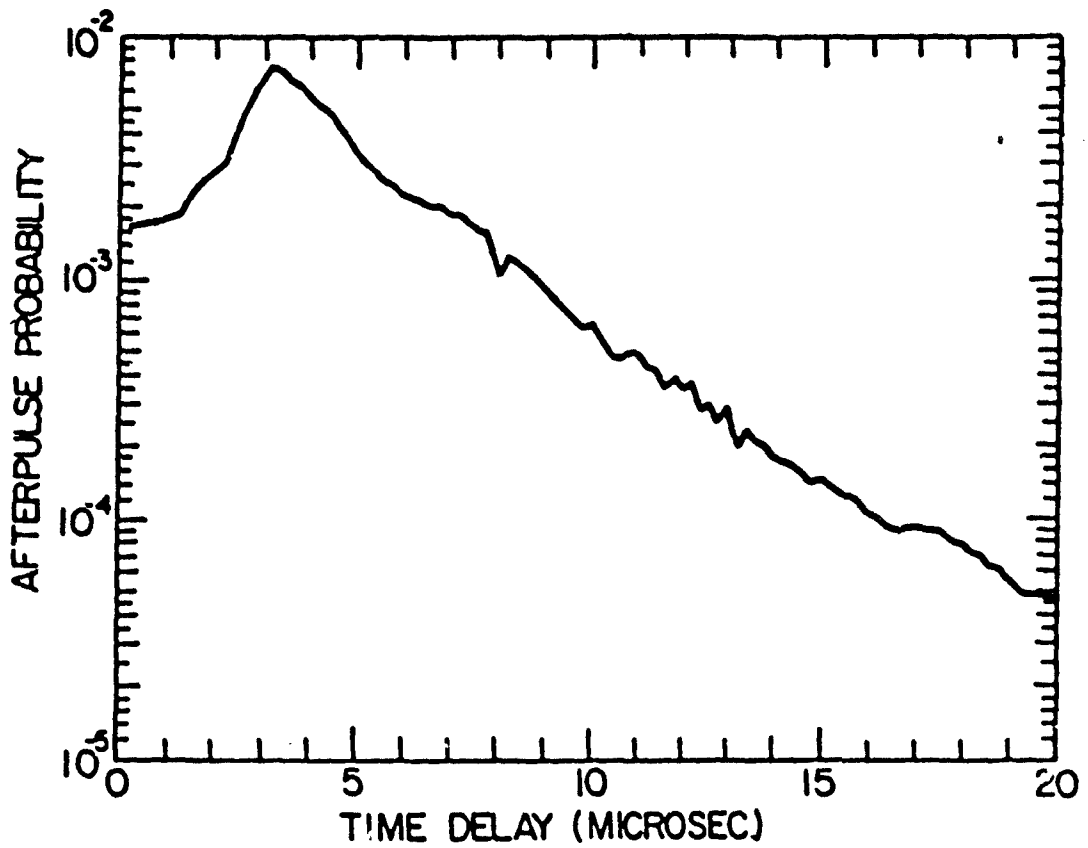

from Shipley et al
U. of Wisconsin

Figure 12. Probability of detecting afterpulse photons in 200-nsec time intervals after an initial photon has been detected by the RCA C31024 photomultiplier. (From Shipley et al, 1983)

used. Thus the processed lidar signal that results has the full dynamic range proportional to T^2, but this occurs within the floating-point computations of the digital computer where it is handled easily.

The advantages obtained from the inherent decrease in dynamic range of the detector signal and the reduced speed at which that range is covered are paid for by having to use coherent detection and having to speckle average.

There is a phenomenon which might occur with the coherent lidar which might be found to have consequences somewhat like those of the T^2 effect on coherent lidar. The author expects that he will be checking out this possibility shortly.

RECOMMENDATIONS

The performance limitations of various incoherent detectors (and amplifiers) need to be determined (or verified) using small, dense clouds generated with known back-edge positions as indicated above.

If these limitations turn out to be severe, ways around them need to be sought. Another detector or a less susceptable variation might be possible. Failing that, the much less attractive alternative of some form of optical range gating might be possible where a number of different detectors observe different range intervals, with the radiation from the near-range intervals not generating significant signals in the detectors meant to observe the far-range signals. The suggested means of doing this (Crawford, 1984) include electro-optical gating (which must have very low leakage in front of the far-side signal detectors) and the use of parallax.

In coherent lidar, the lack of a problem with the tail effect of near-side cloud when the focus is on the far side needs to be confirmed. (This

should be done by the author as matter of course in an upcoming project, which at this writing, however. has not come through procurement.)

G. THE MULTIPLE SCATTERING PROBLEM AND THE MEANS OF OVERCOMING IT

INTRODUCTION

The current lidar equations (Sections B, C and E) require that most of the radiation which is backscattered and then detected by the lidar must be scattered only once if it is to be used. Such scattering events necessarily occur in the transmitter beam. From the lidar range information the path is therefore known over which the radiation traveled as it underwent attenuation in goint out from and back toward the lidar. More importantly, the location at which backscattering took place is known, so the radiation is dependent on the backscattering properties of that one position (even if the backscatter coefficient is the same everywhere--as it may be in scattering from the atmospheric gas) and the attenuation on the path out to, and back from, that position. On these facts the interpretation techniques of Sections C and E are built.

If radiation scattered toward the lidar from a point in the lidar receiver field of view has been previously scattered elsewhere (the significant radiation will be cloud scattered), the radiation being detected is dependent on the scattering properties (and not just the backscattering properties) at more than one point in the cloud (and on the attenuation on the paths between them). Unraveling the optical cloud properties at one point from the signal created by scattering at multiple points has not yet been adequately achieved, even conceptually.

Until (and if) such a theoretical capability is achieved (which must be applicable to lidar observations of clouds in general, including the presence of signal noise), effort must continue to be directed, first, at avoiding or

minimizing multiple scattering effects in lidar returns to be used quantitatively and, second, to knowing when such effects are present in significant amounts and, if possible, removing these effects.

MINIMIZING MULTIPLE SCATTERING EFFECTS.

The predominant way to minimize multiple scattering effects is to narrow the lidar transmitter beam divergence and the observing receiver field of view. These need to be much narrower than the forward diffraction lobe on the scattering pattern from the aerosol particles. This lobe has an angular dimension of the order of λ/D_p where λ is the lidar wavelength and D_p is an effective particle size. With θ the angular dimension of the field of view (usually somewhat greater than the angular dimension or divergence of the transmitter beam for stability purposes), the approximate fraction of the once-scattered radiation which remains in the field of view is the order of $\theta^2/(\lambda/D_p)^2$. [This is true where the cross-sectional dimension of the field of view in the cloud is small compared to $\sigma^{-1}(\lambda/D_p)$.] Some of the backscattered portion of this fraction will then contribute to the lidar return signal in addition to the desired contribution from radiation scattered only once.

Going into the cloud along the lidar beam, the direct (unscattered) radiation in the transmitter beam continues to decrease exponentially due to attenuation. If the cloud attenuates predominantly by scattering rather than by absorption [it is then said to have a high albedo, an albedo near 1], and the field of view is not much smaller than the forward diffraction lobe (which contains a large to very large fraction of the scattered radiation),

significant scattered radiation remains in the field of view after each successive interaction with the aerosol particles. [The angular spread of the forward scattered radiation is the order of $\sqrt{N}(\lambda/D_p)$ in such a situation where the depth of penetration is $N\sigma^{-1}$ with, very roughly speaking, each surviving "photon" interacting once every σ^{-1} traveled into the cloud.] Thus, in such a situation, with increasing optical depth in the cloud, the contribution to the lidar signal from multiple scattering can become much greater than the single-scattered (lidar equation) contribution.

The amount of multiply-scattered radiation observed by the lidar in a given situation can be numerically calculated, but the calculation is usually expensive. A good estimation technique exists, however, where the forward diffraction lobe angle (in radians) is small compared to 1 (Eloranta, 1982).

USE OF LONGER WAVELENGTH RADIATION. From the above, very crude arguments one can see that, for typical fields of view, multiple scattering problems are decreased by going to longer wavelengths due to the greater spread in forward diffraction [$\theta^2/(\lambda/D_p)^2$ decreases 100x from 1.0 μm to 10 μm]. Further, many of the materials present in smoke/obscurants, whether present deliberately or as impurities, have increased absorption in the mid IR so that one rarely sees the 98%, 99% (white cloud) albedos which occur in some smoke/obscurants in the visible.

USE OF THE TOP-DOWN APPROACH. From the above arguments one can see that multiple scattering will be less of a problem at larger cross-cloud transmittances--all other aspects remaining constant--as the singly-scattered lidar signal component is, at least grossly proportional to T^2, and so will be reduced less at larger T, and therefore the multiply-scattered component will

be less significant as a fraction of the total lidar signal. Using the same example as in Section F concerning the T^2 problem, a horizontal path through the 40 m wide cloud of Figure 11 has a cross-cloud T^2 value of 10^{-6}, but if the lidar observes the same cloud from above and the cloud is 10 m high, the cross-cloud T^2 value is 3.2×10^{-2}, a three-hundred-fold increase.

DETECTING MULTIPLE SCATTERING IN THE LIDAR RETURN.

Several approaches to detecting the presence of a significant multiple scattering contribution in the lidar return signal were mentioned in the survey.

USE OF EXCESS SIGNAL. Evans of DREV suggested an approach which is helpful. Its requirements for quantitative use are the same as those currently required for quantitative use of the lidar signal, that is, a constant ratio, C_0, of backscatter coefficient to attenuation coefficient in a cloud and the determination of the calibration factor that is regularly used (C_2 or its equivalent--See Section C). This approach also uses the fact (Equation (27)) that the integral of the beam-geometry-corrected single-scattering lidar signal is $C_2[1 - T^2(L)]$ where $T(L)$ is the transmittance from the lidar to distance L on the lidar beam, the integral is done from the lidar to L, and C_2 is constant. The constant of proportionality, C_2, is the product of $\frac{1}{2}C_0$ and the lidar instrument constant, C_1. (The latter requires correction for any lidar output power or receiver sensitivity fluctuation.) Measurement of the integrated lidar signal over a path over which T is simultaneously known gives an evaluation of C_2. (T must not be too low [where multiple scattering may be present] nor too close to 1 [where the experimental error in $(1 - T^2(L))$ is too large].) If only single scattering is present, note that as T goes below 0.3 the path-

integrated lidar signal will be above 0.9 C_2 with C_2 as an upper limit. Thus observation of a path-integrated lidar signal greater than C_2 is a clear indication of multiple scattering under the above conditions. Also note that, for reasonable lidar systems, multiple scattering should not be a problem at cloud transmittances above 0.3.

This appraoch is applicable to coherent and incoherent lidar. Illustration of this approach, but where C_2 is varying significantly, is shown in Figures 8 and 9. Unfortunately, even where C_2 may not vary, a single path-integrated lidar signal between 0.9 and 1.0 times C_2 does not imply that there is no significant multiple-scattering contribution present in the lidar signal.

This method allows detection of multiple-scattering effects in some cases, but does not allow their removal in any significant way.

USE OF FIELD-OF-VIEW EFFECTS. Use of field-of-view effects were mentioned by survey respondents Lutomirski of Pacific Sierra and Houston of Optech. Basically, for incoherent lidar, the idea is to have one detector observe the lidar transmitter beam (from which the singly-scattered radiation must come--in addition to any multiply-scattered radiation) and one or more detectors (behind the same receiver optics) observe the volume about the transmitter beam from which radiation can come only if multiple scattering effects exist. This idea is further developed in Appendix E, where it is shown that some modification is needed to the simple statement of the approach given here, but this idea appears to have some merit, particularly for detecting whether or not significant multiple scattering effects are present.

However, this approach is not a panacea for removing or subtracting out the effect of multiple scattering. Subtraction of the multiple-scattering

effects from the lidar signal can be adequately accomplished with this method provided the relative error in the difference between the total signal from the detector observing the lidar transmitter beam and the multiply-scattered component of that same signal is less than the required relative error in the single-scattered lidar signal result. In a smoke/obscurant of high albedo, therefore, the decrease which this approach will allow in the minimum transmittance to which a lidar signal can be interpreted--the decrease from the transmittance value at which the multiply-scattered component of the lidar signal first reaches 5% (and so first becomes significant) to the transmittance value at which the multiply-scattered signal component can just be subtracted from the total signal and yet reasonably give a 5% error in the result--is a factor more like 0.37 (T^2 decreases by a factor of about 0.14) than 0.14 (T^2 decreases by 0.02). The transmittance reduction factor will be the same (at best) or even larger if the maximum error allowed in the single-scattered lidar signal is above 5%.

It is not at all clear that this approach, looking for scattered radiation from outside the transmitter beam, can be readily adapted to coherent lidars.

USE OF POLARIZATION EFFECTS. Houston of Optech mentioned the supplementary and separate uses of polarization effects in looking at multiply-scattered radiation coming from outside the transmitter beam. [He is referring to the effects described by Carswell (Carswell and Pal, 1980).]

Polarization effects may need to be taken into account in designing a multiple-scattering detection system which observes the volume outside the lidar transmitter beam. (For example, multiply-scattered radiation in aerosols of small spherical particles illuminated by 10 μm linearly-polarized lidar radiation will tend not to come from the regions outside the lidar transmitter

beam which lie along the linear polarization direction relative to the transmitter beam, so those portions of detectors observing these regions will only contribute noise, not signal, in such a case. (See Carswell and Pal, 1980))

But sole use of polarization effects in general obscurants, especially non-spherical ones, would appear to be asking too much.

RECOMMENDATIONS

Multiple scattering is not a problem in optically thin tracer clouds. In the use of lidar on smoke/obscurant clouds, its consideration ranks after the obtaining and demonstrating of a valid interpretation scheme in clouds of transmittance of 10% or less. It is a more pressing, higher ranking problem in the visible and near-infrared than at 10 micrometers.

As no satisfactory theory is yet known for unraveling the multiply-scattered signal in any situation, particularly a general particle, nonuniform obscurant producing a noise-containing lidar signal, the emphasis until such a theory may be developed must be on detecting the presence of significant multiply-scattered signal contributions and on the reduction of that presence in the signal used. To test the limits of their capabilities in overcoming multiple-scattering effects, lidars should be challenged with obscurants of large particle size and high albedo (at the lidar wavelength) and with situations that challenge the weaknesses in the technique used to detect the presen of significant multiple-scattering effects. The test results need only be the production of valid attenuation coefficient values along various paths as independently confirmed by transmittance measurements and the valid indication of when and/or where in the cloud such lidar-determined values cannot be trusted.

It would appear from the above overview of current approaches that, considering multiple scattering by itself, emphasis should be placed on avoiding or minimizing significant multiple-scattering effects and detecting their presence rather than correcting for them.

H. DESIRED DATA ACCURACY, SPATIAL AND TEMPORAL RESOLUTION AND SCANNING/DATA RATE CONSIDERATIONS

As, in present smoke test methodology, there is no routine, quantitative two-dimensional or three dimensional measurement of any local smoke/obscurant cloud property throughout a cloud, almost any such measurement, by lidar or otherwise, is a step forward. It is worth considering, however, what the desirable qualities of such measurements might be. The following is a beginning. Most of it is a contribution of Ronald H. Kohl & Associates.

DATA ACCURACY: DESIRABLE ERROR LIMITS IN THE MEASUREMENT OF THE ATTENUATION COEFFICIENT

EFFECT OF ERROR IN THE ATTENUATION COEFFICIENT. Consider the goal of the attenuation coefficient, σ, measurement to be obtaining the transmittance, T, on arbitrary paths through the clouds. The relationship between the actual transmittance and the actual attenuation coefficient on a path is

$$T = e^{-\int \sigma \, dL} \tag{40}$$

where the integral is along the path. The same relationship is used to obtain the lidar-determined transmittance T_m, from the measured attenuation coefficient, σ_m, along the path,

$$T_m = e^{-\int \sigma_m \, dL} . \tag{41}$$

With $\Delta\sigma$ the difference between the actual σ and the lidar measured σ_m (that is, $\Delta\sigma$ is the error in σ_m),

$$\Delta\sigma = \sigma_m - \sigma, \tag{42}$$

and with the other errors in the determination of T_m (distance measurement and integration errors) being negligible, the determined transmittance can be expressed as

$$T_m = e^{-\int \sigma (1 + \frac{\Delta\sigma}{\sigma}) dL} . \tag{43}$$

Let us define an average value of the relative error in the measurement of σ,

$$\left\langle \frac{\Delta\sigma}{\sigma} \right\rangle \triangleq \frac{\int \sigma (\frac{\Delta\sigma}{\sigma}) dL}{\int \sigma dL} = \frac{\int (\Delta\sigma) dL}{\int \sigma dL} = \frac{\frac{1}{L}\int_0^L (\Delta\sigma) dL}{\frac{1}{L}\int_0^L \sigma dL} , \tag{44}$$

where the average value, $\langle \frac{\Delta\sigma}{\sigma} \rangle$, is the attenuation coefficient weighted, path averaged value of the relative error in σ. From the definition, Equation (44), one can see that on those portions of the path where σ is large the contribution per unit length to this average relative error is greater. From Equation (44) we can write

$$T_m = T^{(1 + \langle \frac{\Delta\sigma}{\sigma} \rangle)} . \tag{45}$$

Note from Equation (44) that an absolute error, $\Delta\sigma$, of one sign along the path, and/or a relative error, $\frac{\Delta\sigma}{\sigma}$, of one sign along the path, both forms of systemic error, will contribute to $\langle \frac{\Delta\sigma}{\sigma} \rangle$. Note also, from Equation (44), that the random error part of $\frac{\Delta\sigma}{\sigma}$, as one integrates over the path, will tend to cancel out as the contributions to the integral fluctuate from negative to positive along the path. This will be true unless the sense of the variations in $\frac{\Delta\sigma}{\sigma}$ are generally correlated with the sense of the variations in σ; this is another form of systematic error. Thus, it is the systematic error in the

measurement of σ along the path and any residual effect of the random error left after the integration over the path which go to make up $<\frac{\Delta\sigma}{\sigma}>$ and, therefore, contribute to the difference in the actual and determined values of the transmittance.

Given estimates of the limiting value of $<\frac{\Delta\sigma}{\sigma}>$, positive and negative, then the resulting maximum range of the lidar-determined transmittance, T_m, about T, the actual transmittance, can be determined from Equation (45).

In all of the following we shall drop the <> symbol from $<\frac{\Delta\sigma}{\sigma}>$, that is,

$$<\frac{\Delta\sigma}{\sigma}> \rightarrow \frac{\Delta\sigma}{\sigma} \tag{46}$$

so that Equation (45) is

$$T_m = T^{(1 + \frac{\Delta\sigma}{\sigma})} \tag{47}$$

in the notation which follows.

The relationship between T and T_m of Equation (47) is plotted in Figure 13 with the curves labeled by the appropriate value of T_m and the "Relative Variation" being $\frac{\Delta\sigma}{\sigma}$. Relative error limits of $\frac{\Delta\sigma}{\sigma} = \pm 25\%$ are shown by the horizontal arrows at T = 0.1 and T = 0.001 with the resulting range of determined values of T indicated by the vertical arrows, found by extending the tips of the horizontal arrows along the curves to the intercepts with the vertical axis as indicated. Thus a ±25% error in measured attenuation coefficient is shown in Figure 13 to give an uncertainty in the determined transmittance at T = 0.1 of a factor of (just under) 2 in increase and in decrease, and, at T = 0.001, to give an uncertainty factor of about 5 ! We see that the relative systematic error in σ_m is considerably magnified in the determination of T_m in the range of

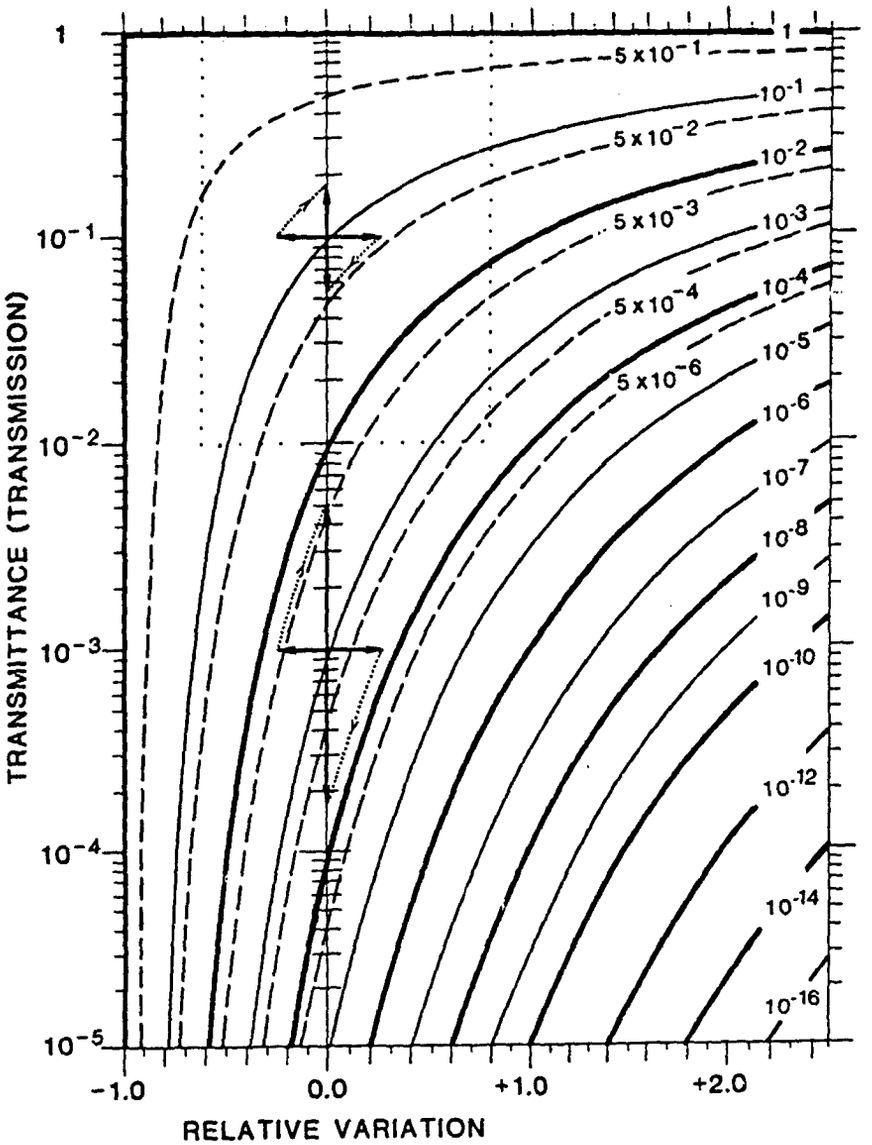

Figure 13. Multiple-use graph. See text. The transmittance depends on a parameter whose relative variation is plotted horizontally. The example shown by the arrows is a relative variation of ±25%. This results, at a transmittance of 10^{-1}, in a variation in transmittance of a factor of almost 2, and, at a transmittance of 10^{-3}, in a variation in transmittance of a factor of 5.

transmittance of interest. The resultant uncertainties in the determined transmittance values with reasonable systematic attenuation coefficient error values seem to be quite large if considered from the viewpoint of an electro-optical system with a threshold transmittance determined in a laboratory by detecting uniformly, statically attenuated radiation. Further, for a given relative error in the measured attenuation coefficient, the relative uncertainties in transmittance are seen to increase as the transmittance decreases (and thereby approaches critical electro-optical system thresholds). Note that these results hold for <u>any</u> determination of the transmittance from local properties, whether from a distribution of the attenuation coefficient or from a distribution of the concentration, no matter how these distributions are obtained, via modeling or experiment.

(As can be seen from the slope of the curves in Figure 13, the magnification of the relative error in σ_m in the determination of T_m remains even when small $\frac{\Delta\sigma}{\sigma}$ are considered in the region of interest away from T=1. For small relative error limits, $\frac{\Delta\sigma}{\sigma}$, a simple expression of the relative error limits on the determined transmittance can be obtained for estimation purposes as

$$\frac{T_m - T}{T} = \frac{\Delta\sigma}{\sigma}(2.30)\log_{10}T \qquad (48)$$

where, for accuracy, the expression should be less than 1. For a relative error in the measured attenuation coefficient of $\frac{\Delta\sigma}{\sigma} = \pm 10\%$, this expression gives a relative error in the determined transmittance of $\mp 23\%$ for each decade in T, $\mp 23\%$ at $T=10^{-1}$ and $\mp 46\%$ at $T=10^{-2}$, etc. [Though these relative error results are hardly much less than 1, the relative numerical error in the value at $T=10^{-2}$ is still only about 20%.])

The situation is nowhere near as bad as it appears at this stage of our development, due to the fact that the transmittance in an obscurant is quite the opposite of a static quantity. The transmittance fluctuations and their impact on attenuation coefficient measurement-error requirements are discussed below, but first note that by taking the negative natural logarithm of Equation (47) for T_m, the Equation (47) can be put in the form

$$\frac{-\ln T_m + \ln T}{-\ln T} = \frac{\Delta\sigma}{\sigma} , \tag{49}$$

that is, the relative error in the determined negative logarithm of T is equal to the relative error in the measured attenuation coefficient which is the cause of it.

TRANSMITTANCE FLUCTUATIONS IN OBSCURANTS. In real obscurants the amount of obscurant along a path or line of sight is not a static, but a fluctuating quantity. Consider the relative fluctuations in the value of the integration of the concentration (the mass of obscurant per unit volume of atmosphere) over the same path on which the transmittance is desired, that is, the short-term relative fluctuations of

$$C_L = \int C dL . \tag{50}$$

With $\langle C_L \rangle$ representing a short-time average C_L, these short-term relative fluctuations, represented as $\Delta C_L / \langle C_L \rangle$, can be expressed as

$$\frac{\Delta C_L}{\langle C_L \rangle} = \frac{C_L - \langle C_L \rangle}{\langle C_L \rangle} . \tag{51}$$

Multiplying the right-hand side of this by 1 in the form of α/α, where α is a characteristic extinction coefficient (the attenuation coefficient per unit concentration) gives

$$\frac{\Delta C_L}{\langle C_L \rangle} \cong \frac{-\ln T_i + \ln T_{\langle\rangle}}{-\ln T_{\langle\rangle}} \tag{52}$$

where $T_{\langle\rangle}$ is the transmittance at the value $C_L = \langle C_L \rangle$, T_i is the instantaneous transmittance arising from the path-integrated concentration C_L and we have neglected the short-term fluctuations in α compared to the short-term fluctuations in C_L.

(The similarity of Equation (52) to Equation (48), and therefore to Equation (47), means that Figure 13 can be taken as a plot with the relative C_L fluctuation, $\Delta C_L/\langle C_L \rangle$, plotted as the "Relative Variation" of the horizontal axis and $T_{\langle\rangle}$ as the "Transmittance" on the vertical axis with the extremes of the transmittance values resulting from the C_L fluctuations interpolated from the appropriate labeled curves as discussed below Equation (47).)

If the magnitude of the relative measurement error in the attenuation coefficient is much less than the magnitude of the short-term relative C_L fluctuations, that is to say (with the magnitude of x represented by $|x|$ and with $\Delta\sigma$ and ΔC_L being representative quantities), if

$$\left|\frac{\Delta\sigma}{\sigma}\right| << \left|\frac{\Delta C_L}{\langle C_L \rangle}\right| \tag{53}$$

then Equations (49) and (52) show us that <u>any transmittance uncertainties due to measurement error in the attenuation coefficient will be much less than the short-term fluctuations in the transmittance</u>, specifically that

$$\left|\frac{-\ln T_m + \ln T}{\ln T}\right| << \left|\frac{-\ln T_i + \ln T_{<>}}{-\ln T_{<>}}\right| . \qquad (54)$$

We expect the size of $|\Delta C_L / \langle C_L \rangle|$ to be reasonably large so that Equation (53) can be met with reasonably-sized attenuation coefficient measurement accuracies. Then if the resultant errors in the determined transmittance, which may be relatively large but will meet the condition of Equation (54), are shown to be small enough to be useful (despite prejudices from the laboratory), good use can and will be made in E-O system performance predictions of attenuation coefficient measurements made with reasonable accuracy throughout a smoke/obscurant cloud. The demonstration that transmittances are useful when the relative error in them satisfies Equation (54), even though that relative error may be large, will be given below, after we consider further the transmittance fluctuations and their size.

Having introduced the C_L fluctuations as the major explanation of the transmittance fluctuations, we leave them and concentrate on the phenomenon of the transmittance fluctuations, themselves, in smoke/obscurant clouds. We want to deal directly with the transmittance fluctuations because these transmittance fluctuations, as we shall see, set the requirements for reasonable attenuation coefficient measurement accuracy, rather than these requirements being set so as to produce a transmittance determination with an error less

than an a priori percentage of an E-O system threshold transmittance value measured statically in the laboratory. (This is just as well, for, as we have seen in the discussion above Equation (48), the latter may be an impossible task for a low transmittance threshold device such as a beam rider.)

At small transmittances, considerable relative transmittance fluctuations are observed along lines of sight through smoke/obscurant clouds. This can be observed in the various DPG Smoke Week reports (such as Smalley, 1981). Such transmittance fluctuations have been observed by all transmissometers observing lines of sight in smoke/obscurant clouds, whether DPG transmissometers or not (Farmer, 1984). In a given cloud the relative size of these fluctuations is smaller the longer the path through the cloud. Where the path is shorter, or passes through less of the cloud, these relative fluctuations are considerably greater, as would be expected given a minimum effective eddy size with different eddies containing different concentrations of obscurant. Similar transmittance fluctuations were observed in natural fogs in the RVR transmissometer program to develop instruments to determine aircraft visibility categories at civilian air terminals (Douglas and Booker, 1977). The fluctuations observed with the RVR transmissometers were an actual and not an instrumentation effect.

While the transmittance along a line of sight is the result of the integration of the attenuation coefficient along that line of sight (see Equation (40)), and the integration along the line of sight reduces the effects of local variations in the attenuation coefficient, this integration occurs in an exponent (see Equation (40)) and when this exponent is significant, and the transmittance is small, the exponentiation magnifies the effects of the integrated variations.

Fogs formed by lowering coastal stratus on the California coast are known for their great horizontal uniformity and lack of turbulance. For this reason in this type of fog the relative transmittance fluctuations on horizontal paths are small, but in all other natural and man-made obscurants the relative transmittance fluctuations are large at small transmittances.

To get an idea of the size of the transmittance fluctuations in smoke/obscurant clouds, the transmittance data from the Smoke Week test reports was reviewed by this author. The data reviewed, therefore, came from a variety of obscurants in numerous trials and circumstances and at all different times in the trials. Small relative variations were particularly sought as they limited the application in mind. Because of the data presentation (small, thick-lined graphs of ln T versus time) transmittance values were limited to the order of 0.1 and down--the region of interest in any case.

Instead of reviewing the magnitude of the relative short-term, fluctuations of the instantaneous cross-cloud transmittance, T_i, about the short-term mean (running average) transmittance value, $\langle T \rangle$, the magnitude of the relative deviation of the negative logarithm of the instantaneous transmittance, $-\ln T_i$, about the short-time mean of the negative logarithmic transmittance value $\langle -\ln T \rangle$ was reviewed. This quantity is

$$\left|\frac{\Delta(-\ln T)}{\langle -\ln T\rangle}\right| \triangleq \left|\frac{-\ln T_i - \langle -\ln T\rangle}{\langle -\ln T\rangle}\right| . \qquad (55)$$

The reason for this choice was the form of Equation (49) as we will be comparing

$$\left|\frac{\Delta\sigma}{\sigma}\right| = \left|\frac{-\ln T_m - (-\ln T)}{-\ln T}\right| \quad \text{with} \quad \left|\frac{-\ln T_i - \langle -\ln T\rangle}{\langle -\ln T\rangle}\right| ,$$

the latter being the quantity reviewed. In fact we shall desire

$$\left|\frac{\Delta\sigma}{\sigma}\right| = \left|\frac{-\ln T_m - (-\ln T)}{-\ln T}\right| << \left|\frac{-\ln T_i - \langle -\ln T\rangle}{\langle -\ln T\rangle}\right| . \qquad (56)$$

The quantity $|\Delta(-\ln T)/\langle -\ln T\rangle|$, the right-hand side of Equation (56), was found to have values in the range 10% to 50% and more in the smoke week data.

One example of the data reviewed is shown in Figure 14. At a transmittance value of about 3.4×10^{-2} (the line marking the value is elongated in time to show up on the figure) the fluctuation in -ln T is seen to be about ±28% as shown by AA' in the figure. (So the quantity in Equation (55), and the one on the right-hand side of Equation (56), is 0.28 .) At a transmittance value of 0.29 the fluctuation in -ln T, BB', is ±16%.

The example of Figure 14 shows a common occurance in the smoke week data, in that the magnitude of the relative fluctuation of -ln T (the magnitude of the fluctuation relative to <-ln T>) on the (cross-wind) line of sight in a cloud is often seen, as in Figure 14, to be larger at smaller T than it is at larger T. In some cases the relative fluctuation of -ln T is about the same at smaller T as at larger T. However, the relative fluctuation of -ln T is not seen to be smaller at smaller T than at larger T unless the nature of the data is that which appears to correlate with the cloud center moving to and away from the line of sight because of wind shifts. This means that if the condition of Equation (56) is met at relatively high values of T on a line of sight passing through the cloud center, it should be met (or improved)

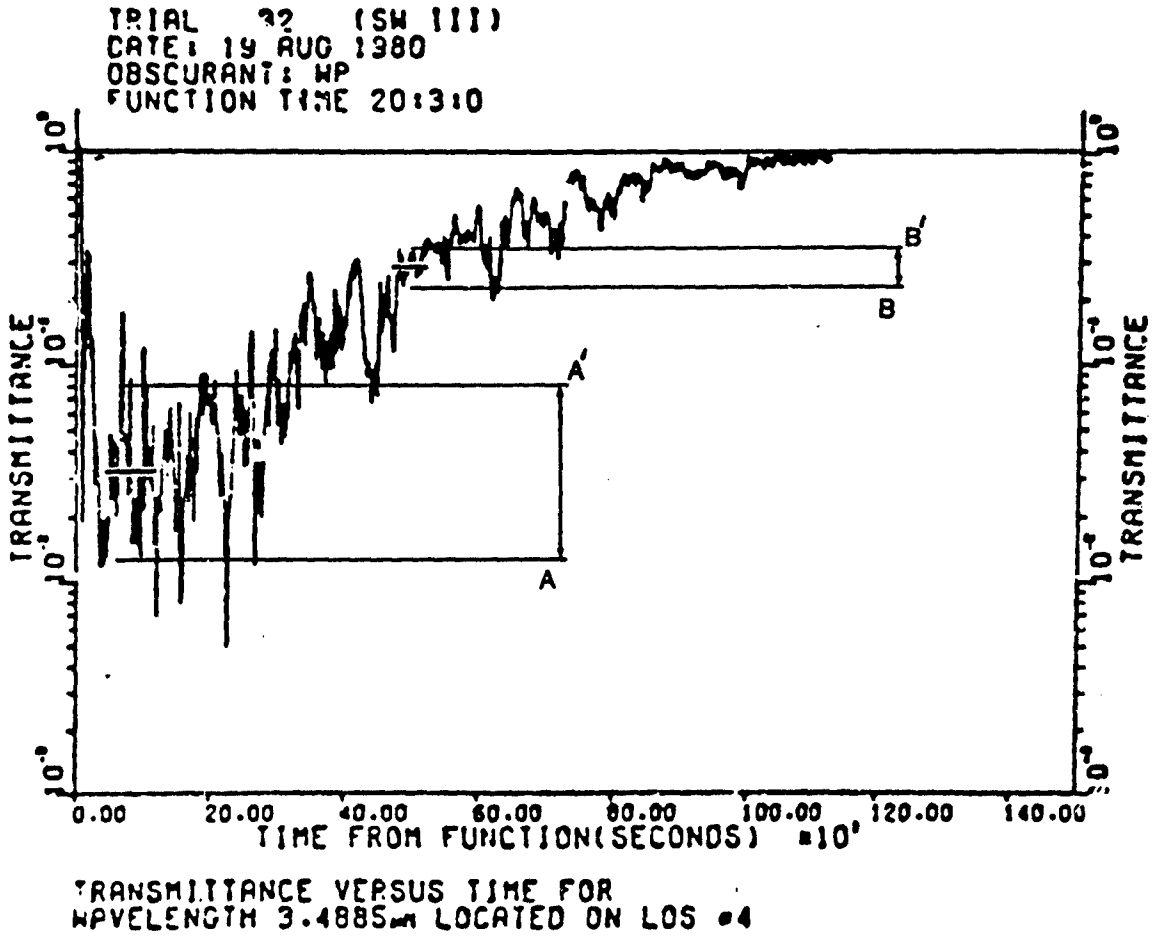

TRANSMITTANCE VERSUS TIME FOR
WAVELENGTH 3.4885μm LOCATED ON LOS #4

Figure 14. Typical logarithmic plot of cross-wind line of sight transmittance as a function of time in a smoke/obscurant. Two local mean log T values are indicated by the central portion of the short solid lines, one at a transmittance of 3.4×10^{-2} and one at 0.29 . The size of associated fluctuations are indicated by AA' and BB', respectively. (Adapted from Smalley, 1981.)

at lower values of T on the same or other lines of sight in the same cloud. (The fluctuations in the vicinity of T=1 must not be used because these fluctuations in the data are instrumentation fluctuations or are due to atmospheric fluctuations of the transmitter beam and receiver field of view, and are not due to the cloud. Such fluctuations are not of interest in any case.)

USEFULNESS OF TRANSMITTANCE DETERMINATIONS WHICH MEET THE CONDITION OF EQUATION (56). To illustrate our point we consider an E-O system whose ability to function (sense a target or a source) at a particular time depends on the transmittance on its line of sight being above a short-term threshold value which depends on the target or source contrast, the background radiance and the path radiance conditions at the time. Let the short-term threshold transmittance be represented by T_{Th}. Consider a typical fluctuation of the actual transmittance on a line of sight of interest which goes from some initial transmittance value to some higher value and back to its initial value so that this transmittance fluctuation intercepts T_{Th}. As a characteristic fluctuation consider this one as starting from, and finishing near the transmittance whose negative logarithm is <-ln T>. See Figure 15. On a logarithmic plot such as Figures 14 and 15 the fluctuation starts at <-ln T> rises to $A = -\ln T_A$ and returns to <-ln T>, intercepting $Th = -\ln T_{Th}$ on the way up and on the way down.

The transmittances in this and all other fluctuations, when determined from measured attenuation coefficient values on the line of sight, will be shifted from the actual transmittance values due to the residual or systematic error in the attenuation coefficient measurements. In particular, the negative logarithm of the transmittances in this fluctuation will be shifted from the actual value by a characteristic amount S. (We define S to be greater than 0

Figure 15. A characteristic transmittance fluctuation along a line of sight is shown with expanded time scale. The fluctuation goes from 1 to 2 to 3, starting from the transmittance whose negative logarithm is $\langle -\ln T \rangle$, and rising to T_A and returning, intercepting the short-term E-O system threshold, T_{Th}, on the way up and on the way down. The solid line is the path of the actual fluctuation of varying transmittance T, and the dashed line is the fluctuation produced from the transmittance T_m which is determined from measured local properties along the line of sight. Due to measurement error $T_m = FT$ with $F \neq 1$. The parameter S is $-\ln F$. If the size of the fluctuation on the logarithmic scale, $\langle -\ln T \rangle - A$, is large compared to S, most fluctuations intercepting the short-term threshold, Th, will yield a determined time above threshold, Δt_m, which differs relatively little from the actual time above threshold, Δt, because most interceptions will have Th - A also large compared to S. (See the text.) This is true despite the fact that effects of measurement error in T_m may be relatively large, causing F to deviate substantially from 1.

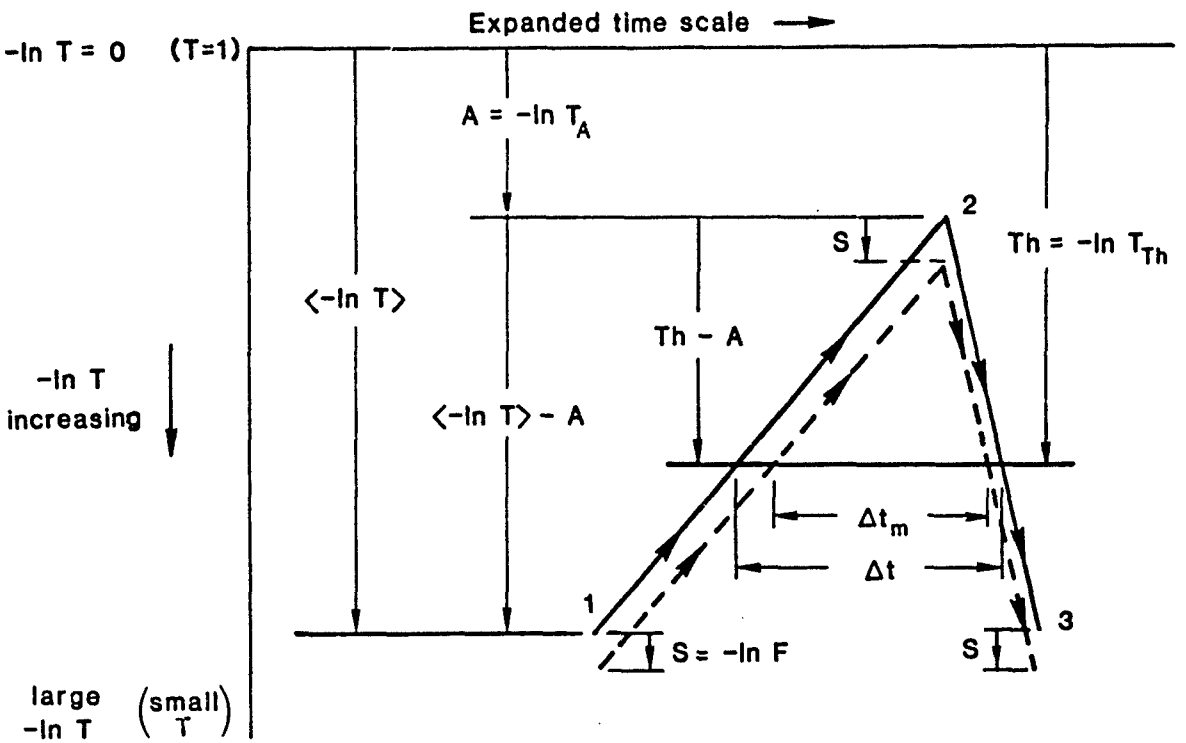

Figure 15. See caption on preceding page.

for a downward shift in Figures 14 and 15.) Note that if the condition of Equation (56) is met, S will be small compared to the size of this fluctuation as seen on a logarithmic plot such as Figures 14 and 15.

Using the short-term threshold T_{Th} and the actual transmittance fluctuation, let the actual operation time of the E-O system (the time interval in which the actual transmittance, T, is above the short-term threshold) be denoted by Δt. See Figure 15. Let the determined operation time, the time interval in which the determined transmittance, T_m, is above the short-term threshold T_{Th}, be denoted by Δt_m. Then (making up the fluctuation with straight-line logarithmic transmittance variations of arbitrary time rate of change [equivalent to arbitrary linear change of attenuation coefficient with time--a good, simple model]) one finds (see Figure 15)

$$\Delta t_m = \Delta t - \left(\frac{S}{Th - A}\right)\Delta t \qquad (57)$$

for Th at least S below A.

Consider taking a plot of the logarithm of transmittance on a line of sight versus time, such as Figure 14, and then marking a displacement S' in toward the short-term mean from the tip of each fluctuation, the displacement being small compared to the size of the fluctuation. Make another, less-varying curve across this plot which intercepts the first one. You will typically find that most fluctuations of the logarithm-of-the-transmittance plot intercepted by this second curve are intercepted at distances from the fluctuation tips which are large compared to the S'.

Similarly, the denominator in ( ) in Equation (57), being typically of a scale of $\frac{1}{2}(\langle -\ln T\rangle - A)$, is, in most fluctuation interceptions, large compared to $|S|$, so that for $|S|$ small compared to the fluctuation size (the condition of Equation (56)), the ( ) in Equation (57), which is the relative error in the determination of Δt, is small compared to 1. Thus we have

$$\Delta t_m \approx \Delta t \ , \tag{58}$$

or the determined time above threshold is approximately the actual time, in most interceptions. In the other interceptions, or near-interceptions, if the effective error in T_m is known, and therefore S or $|S|$ is known, indeed one knows that Δt_m is not approximately equal to Δt, i.e., one knows that Th has approached a fluctuation in the logarithmic plot of T_m within about $|S|$ of the tip.

A similar analysis with similar conclusion holds for fluctuations of decreasing transmittance intercepted by the short-term threshold. The determined blockage time, the time the transmittance, T_m, is determined to be below the short-term E-O system threshold, is approximately equal to the actual blockage time in most intercepts if Equation (56) is satisfied.

It should be noted further that not only is there a threshold effect in the transmittance, operationally there is also a threshold effect in the time, that is, there is a minimum time interval with the transmittance above the short-term threshold in which an E-O system can accomplish its task of the moment and there is a minimum time interval with the transmittance below the short-term threshold in which an E-O system will have its task fail or be revised

(the time interval for a beam rider to lose lock, for example). Thus if the negative logarithm of the short-term threshold, Th, comes within $\pm|S|$ of the tip of a fluctuation, that is, where Δt is not well known, still the possible range of the operation (or blockage) time, Δt, may be so short compared to the required time that its actual value is of no importance. In this case satisfaction of Equation (56) will go beyond giving useful data at most times and will give useful data at all times.

ERROR LIMIT DESIRED IN ATTENUATION COEFFICIENT MEASUREMENT. Given that we need to met the condition of Equation (56) and that the values of the right-hand side of Equation (56) range from 10% to 50% and more, the maximum limit of the desirable systematic and residual relative error in the attenuation coefficient measurements is estimated to be about 5%. [See the discussion below Equation (45) for the definition of the systematic and residual relative error.] Errors less than this will give improved values, but errors much less than this will not contribute additional useful improvement. Measurements with error greater than this will still be useful for obtaining cloud dispersion and transport, and for obtaining the relative attenuation effectiveness of various regions of the cloud, but the transmittance values obtained from them will not be of as great a use as transmittance values obtained from attenuation coefficient measurements of error less than about 5%.

The effect of a 5% relative attenuation coefficient measurement error relative to the measured transmittance fluctuations AA' and BB' of Figure 14 are shown in Figure 16. The transmittance fluctuation range (the set of large vertical arrows) imply a relative variation range (the set of large

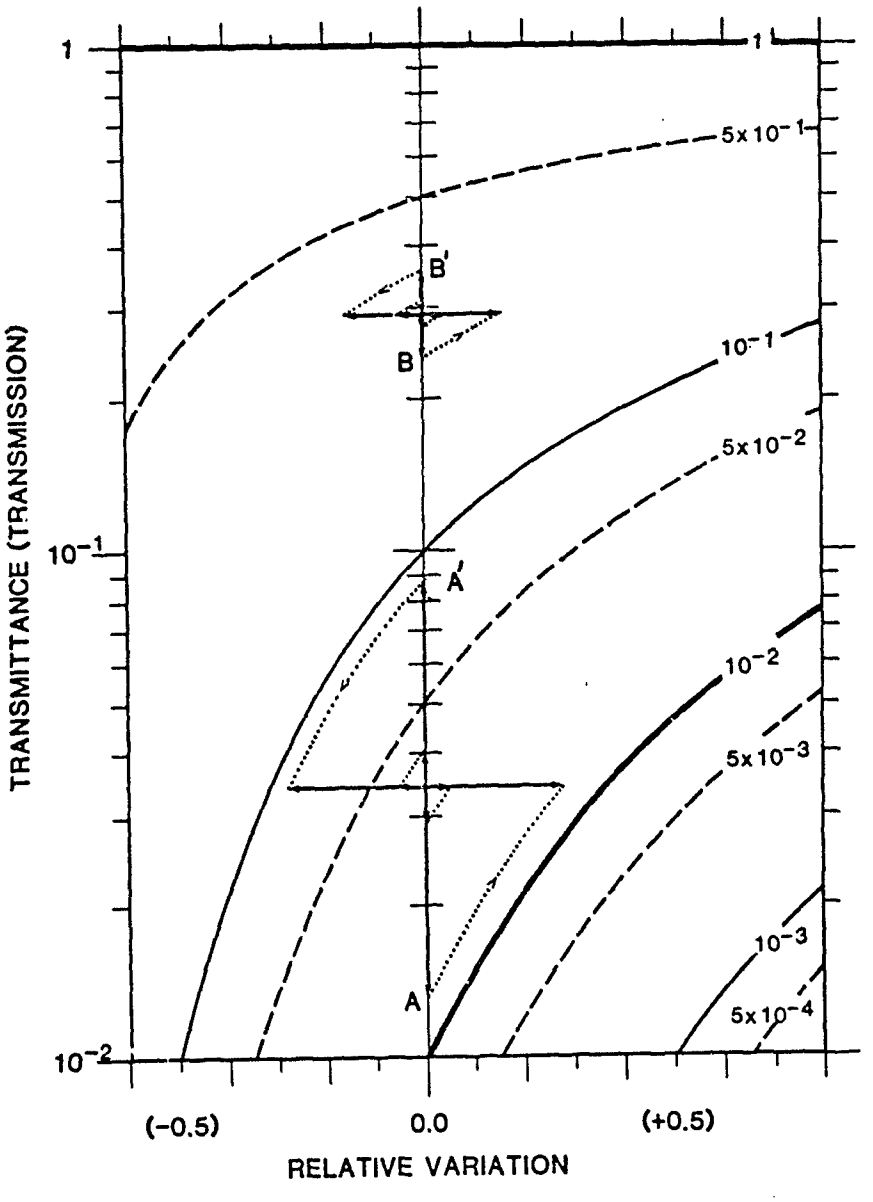

Figure 16. The upper left portion outlined by dots in Figure 13, enlarged, with the fluctuations of Figure 14 plotted thereon (AA' and BB'). The uncertainties due to a 5% residual or systematic relative error (inner horizontal arrows) in the attenuation coefficient measurements used to determine transmittance are shown by the inner vertical arrows.

horizontal arrows) which is twice the right-hand side of Equation (56). Application of 5% systematic and residual relative attenuation coefficient measurement error (the set of small horizontal arrows) yields the transmittance uncertainty shown by the set of small vertical arrows. With the lower set of arrows (AA'), the 5% relative error in the attenuation coefficient will cause the relative error in the transmittance to be ±20% (it would be even more if the cloud were denser and the transmittance were lower still), but, in as much as Equation (56) is satisfied and the outer vertical arrows are much larger than the inner vertical arrows, the results will still be very useful.

Note that the attenuation coefficient accuracy requirements apply whether the attenuation coefficient is obtained directly in a smoke/obscurant cloud or indirectly by using an appropriate tracer cloud in place of a smoke/obscurant cloud.

RECOMMENDATIONS. The achievement of local cloud-property measurement throughout a smoke/obscurant cloud or throughout a cross section of such a cloud is a step forward at almost any measurement accuracy. Some idea of the accuracy of the lidar measurement is needed, however. The local property lidar measurements should be compared with local property measurements made by other means, or, if the local property is the attenuation coefficient, comparison of the derived transmittance with transmittance measurements made directly by transmissometers is recommended. In the latter the derived transmittance error is ideal if it is small compared to the transmittance fluctuation--even if the derived transmittance error is large--as shown above.

(Incidently, the above derivation of this ideal transmittance error criterion is based on the sensor threshold transmittance being less variable than the actual transmittance, but no thorough investigation has been conducted to see if this is indeed the situation for particular types of sensors or sensors in general, and this needs to be done.)

If comparison is made between results of a local property measurement made with lidar and measurement of the same local property made by another methodology, some precautions must be taken. With no knowledge of the spatial and temporal correlation lengths, the volume and time period sampled by each method must be the same (as well as the weighting of the sampling over this volume.) A single measurement instrument with a $(1\ cm)^3$ sensitive volume cannot be expected, a priori, to correlate well with a lidar of sensitive volume $1\ m^3$. There may be some correlation, as both sample eddies of $1\ m^3$ in size, but the lidar will average 10^6 eddies of size $1\ cm^3$ while the instrument responds to only one of them. At least several of the smaller sampling volumes should be distributed within, or, barring that, around the lidar volume.

Error theory shows that comparison of lidar results with results obtained by another methodology (type X) cannot be significantly better than a comparison of the results from two independent measurements made by the methodology of type X. The two type X measurements should be made, at least, under the same conditions as the lidar-type X measurements and, at best, they should be made in conjunction with the lidar measurement as described above.

Lidar attenuation coefficient measurement may be compared with local measurements of the same quantity, but a much easier, and perhaps better way is to use the lidar measurements to derive transmittance values along lines

of sight on which transmissometers are operating. The lines of sight should be across the lidar beam as it sweeps the cloud as well as along the lidar beam. Ideally, the lines of sight should include lines which are horizontal along the wind, horizontal across the wind and vertical. The comments on sampling volumes, times and errors in comparisons, which were made above, apply here with respect to each transmissometer beam volume and the corresponding lidar sampling volumes used along it. The recent, apparent discrepancy in transmissometer results from different transmissometer methodologies is unsettling and needs to be cleared up before transmissometer results can be used for comparison purposes. Once cleared up, the criterion for ideal lidar-derived transmittances is that they vary from transmissometer measured transmittances by amounts which are small compared to the fluctuations in the transmittances.

SPATIAL AND TEMPORAL RESOLUTION

Any two dimensional or three dimensional local optical property measurements in smoke/obscurant clouds will be an assist and an advance over current practice, but, independent of any hardware considerations, there are some desirable spatial and temporal resolutions beyond which still finer resolution only adds to the data burden, but does not allow better prediction of E-O system function. We seek estimates of these optimum resolutions here. We also compare current lidar spatial resolutions with these optimum spatial resolutions, reserving temporal resolution comparisons for the section on scanning and data rates.

ON THE MINIMUM OPTIMUM SPATIAL RESOLUTION REQUIRED TO PREDICT E-O SENSOR PERFORMANCE. Consider a ray of single-wavelength (monochromatic) radiation starting from the furthest point in its reverse direction in a scene and traveling (in a straight line) directly to the E-O system sensor aperture. It brings with it an amount of flux to the sensor which depends on the optical properties, the radiation field distribution and the source distribution in the space through which the ray travels. These properties and distributions have added radiation to and taken radiation from the ray.

Consider a small group of similar, near-by rays surrounding the first. Do these rays differ significantly from the first in terms of the flux delivered to the sensor? If so, then if sensor performance is to be predicted, the optical scene must be described in sufficient detail that the differences in the rays can be generated. If so, also, there should be a smaller, closer group of similar near-by rays which do not differ significantly from the first in terms of flux delivered to the sensor, these form an optical pencil. All the rays inside such a pencil may be described as is the first ray, and optical properties and distributions within the pencil need noly be described to a spatial resolution of the order of the width of the pencil, all finer spatial structure being averaged over the width of the pencil.

A given spatial resolution as stated here implies that structures of smaller spatial scale are averaged over dimensions of the order of the spatial resolution, not that a structure is sampled with distances between the samples equal to the spatial resolution.

If a sensor views a two-dimensional scene (through an unscattering, transparent, source-free medium) the largest pencil widths that can be used,

and therefore the spatial resolution needed in describing the scene is set by the larger of, first, the spatial scale of the optical structure of the scene at sensor-detectable contrast, and, second, the directional resolution of the sensor.

Note that if the scattering properties of the scene (as opposed to the scattered radiation from the scene) have a spatial scale larger than the spatial scale of the directional resolution of the sensor, these scattering properties still need only be described using the former, larger scale, even though they may be illuminated by radiation with a smaller, sensor-detectable spatial scale and the resulting scattered radiation itself would also have to be described using that smaller spatial scale. A similar statement can be made with respect to the emissivity: it can be correctly described by a scale which is much larger than the scale of an impressed, sensor-observable temperature distribution where the latter will require that the emission be described by the smaller scale also.

We now consider allowing the medium through which the sensor is looking to contain distributed scatterers and sources but without attenuation being present, somewhat--in the visual region--like household dust as observed in a sunbeam. Here, similarly, the spatial resolution needed to describe the local optical properties of the region (or a part of the region) is the larger of the spatial scale of those local optical properties (determined as if each volume element were the only one present) and the spatial scale determined by the directional resolution of the sensor.

When we deal with local attenuation properties, however, the local spatial resolution required to describe them cannot be set for each volume element independently. The significant local scale which must be used is

the distance between rays entering the sensor as they spread apart in the medium and first encounter the condition that the transmittance along the rays differs significantly. The spatial scale determined by the directional resolution of the sensor does not enter into consideration. A pencil of rays of the size of the directional resolution of the sensor may vary greatly in the amount of flux conveyed along it depending on how the attenuation coefficient is distributed in the cross section of that pencil (see Appendix F).

The minimum spatial resolution required for description of the attenuation coefficient (in some smoke/obscurant clouds, 2 meters off the ground, at typical Smoke Week instrumentation distances from the cloud source and for observation on crosswind lines of sight) is indicated in Appendix F to be about 1 meter. This is the spatial resolution in the vertical direction, and, since cloud properties are expected to vary most in this direction, it is, under the conditions cited, a minimum spatial resolution with a corresponding minimum volume element 1 m by 1 m by 1 m.

The minimum spatial resolution for description of cloud scattering and emissive properties is indicated (much more tentatively) in Appendix F to be about 1 meter also, under the same restrictions.

It is interesting to note that at threshold contrast conditions in smoke/obscurant clouds, the fine features on a target, as they are often of low initial (no smoke) contrast, will tend not to be discernable, and target structures of the order of 1 meter will be the just-discernable structures under threshold conditions, one meter being the order of a typical dimension on a man or a major feature on a tank or other vehicle. So the description scale of the target and background and the spatial resolution scale of smoke/obscurant clouds, under the above conditions, are about the same.

The pencil of rays from a just-discernable feature on the target starts with a width the size of this feature and decreases to the size of the sensor aperture on entering that aperture. Thus this pencil will travel through smoke/obscurant cloud structure of roughly the same size as the pencil cross-section if the cloud is on the far half of the line of sight, and through relatively larger structure if the cloud is on the near half of the line of sight--again under the above conditions. But where the target-ray pencil passes through the smoke/obscurant cloud near to the source of the cloud (where the smoke cloud structures may reflect smaller, source dimensions) or closer to the ground than 2 meters (the atmospheric eddies have maximum vertical scale dimensions of the order of the height above ground), the target-ray pencil may encounter significant smoke/obscurant cloud structure smaller, and maybe much smaller than 1 meter in dimension. In addition, if the sensor is near to the cloud these structures may be the same approximate size as the target-ray pencil cross section in the cloud (an inherently more difficult situation for discrimination). Such a situation as the latter might occur when the cloud is being used to protect the vehicle or system on which the sensor is mounted, or to which the sensor is traveling.

ON SIGNIFICANT CLOUD STRUCTURE LESS THAN ONE METER IN SIZE. The occurrence or extent of significant smaller-sized structure in various smoke/obscurant clouds at various times is unknown. Collected here are a few thoughts concerning such smaller-sized cloud structure.

There is a natural tendency for a lidar developer to shun a smaller spatial scale size. For if a lidar system can be developed to adequately describe the local optical properties of a cloud, throughout a volume of the cloud, at the 1 meter spatial resolution size, it may very well not be

possible for such a system to be developed to meet the requirements of a smaller spatial resolution and a thousand (million) more determinations as imposed by a 0.1 meter (1 centimeter) spatial resolution size. The question is, are the specifications of the latter system necessary even if such a system could be developed?

One mitigating circumstance is that a smaller spatial resolution size, if required, may be required over only part of the cloud and/or only part of the time the cloud is in existence (i.e., during the time of cloud formation)

There is a temporal aspect also to the effect of optical structures much less than 1 meter in size, and this must be considered in setting the minimum significant optical-property resolution size. A 1 centimeter structure will only take 0.02 seconds to pass through a 1 centimeter-sized optical pencil even at a relative speed orthogonal to the pencil as low as 1 meter per second. A projectile moving at the speed of sound moves only 6 meters in that time. Is the 0.02 seconds a significant time interval? A 0.1 meter structure will take 0.2 seconds to move through a similar-sized optical pencil. This is a more significant time interval on the scales of both human observation and projectile motion.

There is a spatial-averaging aspect to the effect of cloud optical structures much less than a meter in size, and this must also be considered in setting the minimum optimum spatial resolution size for optical properties. If the smaller of the length of the optical pencil in the cloud and the attenuation length (the length in which the transmittance is reduced by a factor of $e^{-1} = 0.4$) along the optical pencil is still much, much larger than the optical structure size, the effect on the rays in the pencil will

be an average effect over a great many optical structures. Unless the cloud properties in the direction along the pencil are markedly different from the cloud properties at right angles to the pencil (such as at a cloud edge), the effect on the rays in the pencil will be the same as that of larger optical structures whose properties are the average of those of the actual optical structures they contain. That is, the effect can be predicted by knowledge of the cloud optical properties at an (averaging) spatial resolution larger than the actual optical structure size.

Finally, there is a common-sense consideration for the question of the significant small-scale dimension. Significant cloud structure (and therefore significant optical structure) which is much less than a meter in size and which exists for more than a very brief time is intuitively anathema to a smoke developer who is trying to develop a shield for an object or scene many meters in extent. The smoke developer wants an optical wall, not a latticework, and will intuitively avoid the development of clouds with significant small optical structure effects.

It appears that the smallest significant optical-property spatial-resolution size may turn out to be not so very much less than a meter, but more thought should be given to the smallest important scale sizes for spatial variation of optical cloud properties and experimental investigation of these thoughts should be done.

HORIZONTAL RESOLUTION. In this section we consider setting the horizontal resolution by considering the temporal variations of a measured, horizontal cross-wind path-integrated optical quantity and using Taylor's hypothesis. This reveals the down-wind scale size and we take the cross-wind scale size to be the same.

The DPG transmissometer data of the smoke weeks was examined to obtain the time scales of significant changes. The DPG transmissometer optical-pencil cross-section size is 0.6 meters. Wind speeds in these tests were above 1 meter per second so spatial averaging could not come into play unless time periods shorter than 0.6 seconds were involved. However, DPG transmissometer data were recorded after a running, 1 second average had been applied. This then is the temporal resolution of the data.

Changes in the logarithm of the transmittance give changes in the path-integrated attenuation coefficient according to $-\ln T = \int \sigma dL$, and the time scales of these changes were examined.

The examination of the DPG Smoke Week data revealed typical significant changes in the logarithm of the transmittance in times of about 2 seconds and up (peak or dip widths of about 4 seconds and up). [There were a few disturbingly large features with significant changes in times of about 1 second.] The lower limit of the significant time intervals is very close to the data-averaging time interval of 1 second and the required horizontal spatial resolution developed in this paragraph may be artificially high for that reason. Applying the individual-trial cross-wind velocity to each individual minimum time interval for significant variation in $-\ln T$ gave the minimum spatial interval along the wind for significant change in the cross-wind integrated attenuation coefficient, $\int \sigma dL$, to be about 6 meters. Using the same cloud-structure dimension across the wind as along the wind implies a 6 m x 6 m horizontal spatial resolution. This horizontal spatial resolution value could well be a function of the time of flight from the smoke/obscurant source, but this was not examined.

(Lidar requirements may be such that the instantaneous sensitive volume of the lidar has dimensions less than these.)

Steven Hanna (1984a) has analyzed some concentration measurements in Smoke Week III from the viewpoint of atmospheric dispersion and transport. Using DPG concentration data, which was averaged over 1 second intervals, Hanna's results show that decreasing the averaging time of the DPG concentration data right down to the 1 second limit gave continuously increasing relative variance with no sign of a decrease in the rate of increase. (The autocorrelogram was exponential.) Thus the concentration fluctuations producing the variance have widths smaller than 1 second.

The same behavior should apply to the path-integrated concentration (Hanna, 1984b). From the wind speed of about 3 meters per second in the trials Hanna examined, the 1 second averaging, which should still be cutting off significant fluctuations, corresponds to averaging over a 3 meter downwind cloud-structure distance. If so, this would imply that the horizontal spatial resolution ought to be down more toward the minimum size set above, or about 1 meter.

VERTICAL RESOLUTION. The comparisons, discussed in Appendix F, between $-\ln T$ ($= \int \sigma dL$) measured on two parallel cross-wind lines of sight separated by 3.5 meters vertically showed that though there were a number of trials in which the two $-\ln T$ curves agreed to less than the size of the fluctuations in $-\ln T$ (see the discussion above on data accuracy), there were an equal number of trials of (generally) lower transmittances which did not. Using linear interpolation between the $-\ln T$ value differences as a function of time (as discussed in Appendix F) showed that for most of the latter trials the separation had to be reduced just below 1 meter to get agreement in all trials to be within the fluctuations of $-\ln T$.

The restrictions of this single determination of required vertical resolution (from the data of Smoke Week II) are that it involves very few smoke/obscurants: fog oil, HC, WP and dust (the fog oil gave good agreement at 3.5 meters in the two trials examined); there was no variation in height (the lower line of sight was at 2 meters); and there was little variation in magnitude of the time of flight from the source.

SPATIAL RESOLUTION OF CURRENT LIDARS. Incoherent lidars have their cross-beam spatial resolution set by their beam divergence and the range from the lidar. The along-the-beam spatial resolution can be computed, to very little error, by considering half of the pulse width expressed in nanoseconds as the along-the-beam sensitive volume length in feet--a happy consequence of the value of c/2.

Typical incoherent lidar beam divergences range from ½ mr to 1 mr to 5 mr (for background and multiple-scattering reduction reasons) so for ranges up to the order of 1 km the cross-beam spatial resolution is less than or equal to the size region believed most desirable. Pulse width in visible and near-IR lidars (Nd-Yag based) imply along-the-beam resolution of 1.5 to 3.0 meters (10 to 20 nanoseconds), again, very favorable. At 10.6 μm, pulse widths for incoherent lidars imply along-the-beam resolution more like 11 m (75 nsec), a factor of 2x to 10x larger than that desired.

Data sampling must be very rapid to make use of these pulse widths. This is discussed below.

While there is only one coherent (CW focused) lidar currently being developed for use in smoke/obscurants, its sensitive volume dimensions will be typical for this type of lidar, current or future. The sensitive volume cross-beam width for this lidar design is just under 1 cm at 180 m and decreases linearly with decreasing focal range. This is very much less than

the desirable spatial resolution, so much so, however, that spatial correlation must be relied on to obtain adequate sampling in typical sampling grids. The coherent lidar along-the-beam sensitive volume length is about 7.5 m at 180 m and decreases as the inverse square of the decreasing focal range. This is in the desirable size range.

MEASUREMENTS NEAR THE GROUND. On the battlefield soldiers and vehicles above ground keep as near to the ground as possible and utilize boulders, knolls, buildings and vegetation as cover. Cloud data from near the ground and near such obstacles is, therefore, important. Lidar return signals from the ground and other solid objects are in many cases much larger than from the aerosols of smoke/obscurant clouds. The instantaneous sensitive volume of a lidar does not cut off sharply at its edges, so in operation near solid objects significant, unwanted signal contribution from the objects or the ground (clutter) can be a problem. In addition, the variation of atmospheric wind with height is greater near the ground and large variations in cloud structures are expected and are observed near the ground, calling for small vertical resolution and close approach to the ground in collecting data.

Lidar returns from vegetation covered ground are a problem with all types of lidar, though with bare ground the velocity difference between the ground and the atmosphere above it allows coherent (and therefore Doppler) lidar the possibility of discrimination. Polarization discrimination might be useable on incoherent lidars but only where the aerosol is made of spherical particles and the ground signal contributions are not much bigger than the aerosol contributions.

Work needs to be done to determine the significant (for E-O system operation) vertical scale near the ground and to develop lidar techniques which can make measurements near the ground on this scale as well as make measurements 1½ to 2 meters above the ground.

TEMPORAL RESOLUTION. Once a whole cloud or cloud cross section is scanned, how often does the scan need to be repeated? We consider this question for whole-cloud scans and then for cloud cross-section scans, in turn.

If a puff of a cloud were an unchanging structure moving with the wind, a scan of the whole cloud puff would not need to be repeated, ever, in whole or in part, except to update the wind velocity at the cloud. If the puff, or a continuously produced cloud, grew regularly as a function of time elapsed, only the few scans required to obtain the parameters of the regular growth would be required. Even laminar shear would not change the scan repetition requirement much. It is the turbulence in the atmosphere, which, by mixing and reshaping the atmospheric eddy volume elements (both cloud-containing and non-cloud containing volume elements), requires that whole-cloud scans be repeated frequently enough to catch the resultant, E-O significant changes in the cloud structure. These changes are observed in riding with a frame of reference traveling with the cloud.

A review of smoke week data showed typica vertical wind magnitudes (obtained from the standard deviation of the vertical wind-vector angle and the wind speed) of about ½ meter per second. This value did not typically vary much over heights from 2 meters up. With vertical structure of the

order of 1 m (see the subsection on vertical resolution above), this structure can be expected to be shifted vertically by its own length in about 2 seconds if the turbulent velocity does not reverse direction in that time. The time interval for significant change of the velocity of a cloud structure is the LaGrangian time scale which, with ½ meter per second standard deviation of the vertical velocity, is about 1.2 sec/m times the vertical scale length of the atmospheric eddies. (See Hanna (1984a) and Pasquill (1974).) The vertical scale length is the height above the ground, so the LaGrangian time scale is about 2.4 sec at 2 m height, indicating 1 meter vertical displacements will take place in about two seconds due to the simple, short-term motions of some of the eddies existing at that height. All clouds of interest are of sufficient extent that where portions are being transported upwards by turbulence, other portions are being transported downwards. Thus significant structural changes should be expected, and whole-cloud scans should be repeated about every 2 seconds. To bracket this time interval we chose to investigate (below) whole-cloud scan repetition times of 1 and 4 seconds.

(Vertical structural shifts were used to set scan repetition times because significant horizontal structural shifts can be expected to be slower. See Hanna (1984a) and Figure 6.4 of Hanna, Briggs & Hosker (1982).)

We now turn from whole-cloud scans to cloud cross-section scans. Vertical, cross-wind, cloud cross-section scans which have width equal to the required horizontal resolution and which are fixed in position with respect to the ground define an imaginary slab into which new cloud material is continuously carried by the wind. With 1 meter horizontal width (an optical pencil width) a wind speed of 1 meter per second fills the slab with new

material every second. The 1 second period is too long to describe the introduction of new material into a 1 meter width at higher, and typical, wind speeds, but correlation of cloud optical properties along the wind direction will mitigate this. We took 1 second as the minimum estimate of a useful repetition time interval for scanning a fixed, vertical cross section, though it could be half of this.

For a maximum estimated useful repetition time interval, the minimum temporal width of significant dips and peaks in the DPG transmittance data, about 4 seconds, was taken (see the subsection on horizontal resolution, above).

SUMMARY AND RECOMMENDATIONS. Any two dimensional or three dimensional local optical property measurements in smoke/obscurant clouds will be an assist and an advance over current practice, but, independent of any measurement hardware considerations, there are some desirable spatial and temporal resolutions beyond which still finer resolution only adds to the data burden, but does not allow better prediction of E-O system function. First attempts at estimating these optimum resolutions were made here.

The spatial resolution used to describe cloud scattering coefficients and cloud emissivity at a location may be obtained as the distance over which these properties change sufficiently to cause a significant sensor response change where the cloud at the location in question is taken to be the only part of the cloud present. The spatial resolution required to describe the attenuation coefficient must be obtained by considering the whole cloud, as it is determined by the separation between optical rays in the cloud which causes a significant difference in the transmittance along the two rays.

Using the criterion of the previous subsection, regarding data accuracy, to determine when transmittance differences became significant, some Smoke Week II data was used to determine that the minimum optimum spatial resolution required to describe the attenuation coefficient was about 1 meter (in the smoke/obscurant clouds for which there were data, 2 meters off the ground, at typical Smoke Week distances from the cloud source and for crosswind lines of sight). This is assumed to be the minimum optimum spatial resolution as it is the maximum spatial resolution allowed in the vertical direction, the direction in which the variation is expected to be greatest.

Using some seemingly reasonable assumptions, this data implies that the minimum spatial resolution limit for description of all optical cloud properties is also approximately 1 meter. Thus the minimum spatial resolution volume element is about 1 m by 1 m by 1 m under the above restrictions, with smaller spatial resolution possibly being required nearer the cloud source and nearer the ground. In sensor-near-the-cloud-source situations reduced spatial scales could play an important role in sensor operation in clouds thrown up for vehicle protection.

Certain data cited above indicates that, due to spatial correlation of cloud properties, horizontal structure resolution might be relaxed as far as 6 m by 6 m, but in the vertical dimension 1 m seems to be required. These conclusions are based on data which are limited in several ways (discussed above) and may not be general.

The spatial resolution of current lidars was found to fit the above size ranges as well as could be expected. There is reduction of the lidar sensitive volume dimensions at close distances, in at least two dimensions, allowing some probing at smaller spatial resolutions close to sources--other aspects allowing.

The importance, in battle, of the region just above the ground and the need for measurements there to determine spatial and temporal scales important to E-O system operation were pointed out.

Finally, desirable scan repetition times were considered for whole-cloud scanning and for cloud cross-section scanning (which differ quite basically) and in both cases were estimated to be typically from 1 to 4 seconds. (These time intervals will be discussed with respect to lidar systems in the following section.)

Much of the above spatial and temporal resolution estimates can be and should be tested with developing lidar systems. Even the scanning time intervals can be tested without having complete scanning of cloud or cross section.

Temporal and spatial resolution can also be tested by transmissometry. In such tests it is important that good data be taken with temporal resolution at the limit imposed by the physics of the situation, that is, the resolution time should be the optical volume cross-section dimension times the wind speed across it, or less, otherwise data is lost. (See the discussion on horizontal resolution above.)

SCANNING/DATA RATE CONSIDERATIONS

An example of a cloud-containing volume to be interrogated by lidar, used as typical and referred to as the grid volume from now on, is a volume 10 meters high and 100 meters by 100 meters in horizontal extent. Consider this volume as made up of smaller volume elements, only one of which gives rise to the backscattered flux observed by a lidar at any one time. In this volume we shall consider two sizes of volume elements in line with the spatial

resolution discussion above: a finer spatial resolution with volume element 1 meter by 1 meter by 1 meter and a coarser spatial resolution with volume element 6 meters by 6 meters, horizontally, by 1 meter, vertically. We shall consider the grid volume divided into the finer volume elements as case A and the grid volume divided into the coarser volume elements as case B. We shall also consider fixed-position, vertical cross-sectional scans of the grid volume, with such a scan using the finer volume element designated as case C, and such a scan using the coarser volume element designated as case D. These cases are given in Table V. Because of the dynamic aspects of smoke/obscurant clouds, discussed above, we shall consider scanning these four cases in a time period of 1 second and in a time period of 4 seconds.

TABLE V. CASES CONSIDERED

REGION SCANNED	CASE	VOLUME ELEMENT SIZE (Horizontal x Vertical)	DIMENSION OF REGION IN NUMBERS OF VOLUME ELEMENTS	TOTAL NUMBER OF VOLUME ELEMENTS
Full Volume (100m x 100m x 10m)	A	1m x 1m x 1m	100 x 100 x 10	100,000
	B	6m x 6m x 1m	16.7 x 16.7 x 10	2,780
Vertical Cross Section (100m x 10m)	C	1m x 1m x 1m	100 x 1 x 10	1,000
	D	6m x 6m x 1m	16.7 x 1 x 10	167

IDEAL SITUATION. We shall first consider the ideal situation. That is we will consider only the end-product information desired and the time periods in which it is desired, independent of the process of collecting the data. We shall thus obtain the minimum data flow for the desired information. Then we shall consider the effects caused by the various means of collecting the data.

The desirable information is the amount of flux returning from a volume element with a desirable accuracy of 1 part in 20 (5% digitizing error) as discussed above. We shall consider the horizontal transmittance across the cloud (grid volume) to be $T = 10^{-3}$. With cloud density the same on the near and far sides, the flux returning from a volume element on the far side of the grid volume will be reduced by $T^2 = 10^{-6}$ compared to the flux returning from a volume element on the near side of the grid volume (cloud). This then is the range of variation of the returning flux for a lidar on the ground. (We neglect any additional L^{-2} and beam geometry effects, where L is the distance from the lidar.) We shall assume the lidar is on the ground in what follows, but, at the appropriate point below, we will discuss the situation of the lidar being in the air and looking down on the cloud.

Since our error requirement is a relative and not an absolute one, we digitize the logarithm of the flux returning, in this, the ideal situation, so we do not waste bits (information) in too fine a determination of large flux quantities.

As a fraction of the maximum flux returning from along the lidar beam, we want to be able to tell 1.05×10^{-6} from 1.00×10^{-6}, while the flux returning may range up to 10^6 times this. Using logarithms, this means we must be able to differentiate $\ln(1.05 \times 10^{-6})$ from $\ln(1.00 \times 10^{-6})$ with the logarithm of the flux ranging from $\ln(10^{-6})$ to $\ln(1)$, or we must know our output to

$$\frac{\ln(1.05 \times 10^{-6}) - \ln(1.00 \times 10^{-6})}{\ln(1) - \ln(10^{-6})} = \frac{\ln 1.05}{\ln 10^6}$$

or 1:283. This resolution is a little finer than that given by 8 bits (1:256) and requires exact matching of the peak signal from the near side of the cloud to the top voltage of the digitizing range. A 10 bit digitization (1:1024) is a little more reasonable from an information standpoint, giving the required resolution and allowing for a factor of almost 4 in variation of the peak flux.

With 10 bits or 1.25 bytes per volume element, Table VI gives ideal data rates in the situations discussed above.

TABLE VI. INFORMATION FLOW IN THE IDEAL CASE

CASE	FOR 1 SECOND COVERAGE OF THE REGION: Average Sample Rate of Volume Elements (sec^{-1})	FOR 1 SECOND COVERAGE OF THE REGION: Average Data Rate (bytes/sec)	FOR 4 SECOND COVERAGE OF THE REGION: Average Sample Rate of Volume Elements (sec^{-1})	FOR 4 SECOND COVERAGE OF THE REGION: Average Data Rate (bytes/sec)
A	100k [10μ]*	125k	25k [40μ]*	31.3k
B	2.8k [260μ]*	3.5k	700 [1.4m]*	870
C	1k [1m]*	1.25k	250 [4m]*	313
D	167 [6m]*	200	42 [24m]*	52

*Quantities in square brackets are average times (in seconds) per volume element for one scan of the region.

These data rates are achievable with microprocessor based systems. For the worst case, case A at the high data rate, up to 2 minutes data could be collected in a common microprocessor followed by about a 1 minute interruption for transfer of the data in one microprocessor to a hard disk.

Thus the ideal case is achievable.

EFFECTS OF LIDAR USE. The actual situation with lidar use differs in two aspects. The first is that there needs to be additional information (such as calibration and position information) with the lidar signal information

in order to obtain the final information desired. This adds little to the data rates above.

The second aspect is that the nature of the lidar used affects the situation, causing deviation from the ideal. Either the lidar signal from some volume elements must be sampled much faster than the above rate (pulsed lidars) or there must be more than one sample of the lidar detector signal per volume element in order to recover the spatial flux information (coherent, CW, focused lidars). In addition there are time interval limitations which tend to limit the coverage of the grids (both types of lidar).

PULSED LIDARS. For pulsed lidars to obtain 1 meter resolution along the lidar beam (a 6.5 nsec pulse length is required), the lidar detector signal must be sampled about every 6 nsec during the flight time of the pulse ($\Delta t = 2\ \Delta r/c$), or at a 167 MHz sampling rate. Such rates can be accomplished with some transient digitizers. Sampling on a 100 m length along the lidar beam implies a group of 100 samples, each sample at this rate. With 1 msec between such sample groups of 100 the entire grid volume, at 1 m x 1 m x 1 m resolution, can be sampled in one second. With 10 bits resolution per sample this would give 125 kbytes per second for the average sampling rate.

There are two limitations to the above aside from detector/logrithmic-amplifier problems discussed elsewhere. The first is that at 200 MHz sampling rates the maximum sampling resolution is effectively 6½ to 7 bits (advertised as 8 bits), not the 10 bits desirable for signal range and accuracy. Ten bits at much lower sampling rates is possible, but 10 bits at 200 MHz sampling rate is out of the question in the foreseeable future (Campani, 1984) [for waveforms arriving at more than 20 Hz]. Seven bits effective sampling resolution at 1 meter resolution along the lidar beam at 5% digital flux accuracy

implies a minimum transmittance of $T = 4.4 \times 10^{-2}$ across the cloud at the lidar wavelength with no leeway for maximum-signal/maximum-digitizing-voltage mismatch. (Detector/logrithmic-amplifier effects [see the T^2 problem section] and--at near-visible wavelengths--multiple scattering effects begin to appear at cloud transmittances of this size also.)

At 6 meters horizontal spatial resolution (cases B and D), with the lidar beam also horizontal, the necessary sample rate along the beam axis is 28 MHz. At this rate appropriate, advertised 10 bit and 12 bit transient digitizers are available.

Thus the limitations of transient digitizers cause the desirable accuracy of 5% to not be achievable with pulsed lidars on the ground with 1 meter spatial resolution along the lidar beam (cases A and C) unless the cloud transmittance is above 4×10^{-2} at the lidar wavelength. This limitation arises because the pulsed lidars necessarily sample the cloud along the lidar optical axis at effectively half the speed of light. Transient digitizers do not prevent the desirable accuracy to be closely approached with pulsed lasers of no more than 39 nsec pulse length for cross-cloud transmittances of $T = 10^{-3}$ with 6 m horizontal spatial resolution (cases B and D) and a horizontal lidar beam. (Note the "desirable accuracy" is just that, essentially a best case accuracy.)

There is another limitation of pulsed lidars which must be considered, that is the pulse rate of the laser transmitter. Pulse rates required for a lidar on the ground to cover the grid examples being considered are given

in Table VII. Current pulsed lidars used in smoke/obscurant work run at pulse rates of 100 Hz and 10 Hz, allowing coverage of the cross-sectional examples, but allowing the full volume scan in only one situation--coarse resolution (case C) with 4 second coverage with the 100 Hz pulse rate.

TABLE VII. PULSED LIDAR PULSE RATES REQUIRED TO COLLECT DATA IN CASES A THROUGH D FROM THE GROUND

REGION SCANNED	HORIZONTAL RESOLUTION	CASE	PULSES PER SECOND FOR 1 SECOND COVERAGE	PULSES PER SECOND FOR 4 SECOND COVERAGE
Full Volume (100 m x 100 m x 10 m)	Fine	A	1,000	250
	Coarse	B	170	43
Vertical Cross Section (100 m x 10 m)	Fine	C	10	2.5
	Coarse	D	10	2.5

The digitizing bit-accuracy requirements would be relieved if the dynamic range of the return signal could be reduced. This can be done, without lessening the cloud densities handled, by putting the lidar above the cloud. For example, with $T = 10^{-3}$ across the 100 m horizontal distance in a uniform cloud (and therefore a dynamic range of $T^2 = 10^{-6}$ for a horizontal-beam lidar) one finds, with T_v the transmittance across the 10 m vertical distance, a dynamic range of only $T_v^2 = 0.25$ for the aerosol signal in a vertical-beam lidar. An accuracy of 1:20 (5 bits) and an amplitude range of 1:4 (2 bits) require only 7 bits without a logarithmic amplifier. With a logarithmic amplifier, only 5 bits are required allowing more leeway for peak voltage mismatch. A 200 MHz transient digitizer at 7 (effective) bits allows data to be obtained at the desired 1 m spatial resolution at the desired accuracy. Thus the top-down pulsed lidar use has the advantage of much less T^2 effect.

Note that detector/loga.ithmic-amplifier and multiple-scattering problems are also relieved. (The advantage of top-down lidar use with dense obscurants was mentioned by Ed Uthe of SRI in the survey).

The $T^2 \approx 1$ tracer technique [ignoring transmittance effects and assuming the lidar signal from distance r is directly proportional to $\beta(r)$] could be used with the desirable accuracy in the top-down approach for 100 m transmittances of about 0.77 and greater as T_v^2 would then be about 0.95 and greater so error in the assumption of $T \approx 1$ would be less than or about 5%.

Putting aside problems of knowing sampling volume positions using high towers and/or aircraft as lidar platforms, the major problem with top-down lidar use with pulsed lasers is that the pulse rate requirements are significantly higher to cover the same amount of cloud region in a given time. This is because the short vertical dimension of the cross section to be covered by repetitive pulsed scanning from the ground is replaced by a longer, horizontal dimension in the cross section to be scanned from above. This is shown in Table VIII. Note that case B is still accomplishable at 4 sec coverage time with a 100 Hz pulse rate but at 10 Hz pulse rate only the 4 sec coverage of the coarse-resolution cross-sectional case (case D) can be achieved.

TABLE VIII. PULSED LIDAR PULSE RATES REQUIRED TO COLLECT DATA IN CASES A THROUGH D FROM ABOVE (TOP-DOWN)

REGION SCANNED	HORIZONTAL RESOLUTION	CASE	PULSES PER SECOND FOR 1 SECOND COVERAGE	PULSES PER SECOND FOR 4 SECOND COVERAGE
Full Volume (100 m x 100 m x 10 m)	Fine	A	10,000	2,500
	Coarse	B	289	72
Vertical Cross Section (100 m x 10 m)	Fine	C	100	25
	Coarse	D	17	4

Adarsh Deepak of STC Corporation is looking into the feasibility of a pulsed, multiple beam lidar, where each pulse output is divided up along multiple beams, like the tines of a fork. Individual detectors and digitizers would be required for each beam. For such a system the pulse rate requirements of Tables VII and VIII above would then be divided by the number of beams.

COHERENT CW LIDARS. The deviation from the ideal data rates in focused continuous (CW) coherent systems does not arise from light time-of-flight considerations because this type of lidar collects data from its focal volume and samples along its beam axis by using small, rapid movements of its optics to move the focal volume position. The deviation from the ideal with focused CW coherent systems comes about because the nature of the receiver detector signal requires multiple samples be taken and/or time delays to be made for each volume element for which the backscattered flux is to be obtained.

In focused CW coherent systems the signal from the receiver detector consists of multiple signal components. Each component arises from and is proportional to the scattered field (observed at the lidar) of a particle in the focal volume. To convert the scattered field signals to scattered flux (power) signals a squaring is required, so that the digital sampling accuracy of the detector signal must be ±2.5% (6 bits) to achieve ±5% accuracy in the flux signal. Having the bit requirement for accuracy, we turn to the bit requirement for signal range. Across a cloud transmittance of $T = 10^{-3}$, the flux will drop $T^2 = 10^{-6}$ but the scattered field amplitudes will only drop $(T^2)^{\frac{1}{2}} = 10^{-3}$ (10 bits). As will be seen below, we do not wish to use the logarithm of this detector signal. (Nor is it necessarily needed as the dynamic range of the coherent lidar detector signal is much less than that of the incoherent lidar detector signal. The former signal varies by T

instead of by $T^2 = 10^{-6}$ (20 bits) as does the latter signal.) We, therefore, need at least 16 bits of digitizing resolution in sampling the detector output. One way this can be achieved is with multiple input channels.

The component of the scattered field signal arising from a particle in the focal volume is at the Doppler frequency determined by the velocity of that particular particle. As we want the flux (square) of each of these single scatterer components, we eventually want the integral over the power spectrum of these components or its mathematical equivalent. What we need is basically the sum of the squares of each component of the signal. When we square the detector signal we square the sum of the components and get what we want plus a sum of cross-product terms between the components. It should be noted that each scattered field component has a phase arising from the position of the scatterer in the focal volume. The cross-products terms, therefore, have random phases and tend to cancel in the average but will make a contribution in any one sample. This is speckle, arising from the coherent and focused nature of the lidar. (Pulsed lidars, being unfocused, average speckle over their receiver apertures.) The contribution from the cross-product terms will change as the relative phases of the scattered waves from the different scatterers changes due to the different velocities of the scattering particles in the focal volume. A number of samples must be taken, each with a different cross-product term contribution. This takes time as we must wait for the particles to shift position. An average of a sufficient number of these samples then gives a cross-product-term contribution below the desirable error limit. Principles of coherent, CW, focused lidar, its hardware, procedures, systems and applications are all still in a state of development. Using

every approach now known to reduce the speckle averaging time, it still appears that about 100 μsec must be spent at each volume element position to obtain 5% error in the flux signal from that volume element. Four hundred samples need to be taken for each volume element. This implies 4 MHz multi-channel digitizing, followed by multiplexing, squaring and summing by a dedicated processor [though an appropriate commerical, general purpose processor should be available in one year], followed by output of one value per 100 μsec to a general processor for storage and manipulation.

The 100 μsec time interval per grid volume element with 1 m separation between elements is compatible with, but near the limits of the focal volume scanning techniques available today, a scanning velocity of about 10^4 m per second along the lidar optical axis. (The limitation is a cycle-time limitation so one would do worse by scanning the 100 m x 100 m x 10 m high grid volume from above.) Using this scanning rate, about a tenth of the grid volume of cases A and B may be scanned in 1 second, 4/10 in 4 seconds. (For case B the 100 μsec speckle averaging time could be increased.) Cases C and D, the fine (1 m) and coarse (6 m) resolution cross-section scans, may be done with ease.

There is an approach that cuts the speckle-averaging dwell time to 10 μsec, considerably increasing the relative error in the local σ determination but keeping the residual random error due to speckle in the integrated σ over a 100 m path at or below the desired 5%. The digital data collection constraints are, on the front end, the same, and on the back end, are a bit more difficult than those of the case above. Using this approach and a focal-volume scanning technique 10 times faster than the present one, the entire grid volume of cases of A and B could be scanned in 1 second.

SUMMARY. Pulse rate considerations limit the current fastest (100 Hz) pulsed lidars to coverage of the full, data-gathering volume used as an example (100 m x 100 m x 10 m) only every 4 seconds at the coarse (6 m x 6 m x 1 m) resolution. Regardless of pulse rate considerations, data collection from the finer spatial resolution examples (1 m x 1 m x 1 m), both whole-volume and cross-section, cannot be done from the ground with the desirable error of 5% unless the cross-volume (100 m) transmittance is increased above 4×10^{-2}. (Transient digitizer bit rates and detector/logarithmic-amplifier properties give rise to this.) From the air (top-down), due to increased vertical transmittance because of the shorter paths involved (and, therefore, a decreased requirement for bits per sample), the fine spatial resolution cases can be handled at the horizontal cross-cloud transmittance of $T = 10^{-3}$ used in the example aside from cloud-volume and cross-section extent considerations. The volume and cross-sectional coverage restrictions due to pulse rate are more severe from the air, however, than with ground-based lidars. For example, pulse rates from the air must reach 100 Hz to collect data from the 1 second coverage, fine-resolution cross-section example used here, from which data can be collected from the ground at 10 Hz, although the latter must be at reduced maximum cloud density. The example at reduced spatial resolution and increased coverage time allow the pulse rate requirement to be reduced considerably.

For CW, coherent focused lidars, current focal-volume scanning rate techniques limit the fractional coverage of the grid volume used as an example here to around 0.1 in one second and 0.4 in four seconds. Data collection from the cross-section examples should be accomplishable with ease. In both

the cross-section and full-volume examples used here, fine and coarse spatial resolutions made no difference as to performance limits. (Current, scanning cycle-time limitations give rise to this result.)

This analysis has not considered the effects of mismatch of the lidar sensitive volume to the spatial volume elements. It has assumed that these match and that the data taken from one is the same as that which would be taken from the other, or its equivalent. It has also assumed that noise floors will not be encountered over the dynamic range of the lidar signals and that the desirable backscatter-to-attenuation coefficient relationship in the smoke is sufficiently constant that the desirable 5% systematic or residual error can be achieved.

Note, from the discussion of this section, the huge amount of data that will be generated from a trial. This amount comes directly from cloud structure sizes and the physics of the interaction of E-O radiation with a smoke/obscurant cloud and the desirability of collecting data useable with almost all E-O system positions relative to the cloud. With the data, the trial can be run, by computer, again and again, making observations along an arbitrary line of sight, or freezing the cloud in time for examination from various angles. If the lidar effort is successful, each field test from which lidar data will be taken will be essentially a repeatable experiment that can be run again and again.

RECOMMENDATIONS. Assuming the desirable spatial resolution and temporal resolution requirements of the preceding section are confirmed--this section is based on these requirements--it becomes evident from this section that further development will be highly desirable to increase volumetric scanning

and data rates. This effort should be of major importance. Application of this effort to one of the various types of lidars used in smoke/obscurants and/or tracer clouds should be done, however, only after it is known that useful data can be obtained by using that type of lidar. For example, for lidars used in smoke/obscurants, this effort should be made after it is known that the backscatter-to-attenuation coefficient relationship is sufficiently constant in important smokes at the wavelength of the lidar, or that any significant multiple-scattering effects can be overcome so that useful data can be obtained from that type of lidar. The needed increase in scanning/data rate capability, however, should be at the back of the lidar developers' minds at all times and various possibilities lined up for trial when the other more fundamental problems are solved, leaving the restrictions in this area to be the major ones.

I. USE OF TRACERS (SIMULANTS)

INTRODUCTION

Figure 17 shows what appears to be a smoke plume issuing from a stack. However, Figure 18, a photograph of the same stack taken in visible light, shows no smoke plume being emitted. What appears to be smoke in Figure 17 is actually sulfur dioxide, a gas which absorbs at the utltraviolet wavelength with which the photograph of Figure 17 was taken. This leads us to consideration of the use of tracers.

If a smoke/obscurant is a passive additive to the atmosphere, and if, once the spatial distribution of its properties are established at some initial time, the spatial distribution of its properties at some later time are all determined by the transport and diffusion caused by the atmosphere, the use of a tracer to determine the results of this atmospheric transport and diffusion in an otherwise relatively clear atmosphere may lead to the determination of the properties of any smoke/obscurant cloud with the same relative initial conditions as the tracer cloud.

The use of a tracer cloud may well make the lidar developer's problems much less difficult by avoiding or ameliorating, for example, such problems as the multiple scattering problem, the T^2 problem and/or the problem due to variation in the relationship of the backscatter coefficient to the attenuation coefficient.

The use of tracers may make it easier for the lidar developer to obtain local optical properties of the tracer throughout the tracer cloud, but such use gives rise to its own problems which must be considered and which are

(a) PHOTOGRAPH TAKEN AT 16:30 EDT WITH A 301.5-nm FILTER AND SHOWING ABSORPTION BY SO_2 (600 ppm at Exit); CENTRAL HALO DUE TO FILTER'S FIELD-OF-VIEW LIMIT

FROM HAWLEY,SRI

Figure 17. Stack at 0.3015 μm in the ultraviolet (Hawley, 1983).

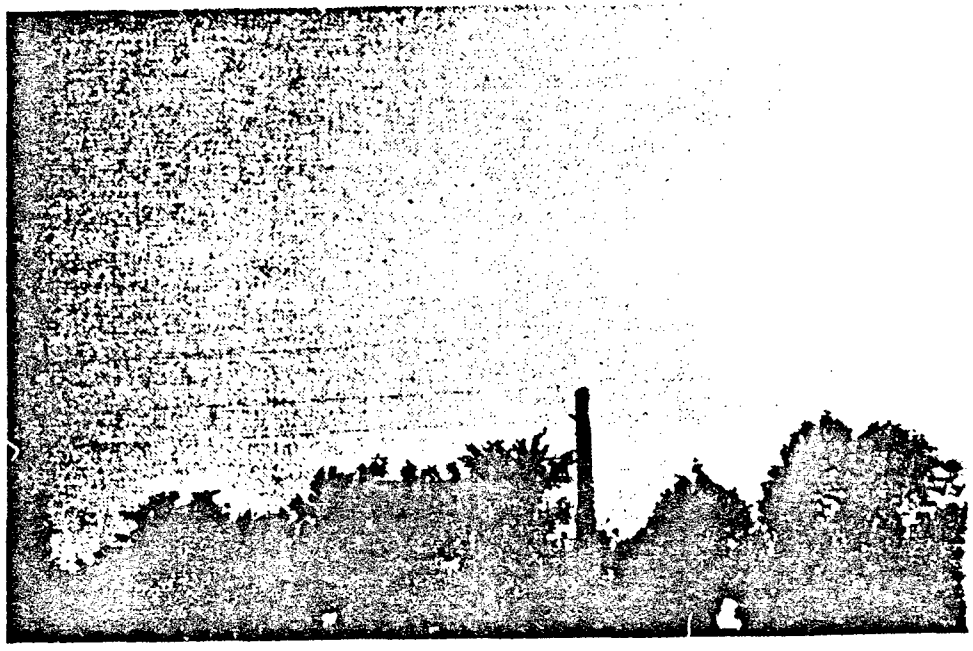

(b) PHOTOGRAPH TAKEN AT 16:45 EDT IN VISIBLE LIGHT

FROM HAWLEY, SRI

Figure 18. Same stack in the visible (Hawley, 1983).

discussed below, namely, the problems associated with relating the lidar-determined optical property of the tracer cloud to the optical property of the similar smoke/obscurant cloud.

First we shall consider various tracer approaches.

USE OF LOW ATTENUATION AEROSOL AS A TRACER

NEGLIGIBLE ATTENUATION. Consider the lidar equation in the form of Equation (4),

$$I(L) = C_1 \beta(L) T^2(L) . \tag{4}$$

If the tracer used is a very low attenuation aerosol so that T^2 is approximately equal to 1 ($T^2 \leq 0.95$ for 5% error), then

$$I(L) \cong C_1 \beta(L) \tag{59}$$

and the (reduced) lidar signal is directly proportional to the local backscatter coefficient of the tracer so that the lidar developer need no longer untangle backscatter effects from attenuation effects. Note that there is no T^2 problem and no multiple-scattering problem, either.

The low attenuation aerosol used may be a special aerosol, it may be the actual smoke/obscurant but extremely diluted, or, in large area screening situations, it might even turn out to be chaff with radar used in place of lidar.

The problems that may be encountered with this approach include obtaining an aerosol sufficiently sparse that $T^2 \cong 1$ but dense enough to give an adequate

lidar signal, avoiding interference from the natural, background aerosol, and having a sufficiently stable relationship between the aerosol backscatter coefficient and the aerosol concentration (the start of the relationship between tracer and smoke/obscurant optical properties).

Chaff has been used as a tracer detected by radar out to 18 km from its source. Its problems include a 30 cm/sec fall speed in still air, ground clutter problems below 100 m height (may be improved by use of 8.6 mm wavelength), variable source output (in one experiment 99.9% of the chaff clumped and fell out of the plume immediately), and relatively coarse resolution -- though the latter may be acceptable in order to get the great range coverage. (See Moninger, 1983 and also Moninger and Kropfli, 1982).

Finally, some other optical property besides backscatter may be detected in an aerosol with negligible attenuation, such as fluorescence. With fluorescence, in particular, the above problem areas may exist along with delay between the absorption and the fluorescence emission by an aerosol particle, causing limited spatial resolution.

LOW ATTENUATION. It may be that with certain aerosols (or with most or certain smoke/obscurants) the relationship between backscatter and attenuation is adequate for lidar signal interpretation, but that difficulties (such as multiple scattering, T^2-related, or far-side boundary-condition problems) that exist with optical depths typical of smoke/obscurants preclude diagnosis with clouds of normal density. It may be possible then to dilute a smoke/obscurant cloud or substitute another cloud of similar source properties so that the local attenuation coefficient, determined in the diluted or substituted cloud by the methods of Section C,

is proportional to the attenuation coefficient which would exist in the actual cloud. This approach would get rid of the problems associated with an aerosol of negligible attenuation.

USE OF A GAS

Another possibility is the use of a gas. The gas must have absorption at lidar output wavelength λ_1 and very low absorption at a second lidar output wavelength λ_2, which must be close to λ_1. The backscattering at both wavelengths is done by the natural background aerosol or an introduced aerosol which must have a backscatter coefficient (and attenuation coefficient) which differs little at the two wavelengths (see Petheram, 1981).

At its simplest, the relevant forms of Equation (4) are, at λ_1,

$$I(L) = C_1 \beta_A(L) [T_G(L) T_A(L)]^2 \tag{60}$$

and, at λ_2,

$$I(L) = C_1 \beta_A(L) T_A^2(L) \tag{61}$$

where the subscript A refers to the aerosol and the subscript G refers to the tracer gas. In Equations (60) and (61) it is assumed that any differences in C_1 at λ_1 and C_1 at λ_2 are already compensated. (Compensation of the C_1's can be tested without the gas present.) Taking the ratio of the lidar signals

in Equations (60) and (61) gives

$$\text{RATIO}(L) = T_G^2(L) \ . \qquad (62)$$

Equation (62) is of the form of Equation (32) of Section E and its solution (for the local attenuation coefficient of the gas) follows accordingly. The extinction coefficient for the gas (the ratio of the attenuation coefficient of the gas to the concentration of the gas) is determined from laboratory data and its application to the attenuation coefficient at a point in the gas plume gives the concentration of the gas there. (Equation (61) assumes negligible absorption by the gas at wavelength λ_2. This need not be the case, as otherwise the solution from the ratio of Equations (60) and (61) will give rise to an attenuation coefficient difference which is also proportional to gas concentration with the constant of proportionality obtainable from laboratory data.)

Note that the spatial scales in the smoke/obscurant cloud and in the tracer cloud, both occurring in the atmosphere, are the same. In fact, the tracer source should mimic the smoke/obscurant source so that, apart from optical properties, the two clouds would be identical in identical atmospheric winds and turbulence. Thus the desired spatial resolution in a tracer cloud will be the same as that which would be desired in the smoke/obscurant cloud and the analysis of Section E, applicable to the form of Equations (32) and (62), indicates (see Table II) that fair to considerable optical depths will be required in the gas plume to achieve such spatial resolution.

Most differential absorption lidar (DIAL) work (as the subject area we are discussing is called) has been directed toward environmental problems and oriented toward detection of trace and pollutant gases, using back-scattering from the natural background aerosol. As such, the spatial and temporal resolutions with which current systems work are much coarser than required for typical Smoke Week trial work, but these may be useful for larger areas of a few square kilometers. (See parts 1 and 3 of Killinger and Mcoradian, 1983.)

GENERAL PROBLEMS IN TRACER APPLICATION

Every tracer solution, to have value, must indicate an optical property of the smoke/obscurant cloud being simulated with some degree of accuracy once the lidar-determined tracer-cloud optical property is recovered. The path this takes is as follows:

Optical Property of Tracer
↓
Concentration of Tracer
↓
Concentration of Smoke/Obscurant
↓
Optical Property of Smoke/Obscurant .

While the use of a tracer may make the lidar developer's problem easier, it may complicate the problem as a whole. The question is: Does the lidar-determined local value of a tracer-cloud optical property correlate well with the value of the desired smoke/obscurant cloud optical property which would have occurred at the same location and time if a smoke/obscurant cloud had been released instead of the tracer cloud? That is: Does the above chain

allow the local value of the desired optical property of the smoke/obscurant cloud being simulated to be determined to useful accuracy?

The relationship of an aerosol optical property to the concentration (mass of particles per unit volume of air) will be discussed in the next section, but assume, since the tracer is chosen, that the lidar-determined value of the optical property of the tracer at a position indicates with little error the value of the tracer concentration at that point. This is the first link in the above chain.

Consider the second link. For the concentration of the tracer (or simulant) to imply the concentration of the smoke/obscurant, the buoyancy of the tracer and the buoyancy of the actual smoke/obscurant cloud must be matched, the initial spatial distribution of the actual smoke/obscurant cloud must be matched by the initial spatial distribution of the tracer cloud and, if sedimentation or evaporation are present in either smoke/obscurant or tracer, they must be matched or the results corrected to account for them.

Finally, concerning the third link in the chain, if, for example, the attenuation coefficient distribution in the smoke/obscurant cloud is desired, and the lidar-determined tracer cloud property is a good indicator of actual smoke/obscurant concentration, is the smoke/obscurant extinction coefficient sufficiently constant and/or well known to get a useful smoke attenuation coefficient value from each indicated value of smoke concentration?

Thus, it appears that a great deal may have to be known about the actual smoke/obscurant being simulated by the tracer before the tracer technique can be used with confidence.

If dilution of a smoke/obscurant may be used, many of these problems may be much more minor.

SUMMARY AND RECOMMENDATIONS

This section simply outlines some of the possible approaches to using tracers (simulants) in place of actual smoke/obscurant clouds and mentions some of the advantages and problems which will be encountered. Simulants should not be used unless the problems in the lidar diagnosis of actual smoke/obscurant clouds should turn out to be too great to overcome. Their use is a natural for the lidar developer, it makes his problems ever so much easier, but the real problem in using a tracer, in most cases, will be in determining the meaning of the lidar-determined tracer cloud values in terms of the smoke/obscurant cloud being simulated. If a diluted smoke/obscurant cloud may be used, this problem may be much less severe as the dilution may not need to be very great (1:4, for example).

J. ON CONVERSION OF OPTICAL CLOUD PROPERTIES TO PHYSICAL AEROSOL-PARTICLE PROPERTIES

INTRODUCTION

PEELING THE ONION. As is clear from the preceding sections, valid interpretation of lidar signals will recover local values of a cloud optical property, most likely the attenuation coefficient, but possibly the backscatter coefficient or some other property. These values are applicable to volume elements (lidar sensitivity volumes) of dimensions much smaller than the cloud but still large enough to contain great numbers of aerosol particles. The cloud optical property these values describe, either by itself or in conjunction with another cloud optical property, gives rise to the lidar signal. This cloud optical property arises from the physical properties of the aerosol, but, like peeling an onion, one must be able, from the lidar signal, to obtain the cloud optical property values which give rise to it, and then, from these values, one may be able to obtain some idea of the physical aerosol properties which give rise to that cloud optical property.

ON FURTHER REDUCTION OF SMOKE/OBSCURANT OPTICAL PROPERTIES. While there are many reasons for desiring to obtain the physical properties of a smoke/obscurant aerosol, it should be noted that the effect of a smoke/obscurant cloud on the performance of any E-O system is based on, and described by, cloud optical properties regardless of the aerosol particle properties which determine them. If the cloud being interrogated by the lidar is a smoke/obscurant cloud and the attenuation coefficient is determined, this, in itself, is an important (if not the most important) cloud optical property for prediction of E-O system operation at the wavelength of the lidar in the presence of

this cloud. It certainly seems (as will be seen below) that the best values of the scattering and/or emissive cloud properties at the lidar wavelength (which are the other cloud properties also affecting E-O system performance), or the cloud optical properties at other wavelengths, can be obtained directly from the lidar-determined attenuation coefficient (assisted perhaps by other inputs) using empirical relationships with empirically-determined variance, rather than by trying to use lidar data to determine physical aerosol properties and then using these properties to calculate the other needed cloud optical properties, even if this last calculation could be readily made.

THE PHYSICAL PROPERTIES OF AEROSOLS AND AEROSOL PARTICLES

We divide the physical properties of an aerosol into two major categories. The first category contains a single property having to do with amount, and is in that sense a category concerning an absolute, as opposed to a relative, quantity. The aerosol property used in that category is either the mass (or volume) of material making up the particles in a unit volume of atmosphere, the concentration (or volumetric concentration), or the property is the number of particles in a unit volume of atmosphere, the particle number density.

The second category is made up of the local distributions of the relative particle number over the possible particle compositions, particle shapes and particle sizes.

The concentration is more used in smoke/obscurant work as an experimental indicator of absolute amount than is the number density or volumetric concentration. Most instruments which directly measure amount deposit particles from a known atmospheric volume and weigh the deposit, a simpler, faster concept in dense aerosols than counting all the particles (or counting all the

significant particles) in a volume of atmosphere or directly determining the total volume of the particles per unit volume of atmosphere. The value of a cloud optical property obtained per unit mass (or per unit volume of particles) is logistically of interest for that part of the mass which issues from the smoke munition or smoke generator, and this reinforces the use of the concentration.

(Use of the concentration as the amount property does have the disadvantages of bringing the density, a non-optical parameter, into the picture and disallowing direct, in-situ measurement, as there currently exists no known way of measuring the mass of the particles while leaving them in the air.)

The property of the material(s) in a particle that determines its optical (i.e., electromagnetic radiation) properties is the complex index of refraction, or alternatively, the complex dielectric constant. This property, in either form, is a function of wavelength. The percentages of particles made up of various materials, and so having various values of the complex index of refraction at the wavelength of interest, is what is meant by the composition distribution. More correctly, allowing for more than one material within a particle, the composition distribution is the percentages of particles having various volumetric fractions of each particle described by the various values of the complex index of refraction. (Even small amounts of certain materials on the surfaces of certain particles can make significant differences in the optical behavior of the particle.)

For each composition there is a shape distribution. Here, describing shape means describing the boundaries on which electromagnetic field boundary conditions would apply. So we include in the shape distribution description

the surface roughness, the distribution of the various materials within a particle, and the (contact) clustering of particles. While there is no known way to parameterize arbitrary shapes, particularly to parameterize shape in terms meaningful to optical scattering and absorption properties, one can imagine the existance of such a parameterization.

For each composition and shape there is a particle size distribution.

In considering the physical properties of an aerosol:

Concentration,

Composition Distribution,

Shape Distribution,

Size Distribution;

it can readily be seen that a number of parameters will each need to be assigned a value in order to obtain a physical description of even a simple aerosol. Certainly much more than the value of one local, cloud optical property will be required to obtain these parameter values and so to describe the physical properties of an aerosol at that location; however, the value of one optical property is the most that can be recovered using a single-wavelength lidar.

Below we shall first consider the possibility of the distribution properties (and the density) remaining sufficiently constant that a relationship can be established between the lidar-determined optical property and the concentration. Then we shall consider, using a few examples, recovering information concerning the distribution properties.

ON CONVERTING THE LIDAR-DETERMINED OPTICAL PROPERTY TO CONCENTRATION

We consider here the conversion of the local, lidar-determined optical property to a concentration value. We shall write in terms of the lidar-determined property being the attenuation coefficient, σ, but, except where specific measurements and situations are referred to at the end of this subsection, this may be replaced by the actual lidar-determined property if it should be different.

The relationship between the attenuation coefficient, σ, and the concentration, C, at a location, $\underline{R}$, and time, t, in an aerosol cloud may be written in completely general form as

$$\sigma(\underline{R},t) = \alpha(\underline{R},t)\ C(\underline{R},t) \tag{63}$$

as $\alpha(\underline{R},t)$, the extinction coefficient, may take on the value $\sigma(\underline{R},t)/C(\underline{R},t)$ at each location, $\underline{R}$, and time, t, and so make Equation (63) an identity at each $\underline{R}$ and t. We note that $\sigma(\underline{R},t)$ and $C(\underline{R},t)$ are both proportional to the particle number density so that $\alpha(\underline{R},t)$ cannot depend on the particle number density. (An argument similar to that given between Equations (7) and (8) is being followed.) The extinction coefficient, $\alpha(\underline{R},t)$, is dependent upon the particle size distribution, the particle shape distribution, the particle composition distribution and the effective density of a particle. If these vary between clouds or in a cloud then $\alpha(\underline{R},t)$ will vary between clouds or in a cloud. But these should vary much less than the particle number density in a cloud, as the latter will vary from near zero, in eddy volumes of clear air folded into the cloud by turbulent mixing, to very high values, in eddy volumes injected

with aerosol particles at the aerosol source. So $\alpha(\underline{R},t)$ will vary much less than the two quantities $\sigma(\underline{R},t)$ and $C(\underline{R},t)$ it relates.

The question is how much $\alpha(\underline{R},t)$ will vary from cloud to cloud and within a cloud and whether that variation is sufficiently small to allow Equation (63) to give a useful relationship between $\sigma(\underline{R},t)$ and $C(\underline{R},t)$. The measurement of the variation of $\alpha(\underline{R},t)$ can be done by demonstrating the capability to measure $\alpha(\underline{R},t)$ with little variation in the results in situations where $\alpha(\underline{R},t)$ is known to vary little (for example, water cloud at 10.6 μm (Pinnick et al, 1983) or perhaps fog oil at 1.4 μm (Kohl, 1983)), and then immediately measuring the variation in $\alpha(\underline{R},t)$ in the aerosol of interest.

The measurement of $\alpha(\underline{R},t)$ will involve measurement of $\sigma(\underline{R},t)$ and $C(\underline{R},t)$ and their comparison. Cautions would need to be followed which are similar to those earlier made regarding comparison of measurements. (See the recommendations following the sub-section on data accuracy in Section H.) Spatially and temporally resolved determinations of $\alpha(\underline{R},t)$ at several point locations in a cloud would be ideal. These would involve local, time-resolved, σ determinations and time-resolved C determinations, such as obtained with a TEOM (tapered element oscillating microbalance). Such measurements have been made to some extent at one location (PCIS trailer) at several past Smoke Weeks. (Concentration instrumentation by its nature takes point or local samples.) Relaxing from the ideal to time-integrated σ and C determinations would allow chemical impingers to be used for the time-integrated concentration (dosage) measurement. Relaxing from the ideal still more allows time- and path-integrated σ and C measurements for comparison between different paths in one cloud and between different clouds. Such measurements, made by DPG, were standard at past Smoke Weeks.

In comparing α-data taken by different methodologies, however, in clouds of the same type, the α values measured in some smoke/obscurants are seen to separate systematically according to the methodology used (Kohl, 1983). This effect remains unexplained despite its being known for some time. Its unexplained existance casts doubt on the validity of all the α values obtained and the techniques used to obtain them, and needs to be resolved so that determination of the variability of α in various smoke/obscurants and aerosols can proceed.

Little has been done regarding the variability of the relationship of the backscatter coefficient to the concentration. Pinnick et al (1983) have investigaged the relationship in water clouds from the visible to the mm wave region and found it very dependent on the particle size distribution.

ON CONVERTING LIDAR-DETERMINED OPTICAL PROPERTIES TO THE OTHER PHYSICAL AEROSOL PROPERTIES

Before citing a few examples involving the use of lidar, we shall consider the results of a calculational investigation that has been going on for several years involving several investigators obtaining size distribution information from given scattering coefficient information--Bottiger's calculation experiment at CRDC.

The particles are known to be spheres; thus there is no distribution over shape. The index of refraction of the single material making up the spheres is known as a function of wavelength; there is no composition distribution. The investigations of interest to us are those involving the backscattering coefficient. This is given at a number of wavelengths. Still a maximum of only 1% to 5% random (simulated) experimental error can be

tolerated in the backscatter coefficient data supplied, if the calculations are to invert the data and obtain the major parameters of a bi-modal size distribution that underlies them--that is, to obtain the two peak locations, the width of each mode and the relative size of the peaks (Kiech, 1984). With backscatter coefficient data at 15 wavelengths from 0.2 to 10 μm, around 5% error is tolerable.

With a shape or composition distribution also included, the capability will be less (Zuev and Naats, 1983).

Some physical property information can be obtained experimentally under limited conditions. For example, Uthe has found a correlation between mean particle diameter and the ratio of the attenuation coefficient at 1 μm and 0.5 μm wavelength in some sub-micron aerosols (Uthe, 1983).

An idea of the difficulty in obtaining physical aerosol property information optically is indicated by Reagan et al (1982) where absolutely calibrated, backscatter and bistatic lidar measurements in horizontally homogeneous media were combined to obtain an effective index of refraction for all particles (assumed to be spheres) and size distribution parameters for a Junge two-slope model. There was no independent particle composition determination or particle sizing confirmation though inversion of solar radiometry data gave a very similar size distribution.

RECOMMENDATIONS

One must be able to recover the cloud optical property which determines the lidar signal before one can recover information concerning the physical properties of the aerosol particles by using that cloud property; like peeling

an onion, one has to be able to peel the outer layers before being able to reach the inner layers.

The lidar-determined cloud optical property is likely to be the attenuation coefficient, and the relationship of the attenuation coefficient to the concentration in smoke/obscurants is already important for figure of merit reasons aside from using lidar to remotely determine concentration. So the determination of both the relationship of the attenuation coefficient to the concentration (via the extinction coefficient, to use the PM Smoke and CRDC lexicon) and its variability is doubly important, and the current apparent experimental difficulties in this regard need to be cleared up and progress resumed in the determination.

To predict E-O system performance with a smoke/obscurant cloud present, it is the cloud optical properties which must be known. One of these will be determined by the lidar at each wavelength. It certainly appears that the best determination of the others will come from the lidar-determined property values (assisted by other inputs) via empirical relations rather than from trying to determine aerosol-particle properties from lidar-derived optical property values and then using these determinations to calculate the other cloud optical properties desired, if such calculations can be made.

Still, indications of the aerosol physical properties of smoke/obscurants as produced in the field can give important clues to generator function, cloud improvement, etc. We recommend support of knowledgeable basic research in this area to determine how one might obtain, from optical properties observable by lidar, clues to the physical properties of the aerosol particles, particularly those properties that may be important in current and candidate smoke/obscurants. It should be understood that any such techniques will be

complex, will contain uncertainties, and will be limited in their capabilities and the types of obscurant to which they will be applicable.

K. SAFETY AND HAZARD CONSIDERATIONS

Here the word "nonhazardous" implies radiation that is safe with respect to the bare eye, the optically-aided eye, and the bare skin; safe as far as all current knowledge indicates. A lidar situation that is hazardous can be made nonhazardous by applying protective gear, using indirect viewing, clearing areas, etc.

A hazardous lidar in smoke/obscurant testing generally increases the nuisance level considerably but does not usually prevent other measurements from being made. This is because the smoke cloud area being diagnosed is cleared of personnel even without the presence of the lidar. Closeup personnel, however, who are viewing the scene directly (rather than via video monitors) may (depending on lidar wavelength and geometric situation) need laser goggles to protect them from specular reflections or direct viewing. Further, the ground and air space painted by the lidar with hazardous levels of radiation, whether by direct radiation or specular or diffuse reflection, should be maintained clear of unprotected personnel.

To obtain nonhazardous use of a hazardous lidar, the methods and guidelines of TB MED 524 (Department of the Army, 1984), supplemented by the Sliney and Wolbarsht handbook (Sliney and Wolbarsht, 1980), should be followed. The use of optically-aided viewing by the human eye must be considered in the wavelength region 0.330 to 4.200 μm (see the appendix "Detailed Technical Hazard Analysis" in TB MED 5234). Atmospheric scintillation effects at all wavelengths may be considered (see the appendix just cited, (Johnson et al, 1970) and (Dabberdt and Johnson, ~1971)) though such effects are currently

believed to be within the safety margins of non-scintillation, nominal hazard calculations (Marshall, 1984).

A nonhazardous lidar should be judged as nonhazardous by using the guidelines of the references mentioned in the previous paragraph.

The Laser/Microwave Division of the US Army Environmental Hygiene Agency (Aberdeen Proving Ground, Maryland 21010) can be used for consultation regarding unusual situations (Av 584-3932/3468 or Commercial 301 671-3932/3468).

It may be noted that radiation of wavelength about 1.4 μm and longer does not penetrate to the retina, and the eye-safe radiation levels for such radiation are the same as for the skin. For this reason, and because many materials transparent to visible radiation are very opaque in common regions of the infrared, hazards in this wavelength region are typically more easily dealt with than are those at shorter wavelengths.

RECOMMENDATIONS

It would be better to have a working smoke/obscurant diagnostic system that is hazardous to unprotected personnel near the lidar than to not have such a system at all. Since the potential payoff from such lidar use is great, since the technical lidar difficulties are also great and since the additional protective constraints required for safe use of a hazardous lidar are not particularly difficult in a typical test situation (though a nuisance), the imposition of a requirement for nonhazardous operation for unprotected personnel at the output of the lidar should not be made. Nor should lidar development in one wavelength regime be preferred over another based on reduced hazard considerations. Minimization of the spatial region and time periods in which a

diagnostically satisfactory lidar is hazardous to unprotected personnel should always be pursued.

The lidar developer should know what safety precautions are required in what areas under the guidelines of the above references. He should be sure that these safety precautions can be met in typical test exercises, particularly any precautions involving long ranges. He should be aware of any specular surfaces in the test area and any changes they require in the required safety precautions.

Further, regarding potential hazard to, or interference with optical instruments operating at the same wavelength as the lidar, the lidar developer should furnish typical irradiance and beam cross-sectional area values as a function of distance from the lidar to those considering operation of such instruments simultaneous with the lidar operation in a test.

III. RECOMMENDATIONS

A. GENERAL RECOMMENDATIONS

INTRODUCTION

It is the problems that impede progress that need to be dealt with in order to make progress, and so it is the problems on which this report concentrates. But in immersing oneself in the problems and in seeking solutions to them, one must not lose sight of the fact that the potential payoff from the quantitative diagnostic use of lidar on smoke/obscurants is very great, so that dealing with the problems is a worthwhile activity, especially when it is done with insight and with utilization of existing knowledge or with the determination of additional knowledge if that is needed, so that with the best use of resources one can determine which problems can be overcome and how, and which problems must be skirted and how.

RECOMMENDED ROLE OF THE DEVELOPMENT SPONSORS

In the early days the capabilities of lidar as a diagnostic of smoke/obscurants were vastly oversold. This is now recognized by the instrumentation development sponsors, but a hold-over attitude from those days tends to remain in some places, that lidar for diagnosis of smoke/obscurants will come off the shelf or from lidar development for other use.

The smoke/obscurant diagnostic lidar requirements include optical depths and space and time scales not found anywhere else. While experience and instrumentation from other fields should be utilized as much as possible, the smoke/obscurant lidar development effort must be undertaken so as to answer

the key questions of smoke/obscurant lidar diagnosis and to overcome or avoid the problems unique to diagnosing smoke/obscurant clouds with lidar.

Efforts must be focused on the questions which will not be answered unless answered by those interested in developing lidar for use as a diagnostic of smoke/obscurants.

The development sponsors must go beyond the role of setting (lidar) instrumentation criteria and determining whether or not they are met, to seeing that the existing technical knowledge is utilized in order that efforts are directed at the key questions to be answered, that efforts are directed where there is the greatest potential for gain from that effort and that aspects of these efforts critical to these aims are supported and encouraged.

Reasonable and useful technical goals for the short-term and ultimate uses of lidar in smoke/obscurant diagnosis need to be developed in conjunction with those experienced in the area. These need to be promulgated, and then they should be revised as more is learned and additional requirements may be laid on by data users. There is currently some uncertainty among some lidar developers about what is desired, just as there is currently an uncertainty among sponsors of that development about what is achievable.

This report has been focused on problem areas. Where it touches on technical, lidar development goals (such as in Section H) its statements should be critiqued by the development sponsors. Perhaps these critiques could serve as a basis, or part of the basis, for the technical goal development mentioned above.

RECOMMENDED INFORMAL MEETING OF SMOKE/OBSCURANT-RELATED LIDAR DEVELOPMENT GROUPS

Of those groups actively working in smoke/obscurant lidar development, no one group has a corner on expertise. Each group has pushed forward the development of lidar for smoke/obscurant use, but in different areas. Each group has worked very independently in the past without any significant contact between groups. All groups have encountered problems, many of which are common. Each group would benefit greatly from informal, in-depth technical interaction with the others, discussing both their individual achievements and their common problem areas. The overall development effort would benefit, as such an exchange would prevent time being wasted on solving problems already solved by another group and would allow a better attack on unsolved problems due to pooling of ideas and experiences.

Furthermore, the individuals in these groups who have hands-on experience may have viewpoints, conclusions or recommendations regarding the subjects taken up in this report that differ from those given in this report. Any such comments should be aired and documented.

Such a meeting would be small, as each group is small, and would involve six to twelve people. There appears to be an interest in such a meeting among potential attendees. One of the groups has offered its laboratory site as a location.

For such an open information exchange to succeed, participation in the meeting itself by observers (particularly observing development sponsors), rather than contributors, must be minimal. This particular meeting must be one of technical peers,without temptation to play to the grandstand.

B. SPECIFIC RECOMMENDATIONS

BOTTOM-LINE TEST

If any local optical property is determined by lidar along a line of sight, in a cross-section,or throughout a smoke/obscurant cloud, it will be the attenuation coefficient, σ, the fraction of radiation lost to its original propagation direction per unit length of propagation, at the lidar wavelength.

The test of an ideal determination of this property is that the values of the attenuation coefficient determined by lidar along a straight line path through a smoke/obscurant cloud, when integrated over that path ($\int \sigma \, dL$), agree with the negative natural logarithm of the transmittance ($-\ln T$) at the lidar wavelength as independently determined by a transmissometer operating over that same path,

$$-\ln T \stackrel{?}{=} \int \sigma \, dL \ . \tag{64}$$

Ideal agreement (derived in this report--see Part II, Section H) exists when differences in the two quantities are less than the fluctuations in these quantities. The cloud volumes and time intervals contributing to the two quantities compared should be the same as much as possible. Matching to dimensions small compared to 1 meter and to times small compared to 1 meter divided by the wind speed should be ideal (see Part II, Section H), but the horizontal dimension and time coincidence can be relaxed if good correlation exists over larger horizontal up-wind distances than 1 meter. (The current

uncertainties with respect to transmissometry measurements need to be understood and cleared up.)

The transmissometer path may be radially outward from the lidar (along the lidar beam) to save the expense of scanning hardware in a developing lidar system, but eventually transmissometer paths along non-radial directions, horizontally and vertically, should be used with lidar scanning in all types of smoke/obscurants.

STEPS TO PASSAGE OF THE BOTTOM-LINE TEST

While the above comparison should be available when lidar is operated in smoke/obscurant clouds as it is being developed, there are intermediate steps to be taken to determine physical possibilities and ultimate limitations, and to overcome problems already known to exist.

These are stated in order of priority.

EFFECT OF AND AMOUNT OF RELATIVE VARIATION BETWEEN BACKSCATTER AND ATTENUATION IN SMOKE/OBSCURANT CLOUDS

All current lidar approaches use lidar signals affected by both the backscatter and the attenuation taking place in smoke/obscurant clouds. In order to use such signals quantitatively, some relationship, and a fixed relationship, must exist between the backscattering and the attenuation along a lidar beam path in such a cloud (see Part II, Section B). What appear to be significantly large variations are observed in current lidar data in a parameter which will vary if the backscatter-to-attenuation relationship varies in smoke/obscurant clouds. It must be determined (a) how much variation in

the backscatter-to-attenuation relationship can be withstood before the techniques used to recover useful information from the lidar signal are worthless, and (b) how much of such variation there is in smoke/obscurant clouds. If (b) is larger than (a), none of the current lidar approaches can work, no matter how good their hardware. (See Part II, Section B and Section D.) If this turns out to be the case, the recommendations concerning Sections E, I and J of Part II move to the top of the priority list and the following recommendation would be dropped.

INTERPRETATION IMPROVEMENT

Current techniques used to obtain quantitative information from the lidar signal (interpretation techniques) contain restrictions (to allow evaluation of a boundary condition) which, for example, do not allow the cloud-scanning freedom one needs in low transmittance smoke/obscurant clouds. There are ways around this which show promise and which should be pursued. In addition, there is an interpretation technique which should work in relatively high transmittance clouds which apparently works at lower transmittances than expected and this needs to be checked. (See Part II, Section C.)

DESIRABLE DATA ACCURACY, SPACE AND TIME RESOLUTION,
AND SCANNING/DATA-RATE CONSIDERATIONS

Desirable Data Accuracy. That the ideal error in lidar-determined or model-determined transmittance is small compared to the fluctuations in the actual transmittance even though such error could be relatively large at small transmittances, is a statement that needs critiquing. Also needing critiquing is the figure of approximately 5% as the optimum systematic and

residual random error in lidar-determined attenuation coefficient values, at least at typical Smoke Week source-instrumentation distances and heights. (These are derived in the early part of Part II, Section H.)

Desirable Spatial Resolution. The vertical and two horizontal directional separations of two parallel lines of sight which still allow the differences in the two transmittances along the lines of sight to be somewhat less than the fluctuations in those transmittances needs to be determined in various smoke/obscurants at various distances from the source and at various heights above ground, particularly lower heights. These set the lowest possible optimum spatial resolution (for the attenuation coefficient in the cloud at least) required for any E-O system performance prediction. These separations are estimated in this report (Part II, Section H) to be about 1 meter vertically and 1 to 6 meters horizontally, at least at typical Smoke Week source distances and heights above ground in some smoke/obscurants.

Desirable Time Resolution. The desirable data repetition rates need to be determined for cloud cross-section scans that are fixed with respect to the earth and for whole-cloud scans that may move with the wind. The scan repetition times estimated for both cases are between 1 and 4 seconds (Part II, Section H) at typical Smoke Week source distances and heights. Whether, in particular, the lower time limit for cross-sectional scans is too high needs to be checked. These can be tested with developing lidar systems without complete scanning of cross section or cloud.

Scanning/Data-Rate Considerations. [In priority order this particular paragraph should occur with the recommendation on lidar hardware below.] It

would be very desirable to increase volumetric scanning rates in both coherent and incoherent lidars, but efforts in this direction should be made only after it is known that useful data can be obtained from the type and wavelength of lidar involved, whether from a smoke/obscurant cloud or a tracer (simulant) cloud. This is discussed at length in the last sub-sections of Part II, Section H.

T^2 PROBLEM

The T^2 problem refers to the fact that radiation flux or energy which has been backscattered from the back edge of a cloud gives rise to a signal, in an incoherent lidar where the detector signal is proportional to the energy flux received, which is the order of T^2 less than the signal from the near side of a cloud, where T is the transmittance through the cloud. For example, if T is 10^{-3}, T^2, the dynamic range of the signal, is 10^{-6}. The dynamic range itself is not a problem so much as the speed (half the speed of light) through which it is swept.

The performance limitations of various lidar-candidate incoherent detector and amplifier combinations need to be determined (or verified) using lidar observations of small, dense clouds generated with known back-edge positions as indicated in Part II, Section F. If these limitations turn out to be severe with respect to use in smoke/obscurant clouds, ways around them need to be sought.

In a coherent lidar the detector signal is proportional to the scattered field and so is proportional to T, not T^2. Further, the front to back edge signal range is swept at the much slower rate at which the coherent lidar's

focal volume is optically scanned from front edge to back edge of the cloud. There is one aspect (called a tail effect) where the cloud front edge contributes signal at the back edge, and this needs to be confirmed as not being a problem.

See Part II, Section F for more details.

MULTIPLE SCATTERING PROBLEM

Multiple scattering will not be a problem in optically thin tracer clouds. In the use of lidar on smoke/obscurant clouds, its consideration ranks after the obtaining and demonstrating of a valid interpretation scheme in clouds of transmittance of 10% or less. It is a more pressing, higher ranking problem in the visible and near-infrared than at 10 micrometers.

As no satisfactory theory is yet known for unraveling the multiply-scattered signal in any situation, particularly a general particle, non-uniform obscurant producing a noise-containing lidar signal, the emphasis until such a theory may be developed must be on avoiding the presence of significant multiply-scattered signal contributions, detecting the presence of significant multiply-scattered signal contributions and correcting for that presence in the signal used.

To test the limits of their capabilities in overcoming multiple-scattering effects, lidars should be challenged with obscurants of large particle size and high albedo (at the lidar wavelength) and with situations that challenge the weaknesses in the technique used to detect the presence of significant multiple-scattering effects. The test results need only be the production of valid attenuation coefficient values along various paths

as independently confirmed by transmittance measurements and the valid indication of when and/or where in the cloud such lidar-determined values cannot be trusted.

It would appear from the overview of current approaches in Part II, Section G, that, considering multiple scattering by itself, emphasis should be placed on avoiding or minimizing significant multiple-scattering effects and detecting their presence rather than correcting for them.

LIDAR TYPE AND LIDAR HARDWARE

Satisfactory answers in other problem areas need to be found with higher priority than the determination of one lidar type over another. Indeed, these solutions, or their lack, should play a major role in determining the final desirable lidar type.

In light of the above, fastening on a single lidar type at this time is too premature, instead, with the higher priority problems mentioned above being satisfactorily addressed, remaining resources should be directed to efforts within each lidar type to obtain solutions to those problems limiting the application of that type, particularly in smoke/obscurants. For incoherent lidars this means attacking or finding a way around the dynamic-range (T^2) / time-of-flight problem. In addition, for incoherent visible and near-IR lidars it means seeing if improvements are feasible regarding the multiple-scattering problem. For incoherent lidars at 10 μm it means seeing if appropriate speckle-averaging techniques might be developed. For coherent lidars, whose development is newer, this means obtaining performance closer to design, probing performance limits including speckle averaging, seeing if signal processing can be improved and, finally, scanning velocities increased.

The major emphasis on current lidar systems should be in using them to obtain those answers which impact the use of lidars as smoke/obscurant diagnostic instruments, as a whole, in the various wavelength regions. An idea of the variation of the backscatter to attenuation coefficient ratio, C_o, needs to be determined in the many different smoke/obscurants at the several lidar wavelengths. This variation, coupled with the sensitivity of lidar interpretation schemes to this variation, will determine to what extent backscattering from the smoke/obscurant particles themselves can be used and whether the development of the use of tracers (simulants) needs to be looked at. Incoherent lidars, being better developed than the coherent, need to be used to address the questions of desired spatial and temporal resolution raised above (they can do this with partial cloud scans), though the coherent lidar, with improved speckle averaging, might be able to assist some in this area also. While experience can be gathered and methods developed for handling the large data flows and amounts resulting from lidar use on smoke/obscurants and/or on tracer clouds, this is a situation that will tend to improve with time, by itself, as better equipment becomes available, so that as a current objective for its own sake it should be given a rather low priority.

The basic aspects of the two lidar types are given in Part II, Section B. Other lidar-hardware aspects are discussed throughout Part II where those aspects impact problem solutions or are, themselves, the problem.

SAFETY AND HAZARD ASPECTS

It would be better to have a working smoke/obscurant diagnostic system that is hazardous to unprotected personnel near the lidar than to not have

such a system at all. Since the potential payoff from such lidar use is great, since the technical lidar difficulties are also great and since the additional protective constraints required for safe use of a hazardous lidar are not particularly difficult in a typical test situation (though a nuisance), the imposition of a requirement for nonhazardous operation for unprotected personnel at the output of the lidar should not be made. Nor should lidar development in one wavelength regime be preferred over another based on reduced hazard considerations. Minimization of the spatial region and time periods in which a diagnostically satisfactory lidar is hazardous to unprotected personnel should always be pursued.

The lidar developer should know what safety precautions are required in what areas under the guidelines of the references given in Part II, Section K. He should be sure that these safety precautions can be met in typical test exercises, particularly any precautions involving long ranges. He should be aware of any specular surfaces in the test area and any changes they require in the required safety precautions.

Further, regarding potential hazard to, or interference with optical instruments operating at the same wavelength as the lidar, the lidar developer should furnish typical irradiance and beam cross-sectional area values as a function of distance from the lidar to those considering operation of such instruments simultaneously with the lidar in a test.

USE OF SCATTERING FROM THE ATMOSPHERIC GAS

If an insufficient relationship should be found to exist between the backscatter and attenuation properties of a smoke/obscurant, so that

adequate interpretation of lidar radiation which has been both backscattered and attenuated by the smoke/obscurant cannot be achieved, investigation of the means of obtaining lidar measurements of a local optical property of the smoke/obscurant leads, apparently solely, to consideration of the use of scattering by the atmospheric gas.

The reasonable form of the lidar equation for use with scattering from the atmospheric gases implies the need, if the desirable 5% error in the lidar-determined attenuation coefficient is to be achieved, for experimental error limits which are extremely stringent if 1 meter resolution along the lidar beam is required, but are not too bad if 6 meter resolution is required, as shown in Table II of Part II, Section E. Note that this is another reason for knowing what spatial resolution is required.

The two types of scattering from the atmospheric gas that occur are elastic, where the scattered photon leaves the internal energy of the gas molecule unchanged (Cabannes [Rayleigh] scattering), and inelastic, where the photon changes the internal energy of the molecule (Raman scattering). In Cabannes scattering the principle problem is the elimination of the interference by the radiation scattered by the smoke/obscurant. In Raman scattering, in the approaches outlined, the problem is the scarcity of photons, causing insufficient accuracy at typical smoke/obscurant cloud transmittance values. (In both types of scattering, there will be a tendency to utilize shorter wavelengths, λ, to take advantage of the $1/\lambda^4$ dependence of non-resonant scattering, but the shorter wavelengths are also those at which multiple scattering effects are worse (see Part II, Section G).)

If the relationship between backscatter and attenuation should be found to be inadequate in some smoke/obscurants, these two types of scattering are

apparently the only alternatives short of replacing the smoke/obscurant with a simulant (a tracer) which makes the lidar-determined optical properties at least once removed (and probably several times removed) from the desired optical properties of the smoke/obscurant. (Use of tracers is treated in Part II, Section I.) In such a situation, further investigation would be warranted into use of these two forms of scattering by the atmospheric gas, but, as significant innovation and improvement in the state of the art is required, lidar hardware should not be built for its own sake unless there is a reasonable chance of success--rather, feasibility studies should be made based on existing knowledge or, if progress-preventing gaps exist in that knowledge, these gaps should be filled.

Note also that the effects discussed in Part II, Sections F and G, the T^2 effects and multiple-scattering effects, will apply to the use of lidars in smoke/obscurants whether scattering from the cloud or scattering from the atmospheric gases is observed.

USE OF TRACERS (SIMULANTS)

Part II, Section I simply outlines some of the possible approaches to using tracers (simulants) in place of actual smoke/obscurant clouds and mentions some of the advantages and problems which will be encountered. Simulants should not be used unless the problems in the lidar diagnosis of actual smoke/obscurant clouds should turn out to be too great to overcome. Their use is a natural for the lidar developer, it makes his problems ever so much easier; but the real problem in using a tracer, in most cases, will be in determining the meaning of the lidar-determined tracer cloud

values in terms of the smoke/obscurant cloud being simulated. If a diluted smoke/obscurant cloud may be used, this last problem may be much less severe as the dilution may not need to be very great (1:4, for example).

ON RECOVERING PHYSICAL AEROSOL-PARTICLE PROPERTIES FROM LIDAR-DETERMINED CLOUD OPTICAL PROPERTIES

One must be able to recover the cloud optical property which determines the lidar signal before one can recover information concerning the physical properties of the aerosol particles by using that cloud property; like peeling an onion, one has to be able to peel the outer layers before being able to reach the inner layers.

The lidar-determined cloud optical property is likely to be the attenuation coefficient, and the relationship of the attenuation coefficient to the concentration in smoke/obscurants is already important for figure of merit reasons, aside from using lidar to remotely determine concentration. So the determination of the relationship of the attenuation coefficient to the concentration (via the extinction coefficient, using the PM Smoke and CRDC lexicon) and of the variability of that relationship is doubly important, and the current apparent experimental difficulties in this regard need to be cleared up and progress resumed in the determination.

To predict E-O system performance with a smoke/obscurant cloud present, it is the cloud optical properties which must be known. One of these will be determined by the lidar at each wavelength. It certainly appears that the best determination of the others will come from the lidar-determined property values (assisted by other inputs) via empirical relations rather

than from trying to determine aerosol-particle properties from lidar-derived optical property values and then using these determinations to calculate the other cloud optical properties desired, if such calculations can be made.

Still, indications of the aerosol physical properties of smoke/obscurants as produced in the field can give important clues to generator function, cloud improvement, etc. We recommend support of knowledgeable research in this area to determine how one might obtain, from optical properties observable by lidar, clues to the physical properties of the aerosol particles, particularly those properties that may be important in current and candidate smoke/obscurants. It should be understood that any such techniques will be complex, will contain uncertainties and will be limited in their capabilities and in the types of obscurant to which they will be applicable.

APPENDIX A

DESCRIPTIVE PAGES SENT TO US RECIPIENTS
AND
SMOKE/OBSCURANT LIDAR SURVEY QUESTIONNAIRE

February 1983

SURVEY OF CURRENT AND POTENTIAL POSSIBLE SMOKE/OBSCURANT DIAGNOSTIC LIDAR SYSTEMS

The US Army Project Manager for Smoke/Obscurants would like to know the capabilities of those lidar systems (whether currently utilized, under development or planned) which might be used to diagnose or to assist in the diagnosis of smoke/obscurant clouds produced in field experiments.

Capability is first sought in the mapping of the spatial distribution of a property or properties of a smoke/obscurant cloud made up of a single type of material. If, in addition, further capabilities may exist, such as the possibility of mapping each component of a cloud made up of two component materials, these capabilities would also be of interest.

Lidar systems which will successfully produce useful data (e.g., the spatial distribution of the volumetric attenuation coefficient) from actual smoke/obscurant clouds in the field are of primary interest. These clouds tend to be optically dense and may present other complications so that signal interpretation, transmittance-squared effects and multiple scattering problems could require focusing attention on mapping optically thinner clouds or plumes of other materials released in simulation of smoke/obscurant clouds or plumes. Therefore lidar systems capable of the latter are also of interest.

The smokes or obscurants that may need to be diagnosed could be primarily absorbers or primarily scatterers at any wavelength. The obscurant particles could be liquid or solid. Particle size and shape distributions may be only roughly known and little may be known about the variation of these properties in a cloud. Cloud and plume thicknesses range from a few meters to a hundred meters and more. The cloud being characterized may be the result of continuous generation or an instantaneous event. Transport velocities are those of the atmospheric winds but may be higher near generators.

In typical field tests, smoke clouds can be generated so that the experimentalist can be assured that they will pass through an imaginary vertical rectangle which is oriented across the wind and which is 500 to 1000 meters long by 100 meters or more high.

If you or your organization has one or more lidar systems which might be of use in the above, or have comments, pro or con, which might be helpful, your participation in this survey would be greatly appreciated. Wherever possible, answer the posed questions with a reference to published work or a readily obtainable report, or attach a report to the questionnaire and reference it as appropriate - the idea is to supply the answers needed, if known, with the minimum amount of time and effort on your part. You may not be able to answer all the questions. You should duplicate the set of questions if you have two or more very different systems to discuss.

Feel free to provide whatever additional information you feel important. The questionnaire was developed with both coherent and incoherent, pulsed and CW, stationary and moving lidar systems in mind. (This causes some parts of some questions to appear a little strange when viewed from the standpoint of only one type of system.) If the very few assumptions that have been made in

developing the questionnaire should happen not to fit the lidar system you have in mind, convert any questions based on such assumptions into more appropriate questions with the same basic theme. Contact Ron Kohl (see below) if you are uncertain about any point.

If your responses to the questionnaire include data which you do not want disclosed to the public or used by the government for any purpose other than establishing the state of the art in lidar technology, add a cover page with the following legend:

> "Some of the data furnished in connection with this questionnaire shall not be disclosed outside the government or Ronald H. Kohl & Associates, and it shall not be duplicated, used, or disclosed in whole or in part for any purpose other than establishing the state of the art in lidar technology. This restriction does not limit the government's right to use information contained in the data if it is obtained from another source without restriction. The data subject to this restriction is contained in sheet(s) [indicate sheet numbers] ."

Mark each sheet containing data which you wish to restrict with one of the following legends, either "Use or disclosure of answers to questions [indicate question numbers] is subject to the restriction on the cover page of this questionnaire," or "Use or disclosure of the data on this sheet is subject to the restriction on the cover page of this questionnaire."

Funds allowing, all USA respondents submitting an unrestricted questionnaire response will share in the results of this survey.

This survey is being conducted by Dr. Ronald Kohl and should be returned to him at:

Ronald H. Kohl & Associates
R 2, Box 283B
Tullahoma, Tennessee 37388

If you have any questions, telephone Dr. Kohl at (615) 454-9060 (Tullahoma is in the Central Time Zone) or correspond with him.

Respondents should forward only unclassified materials. If this presents a problem, contact Dr. Kohl.

WE WOULD APPRECIATE THE RETURN OF THIS SURVEY WITHIN 21 DAYS AFTER YOU RECEIVE IT, IF AT ALL POSSIBLE.

Thank you for your cooperation and assistance.

QUESTIONNAIRE ON

LIDAR FOR DESCRIBING SMOKE/OBSCURANT

PLUMES AND CLOUDS

(Continue any answer on the back of a sheet or on additional sheets if needed.)

1. Please give your name, mailing address and telephone number:

2. Describe very briefly (as a one or two sentence abstract) the lidar system you have in mind in answering this questionnaire.

3. Is it -in existence? -in use? -under development? -being planned?

4. Are you thinking of the lidar system for use with actual smoke/obscurants or with tracer material released to form optically thin clouds or plumes to simulate smoke/obscurant plume behavior?

5. Is the scattered radiation you observe scattered by particles in the atmosphere? (If so, which?) By gases in the atmosphere? (If so, which?)

6. Would you cite an available reference here or attach a copy of the appropriate pages from a report or other description giving the approach you use to unravel (interpret) your lidar receiver signal(s)? If the values of particular parameters must be assumed, please be sure that the values you would use or the methods that you would use to determine them are indicated.

7. Note: If the lidar system is to be used with actual smoke/obscurant clouds (see question 4), take the two properties referred to here as those of cloud backscatter and attenuation. If the lidar system is to be used with optically thin tracer clouds (see question 4), take the two properties referred to here as those of cloud backscatter and concentration (mass of particles per unit volume of air).

   Do you know that the relationship between the two properties in question will vary sufficiently little within the clouds that you can interpret your lidar signal (i.e., determine attenuation in smoke clouds or concentration

in tracer clouds)? How much may the relationship vary and still allow you to interpret your signal? To what error? Please cite any analyses or tests and/or data that support any contention you make here.

8. What is (are) the transmitted and detected wavelength(s) of the lidar system?

9. For a lidar system using optically thin tracer clouds:
(a) Of what materials/particles must the cloud consist? (b) Could the lidar system handle tracer clouds where attenuation begins to play a role? If so, how? (c) Could the fact that attenuation was playing a role in the lidar signal be detected if this situation needs to be handled specially or be avoided? (Proceed to question 11.)

10. For a lidar system for use with smoke/obscurants: If you do not anticipate problems from multiple scattering, please indicate as specifically as possible why you do not. Could the presence of a significant multiple scattering effect be detected from some characteristic of the lidar signal? From analysis? How? If a significant multiple scattering effect should be present, is there a way to correct for it? If so, how?

11. (a) What is the minimum fraction* of the outgoing, transmitted power (CW) or energy (per pulse) that can be detected and utilized at a signal**-to-noise ratio of 1 or signal** uncertainty of 50%? (Or give the criterion you use, if different.) Describe the optical or radiation background for which this applies, whether experimentally (even qualitatively) observed or calculated. It should be typical of a daylight situation on a clear day, around 300°K, with high sun. [If you wish a specific example for calculation, for a shorter wavelength lidar assume the lidar is viewing a 50% reflecting, ideal diffuse-reflecting surface of infinite extent normal to the sun's rays with a standard clear-day air mass near 1 (sun near zenith at sea level). For a longer wavelength lidar assume the lidar is viewing an infinite, 300°K, ideal blackbody surface.] Assume the most favorable range (and state it)

*For each wavelength or spectral channel if more than one.
**Power spectrum signal in a homodyne or heterodyne lidar.

if the unattenuated signal is range dependent. (b) Is this fraction in (a) limited by an instrumentation effect (e.g., a digitizing minimum)? by internal noise? by background radiation induced noise? (c) Is time integration or noise averaging involved in your answer to (a)? If so, over how much time? (d) If the lidar system is pulsed, what is the pulse repetition frequency for your answer to (a)?

12. (a) Given the lidar system set up to produce the minimum fraction of question 11, what is the maximum fraction of the outgoing transmitted power (CW) or energy (per pulse) that can be detected and utilized? Again use a 50%

uncertainty in the result or give the criterion you use, if different. (b) Is this limitation due to digitizer range, non-linearity of the detector/amplifier or what?

13. How does or how would the fraction of the transmitted power or energy that is detected or utilized vary with range (distance out from the lidar) in a uniform, non-attenuating scattering medium? Start at range zero. What is the minimum range to which a cloud may approach and still allow lidar signal interpretation?

14. Could the lidar system currently handle the field test cloud/plume geometries and sizes described above the beginning of the questionnaire? In the future? In part?

15. As a function of range for a single lidar beam direction, what is the spatial resolution of the data resulting from the lidar system (a) along the beam, (b) perpendicular to the beam? (c) As a function of range, how accurately is any position along the beam known from which data is collected?

16. (a) For a single lidar beam direction, how much total time is required to take or store data from each of the spatial resolution elements of question 15(a) from the minimum range of interpretation (see question 13) out to 500 m (or cite the maximum range used) and to complete any preparation required to repeat the process? How much of this cycle time is spent collecting optical radiation at the receiver? Is this radiation-collection time continuous within a cycle? If not, please discuss how it is divided up. (b) What is the maximum data signal-to-noise ratio or minimum data uncertainty (including any variation due to speckle effects) for your answer to (a) and what is the cause of the limitation? (c) How long can the longitudinal scanning in (a) be repeated without pause at the rate in (a) and what causes the limitation? (d) How do the times in (a) and/or (c) change with changing maximum range? Please indicate any relationships which may apply from maximum range equal to the minimum range of interpretation to maximum range equal to 1 km (or cite the upper limit, if different).

17. Consider the displacement of the lidar beam (latitudinal scanning) in the two directions which are perpendicular to the lidar beam as appropriate to the lidar system (e.g., displacement in azimuth and elevation or, e.g., displacement in translation along the direction of lidar system motion and translation perpendicular to this direction of motion). Describe this latitudinal scanning including: (a) In each perpendicular direction is the displacement continuous, occurring during optical data collection from the lidar beam, or discrete, occurring between one or more samplings of the lidar beam? If continuous in a direction, give the continuous rate(s) of displacement used.* If discrete, how much time is spent in starting and stopping motion, how much displacement occurs during such starting and stopping, and, in between the starting and stopping, what are the rate(s) of displacement? (If discrete displacement occurs between individual lidar beam positions, how much overlap is there between the cycling time in question 16(a) and the time to make the discrete displacement?) (b) What are the displacement limits in the two perpendicular directions? (c) How accurately are the individual beam locations known within these limits?

*If the cycle times of questions 16(a), (c) and (d) change due to the longitudinal scanning or related data flow, indicate how.

18. Is the lidar system eye safe? By what standards and at what ranges?

19. Can you cite accuracies in either volumetric attenuation or concentration determination as obtained by independent checks? If so, describe the test and atmospheric dispersion used to determine the accuracies.

20. If known, how often or under what circumstances has calibration, checking, re-adjustment or maintenance been required to maintain the specifications given above or to assure proper operation of the lidar system? What maximum to minimum range in man-hours per unit calendar time does such activity require?

21. For those lidar systems for use with smoke/obscurants: Please comment on or reference any means you believe suitable to convert the recovered volumetric optical properties to particle or particle distribution properties. Be sure to include the limitations of the techniques.

22. Please make any additional comments or references you may wish.

APPENDIX B

THE $k \neq 1$ FORM OF THE RELATION BETWEEN β AND σ

Occasionally, e.g. (Klett, 1981), mention is made of the form

$$\beta(L) = C_0 \, \sigma(L)^k \tag{B-1}$$

with $k \neq 1$.

Where the author has seen this form obtained as a fit to calculated or measured β's and σ's (generally in natural aerosols), one of two conditions have existed. The first is with β and σ values for many aerosol types plotted on one plot with limited range of σ within types. From the discussion in section B it can be seen that C_0 will vary with aerosol type (see also Appendix C) and a plot containing data of different C_0 with limited σ ranges for the different C_0 will appear to give data best fit by a curve. For any one aerosol and particularly for any one line in any one cloud, however, the form of Equation (B-1) with $k = 1$ (i.e., Equation B-2 or Equation (8) of section B) gives a better fit.

(Note that an aerosol mix with varying percentages of the component aerosols about the cloud will destroy the form of

$$\beta(L) = C_0 \, \sigma(L) \tag{B-2}$$

if the C_0's of the components are quite different, for example, if β is predominantly supplied by one aerosol and σ by the other.)

The second type of encounter with the form of Equation (B-1) was in data where the lengths involved in the measurement had become a significant fraction

of σ^{-1} so that the values being measured were no longer local property values. This occurred at larger σ values and caused the data to deviate from the straight line of Equation B-2.

APPENDIX C

REVIEW OF DATA ON THE VARIATION OF THE RELATIONSHIP OF β TO σ

A review of the data in existence regarding variation in the backscatter to attenuation coefficient relationship is given here. Relatively little data exists regarding man-made smoke/obscurants; much of it is for water clouds and hazes. As lidar may be applied to diagnosing such natural obscurants and as the properties of some battlefield obscurants approach those of water droplet aerosols, the water droplet aerosol data--such as it is--is also reviewed here.

The relationship of β, the backscatter coefficient, to σ, the attenuation coefficient, in natural and man-made obscurants can be described in two ways. In the first, β and σ are obtained by calculation or measurement as samples within one or more classes of obscurants. The relationship of β to σ is seen to vary from sample to sample. In the second, which is more appropriate for obtaining an idea of the variation of the relationship along a lidar beam, β and σ are determined along a line in an obscurant. So far this has been done either by movement of an instrument through an obscurant or by letting an obscurant flow over the instrument and using Taylor's hypothesis. Where β/σ data exist both from sampling various obscurant clouds of a given class and from measuring along a line in individual clouds of the same obscurant class, the variation of β/σ along a line in a given cloud is less.

Several results are described here. (The existing data are far from complete for lidar use purposes.) The variation in β/σ for different obscurants and wavelengths is found to range from perhaps as little as $\pm 3\%$ up to a multiplicative or divisible factor of 3.2 ($\sqrt{10}$). Work in the visible and near-IR

shows that there can be factor of 2 or larger differences in the value of β/σ between various obscurants and various states of the clear atmosphere.

ELABORATION

Samples from within different clouds or classes of obscurants are considered first. Figure C-1 shows a plot of β versus σ in water clouds (Stapleton, 1972). The circles are values obtained by flight measurements at 0.9 μm. The other symbols are calculated values from the cloud models of Carrier, Cato and von Essen (1967) which are based on size distribution measurements. The value $\beta/\sigma = 0.053$ gives a good fit, and a variation of ±16% includes all measured points but one.

Brinkworth (Brinkworth, 1971 and 1973) found a range of β/σ from about 0.040 to 0.056 (despite his statement in his 1973 paper), or a range of ±17% about 0.048, in cloud and fog for visible and near-IR wavelengths. This range in β/σ was obtained from using a range of parameters in a Best (Best, 1950) size distribution which was considered "likely to be encountered in practical situations."

The large scatter in the ratio β/σ plotted versus σ by Twomey and Howell (Twomey and Howell, 1965) may well be misleading in the present context. (Their results are fine for what they intended to do.) They normalized their distributions to a fixed liquid water content which will contribute scatter to relationships other than that of β/σ equal to a constant. More to the point, they used a wide range of mathematical size distributions including some distributions of very small particle size and some which were very narrow. Some of this was done to include distributions which might be "probable" (using their word) for haze. Such distributions should give more scatter in β/σ at the 0.7 μm wavelength used

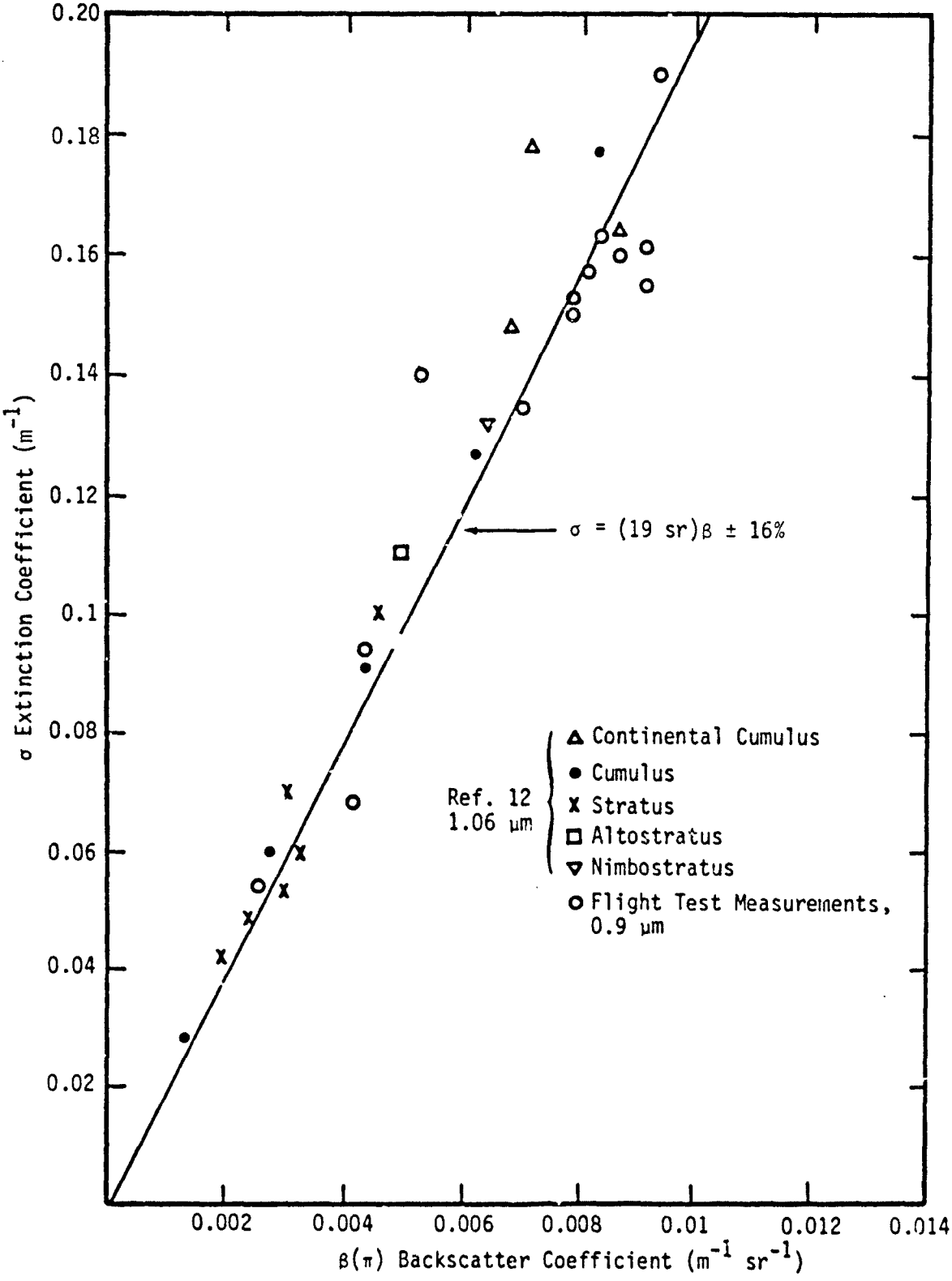

Figure C-1. Water Cloud Values from Stapleton (1972) and Carrier, et al. (1967).

by Twomey and Howell than those more representative of cloud and fog. The results from such distributions were not separated, in the plots presented, from those obtained from distributions which might represent cloud and fog. The scatter in β/σ they obtained is around ±80% about a value of approximately 0.06.

Values of β/σ in haze and clear air can range downward considerably from the values around 0.05 typical of cloud and fog in the visible and near IR. Herrmann, et al. (1981), report the β/σ values given in Table C-I calculated from the aerosol models of Hanël and Bullrich (Hanël and Bullrich, 1978). Thus β/σ may differ considerably between an obscurant cloud and the relatively clear air around it. (Man-made obscurants are discussed below.)

TABLE C-I. SOME VALUES OF β/σ BASED ON PARTICULAR HAZE MODELS*

HAZE MODEL	β/σ (sr^{-1})
Maritime	1.55×10^{-2}
Maritime plus Desert Dust	5.11×10^{-2}
Pollution	0.90×10^{-2}
Continental Clean	2.26×10^{-2}

*Herrmann, et al., 1981, and Hanël, et at., 1978.

(Reagan, et al. (1980), have indicated the sensitivity of the β/σ ratio to the haze aerosol size distribution and material at 0.7 μm by using varying Junge size parameters and "mean" index of refraction values applicable to haze aerosols in a Mie calculation of β/σ .)

More to the point for the use of lidar within haze, Waggoner, Ahlquist and Charlson (Waggoner, et al., 1972) measured β and σ at 0.7 μm over three consecutive days in the background or haze aerosol in Seattle. For relative humidities below 75%, they found $\beta/\sigma = 0.012 \pm 20\%$ for the aerosol with all values included in the indicated variation.

Pinnick, et al. (1983), have extended the work of Carrier, Cato and von Esse (1967) by calculating β/σ from 155 actual cloud droplet size distribution measurements (including some of those used by Carrier, Cato and von Essen). No adjustments were made for particle size limitations of the different instruments; the size distributions were used as measured. Pinnick, et al. (1983), have also added theoretical understanding of the relatively tight clustering of β/σ values in water cloud in the visible and near IR. See Figure C-2. The line in Figure C-2 indicates the ratio $\beta/\sigma = 0.055$. A variation of $\pm 27\%$ in β/σ from the line includes all but one or two points in the figure. Similarly, values of β/σ for these same size distributions at 10.6 μm are plotted in Figure C-3. Here the spread in β/σ occurs over a range of 10X. (This result is significantly different from the spread in the values one obtains from the Carrier, Cato and von Essen (1967) results at 10.6 μm where the range is over a factor of 2X.)

Shipley (1978) obtained values of the ratio of the backscatter and extinctic coefficients over an approximately 30 fold range in extinction coefficient in rainfall using two drop-size distribution models, Marshall-Palmer and Joss-Gori, which are based on observed drop-size distributions. These gave β/σ of about 0.066 with variation $\pm 8\%$ between the two models at low σ (3×10^{-1} km^{-1}) and about 0.059 $\pm 3\%$ at higher σ (6.0 km^{-1}). With fixed mean β/σ of about 0.064, the variation is $\pm 11\%$. These numbers give only rough, temporary ideas of the range of β/σ in rainfall in the visible and very near IR.

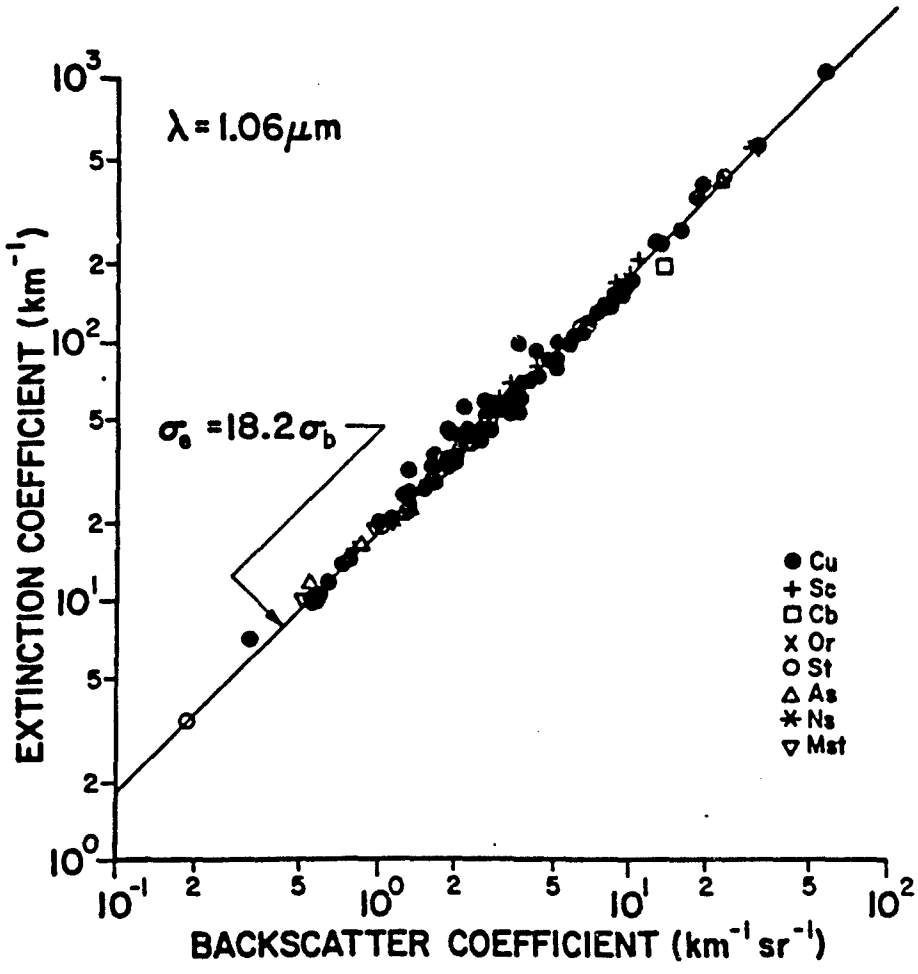

Figure C-2. Figure 4 from Pinnick, et al. (1983). (The symbol σ_e is σ in this proposal and σ_b is β.)

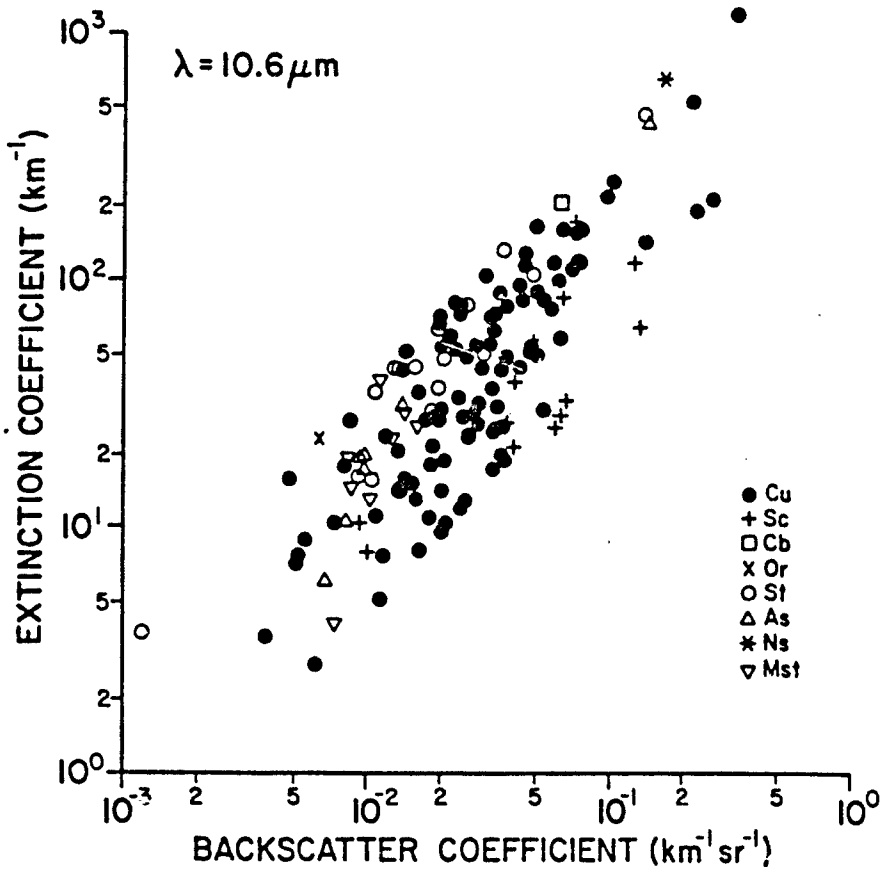

Figure C-3. Figure 7 from Pinnick, et al. (1983).

The only measurements of β and σ known by the author to have been taken along paths in obscurants have been done under Sztankay at HDL. The first published example involved flying a xenon arc lamp dual-channel nephelometer through fair-weather cumulus with some vertical development (Giglio, et al., 1974). The wavelength band used was 0.7 μm to 1.0 μm. Figure C-4 shows the data from one such cloud traversal with the resultant β/σ values in Figure C-5. Figure C-6 shows the β/σ values taken to be valid for each of the four runs reported by Giglio, Rod and Smalley (1974). Variations in β/σ, within which reside most β/σ values measured in that cloud traversal, range from about ±8% to about ±18%.

The second published "path" measurement example was done with fixed instrumentation at 0.9 μm on the ground with obscurant blowing by in Smoke Week III (Sztankay, et al., 1980). Taylor's hypothesis and the wind velocity convert the time varying data into spatial variations along the wind. A sample measurement of β/σ versus time is shown as Figure C-7. In fog oil, Hc, IR#1, IR#2 and IR#3, the mean values of β/σ as measured (one trial each) were found to range from 0.014 to 0.13 with measured variations within a trial of from ±30% to ±50%. (A run with an appropriate water cloud [or phosphoric acid cloud(?)] to demonstrate the relative lack of variability due to instrumentation effects would have been most suitable.) In one trial negative correlation between β/σ and σ occurs, but the data are few.

In addition to the published data, Sztankay's group has a large amount of unpublished β/σ ratio data obtained in flights through strato-cumulus clouds. Very often on the cloud edges and in relative voids in the clouds, well-determined β/σ values are obtained which are as low as half of the 0.05 value commonly

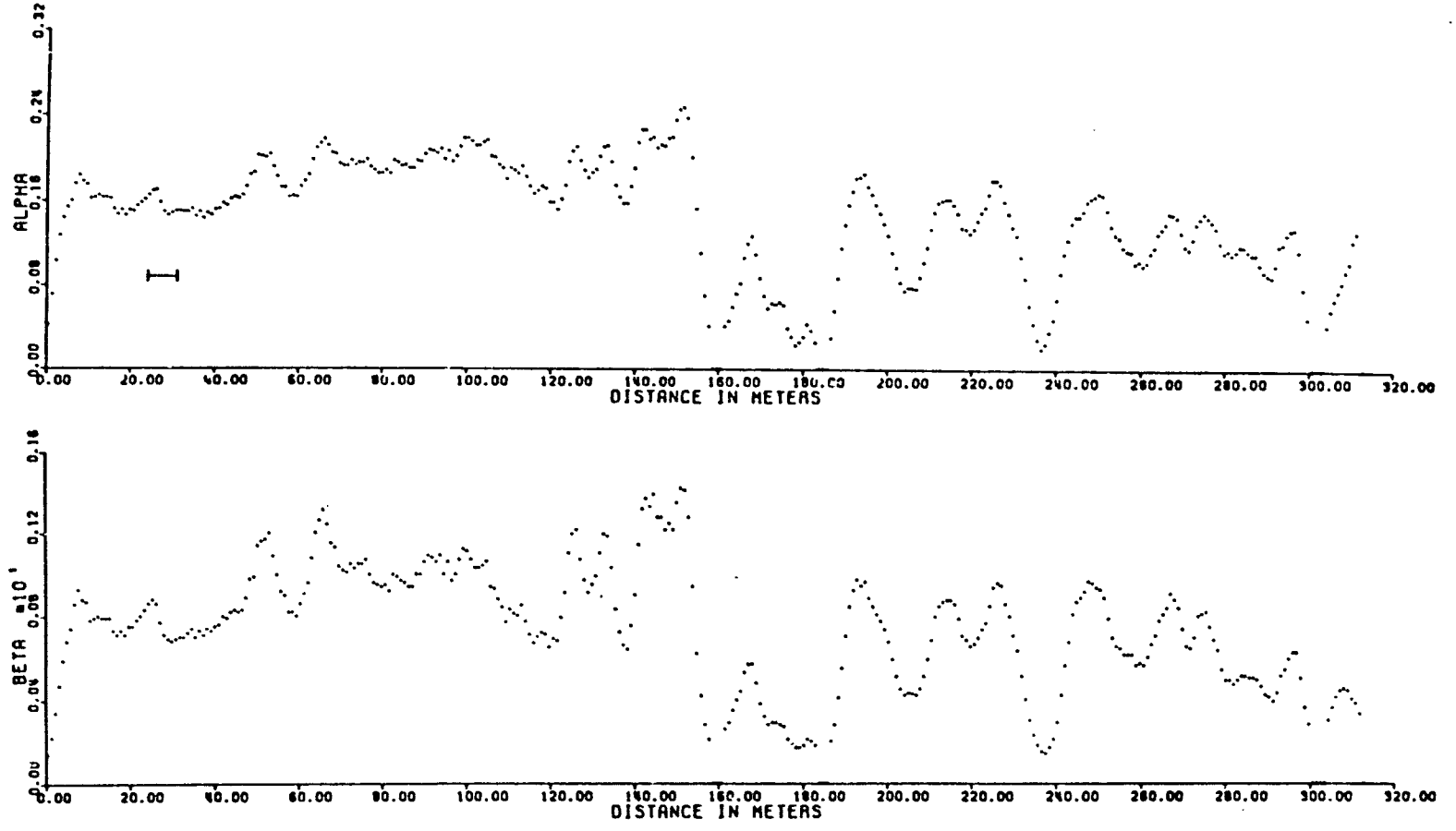

Figure C-4. Figures 5 and 6 of Giglio, et al. (1974). Plot of measurements of extinction coefficient σ (α here) and backscatter coefficient β along a cloud traversal. The bar at 20 meters in the upper plot indicates the 7 meter resolution of the device over which cloud properties must not vary significantly for the measured values to be meaningful. For this run the meaningful data were taken to be that from 10m to 105m.

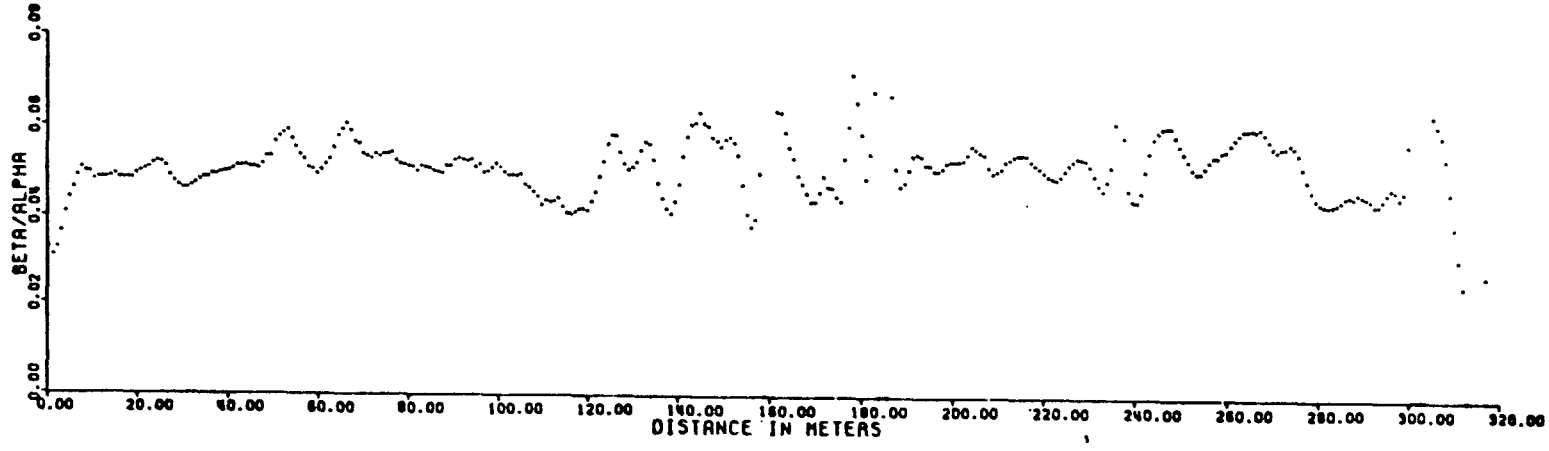

Figure C-5. Figure 7 of Giglio, et al. (1974). Beta/Alpha is our β/σ. Data from 10 to 105 meters is considered meaningful.

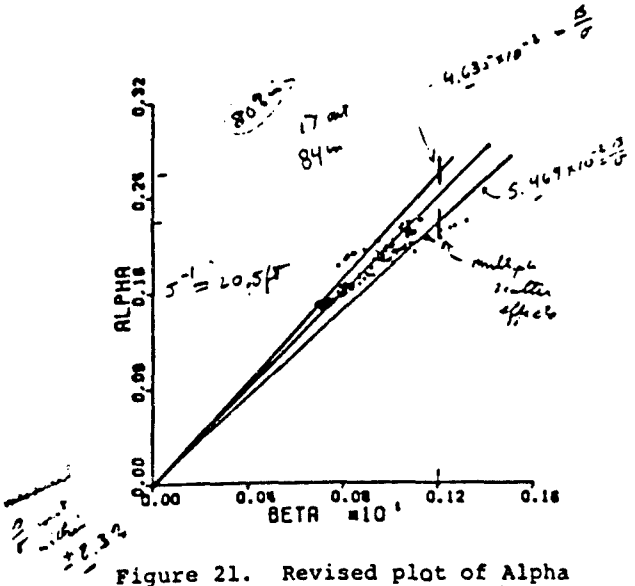

Figure 21. Revised plot of Alpha versus Beta for first sample cloud.

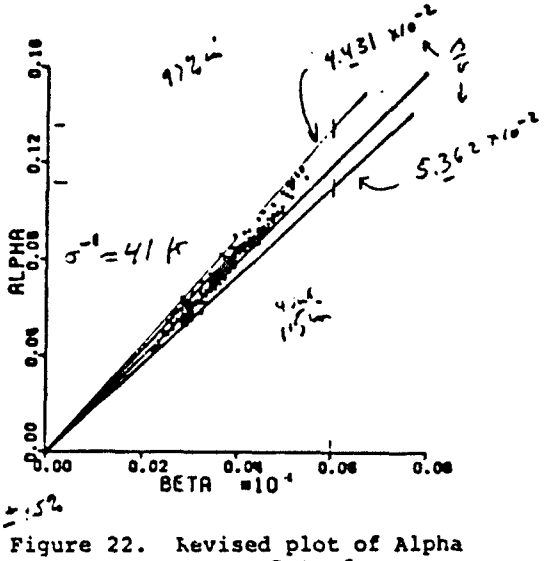

Figure 22. Revised plot of Alpha versus Beta for second sample cloud.

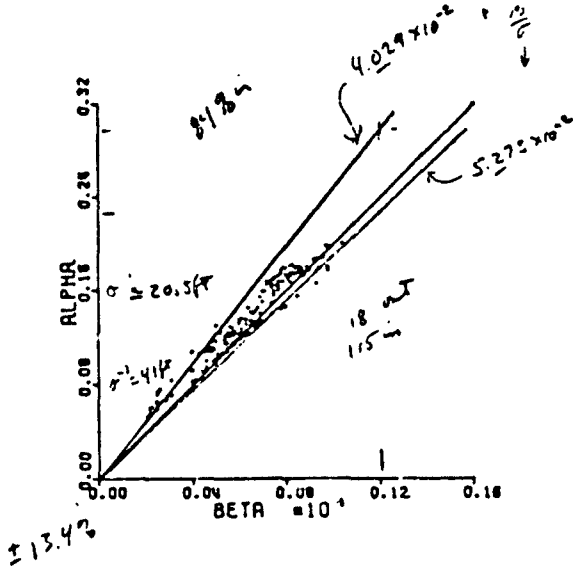

Figure 23. Revised plot of Alpha versus Beta for third sample cloud.

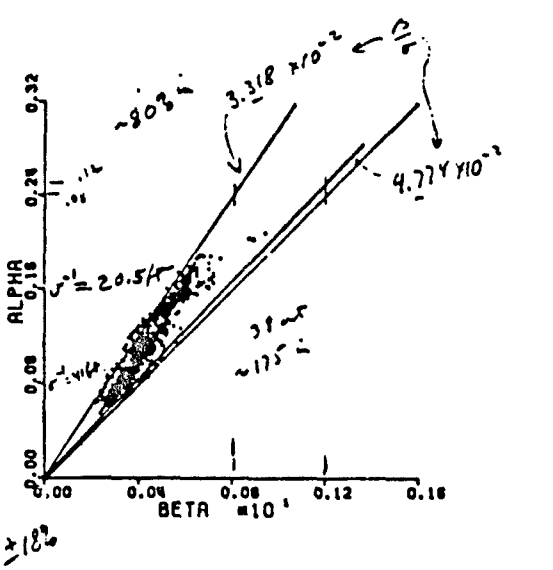

Figure 24. Revised plot of Alpha versus Beta for fourth sample cloud.

Figure C-6. Kohl's notated copy of Figures 21 through 24 of Giglio, et al. (1974). The four cloud traversals reported in that reference, shown here, show β/σ varying within a cloud from about ±8% to about ±18%. Three of the mean values of β/σ are near 0.05 with one near 0.04.

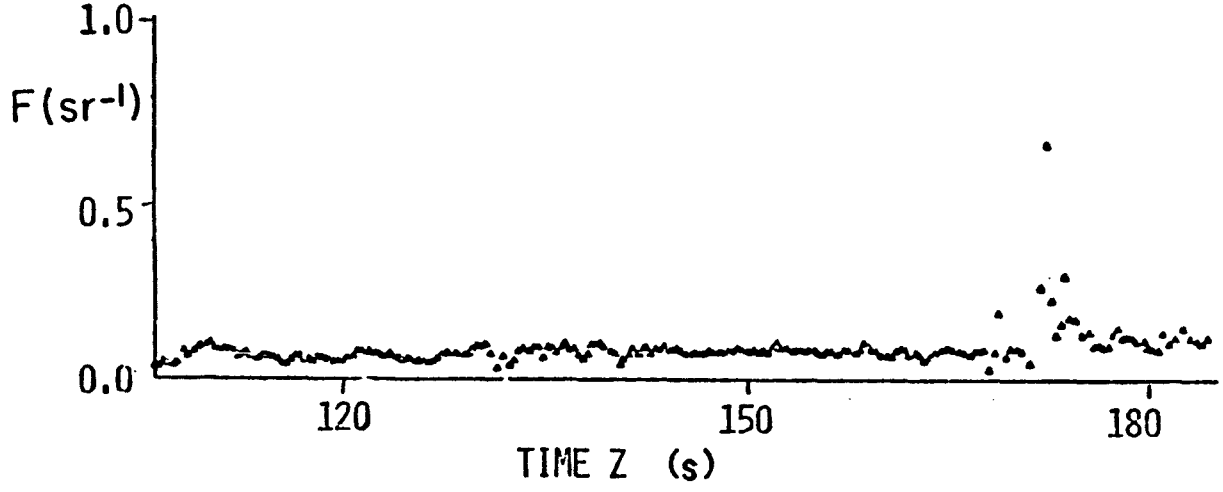

Figure C-7. Figure 8(c) of Sztankay, et al.(1980). F is β/σ for IR#2 in Smoke Week III. Fluctuations at about 130 sec, 140 sec and around 170 sec occur with low signal levels in β and σ and should be false.

measured and calculated inside the cloud. These are considered to be indicators of a more haze-like aerosol (see Table C-1) with particles which are growing toward or shrinking from size distributions characteristic of clouds.

[We wanted to incorporate an analysis by G. de Leeuw (1982) involving the influence of size limits and complex refractive indices on the calculated extinction and backscatter coefficients, but it was not recieved in time.]

Current and near-future efforts to collect data on β/σ at 10.6 μm in obscurants include that of Kent Bullock at NWC and Lockheed-DPG tests to take place at DPG. In the former, the results may not be very quantitative. In the latter, the measurement of the variation of the T^2 weighted, path-averaged β/σ has been made one of the goals of the effort. Knowledge of the effects of variations of β/σ on the various lidar interpretation schemes should help spur the measurement of these variations in actual obscurants.

APPENDIX D

BISTATIC LIDAR

With bistatic (two-site) lidar the situation is more complex than with the usual monostatic lidar. Consider every volume element in a cross-sectional plane or slice containing the lidar transmitter site, receiver site and a cross section of a cloud. Consider all the straight-line paths leading from the lidar transmitter to each of the volume elements in this cross-sectional plane and from each of the volume elements to the lidar receiver at the second site. To prevent a hopeless garble of information, the lidar transmitter beam and the receiver field of view would have to be narrow enough and their scanning synchronized so that they systematically crossed at one volume element at a time at each volume element in the plane in turn. The product of the transmittance on the path from the transmitter to the volume element, the transmittance on the path from the volume element to the receiver and the scattering coefficient at the volume element (at a known angle of scattering) would imply the lidar signal at any one time. When the lidar illuminated and viewed a neighboring volume element, in general the path from the transmitter, the path to the receiver, and the scattering coefficient would all be different.

If scattering from the cloud were being observed, it would appear that the scattering coefficient of the volume element would have to be replaced in a mathematically reduced lidar signal by the attenuation coefficient of the volume element so that the reduced lidar signal from a volume element would depend on the attenuation coefficient value of that element and the attenuation coefficient values on the two paths, the one to and the one from the element--i.e., the lidar signal would depend on the volumetrically distributed attenuation

coefficient alone. This would require the scattering coefficient to have a known relationship to the attenuation coefficient with a known relative scattering function (phase function), that is, the scattering coefficient would have to have a known dependence on scattering angle except for an overall multiplier which was related to the attenuation coefficient at the same location. What form of boundary condition would be required in such a case is not known.

If scattering from the atmospheric gases was being observed, the scattering coefficient would be known and the lidar signal would already depend on the attenuation coefficient distribution alone through the dependence on the transmittance on the two paths, to and from each volume element. Note that in this case no interpretation would be possible on the line running from the lidar transmitter to the lidar receiver.

Whether a solution can be shown to exist and can be found, or whether a solution can be shown not to exist in these two cases is not known. If a solution does exist in one or both cases, the lidar implimentation for its use would be more complicated than with monostatic lidar.

With a monostatic lidar the situation is much simpler. When a monostatic lidar observes in a given direction, it is observing scattered radiation from various depths in the cloud which has traversed the same path to and from the lidar. The scattering from one increment of length of the lidar beam at a given depth and the scattering from the next deeper increment of length differ in their round-trip transmittance only in that the transmittance from the second increment is decreased by the attenuation taking place in the first increment. If the backscatter from the cloud is being observed, a relationship of known form between the backscattering coefficient and the attenuation coefficient in

the cloud allows attenuation in the first, and all other path increments to be obtained once a boundary condition at one point on the path, or over some interval of the path is obtained. (See Section C.) If the backscatter from the atmospheric gases is being observed, the attenuation in the first increment and all other increments can be obtained directly. (See Section E.)

The bistatic configuration has been used, along with monostatic backscatter, to obtain information in tne situation where the aerosol is arranged in horizontal layers, each layer being uniform horizontally (Reagan, Byrne, King, Spinhirne and Herman, 1980 and Reagan, Byrne and Herman, 1982), but this does not fit smoke/obscurant situations.

APPENDIX E

MULTIPLE SCATTERING DETECTION USING FIELD-OF-VIEW EFFECTS

To detect the presence of multiple scattering in incoherent lidars, a scheme like that of Figure E-1 comes to mind. A central detector, A, in the focal plane of the receiver observes the radiation coming from the volume encompassed by the transmitter beam. Other detectors--B, C, D in Figure E-1--observe the multiple-scattered radiation coming to the receiver from outside the transmitter beam volume. An interpolation as shown in Figure E-1 (with some type of noise threshold for B, C and D) is done at the various ranges of interest (particularly the furthest ranges at which A observes a return), and the fraction of the signal from A due to multiple scattering effects can be estimated.

If none of detectors B, C, D is to observe single scattering, the condition derived in Figure E-2 must hold. If detector B (where multiple scattering will first give a signal) is to observe significant multiple scattering when it is present, the condition derived in Figure E-3 must hold. These two conditions give an upper and lower limit to the minimum off-axis angle, ϕ_B, observed by detector B.

If the relative roles of detector A and detectors B, C and D are to remain unchanged over the lidar ranges of interest, then these two limits come into conflict as the dimensions of the aerosol particles significantly contributing to the radiation scattering increase. This is illustrated in Table E-1 for diagnosis between a minimum range of 30 meters (L_1) and a maximum range of 1 kilometer (L_2) with minimum attenuation length (σ^{-1}) of 6 meters (or a maximum attenuation coefficient (σ) of 0.17 m^{-1}, corresponding to transmittance (T) being reduced 10^{-3} in 40 meters). The lidar parameters given

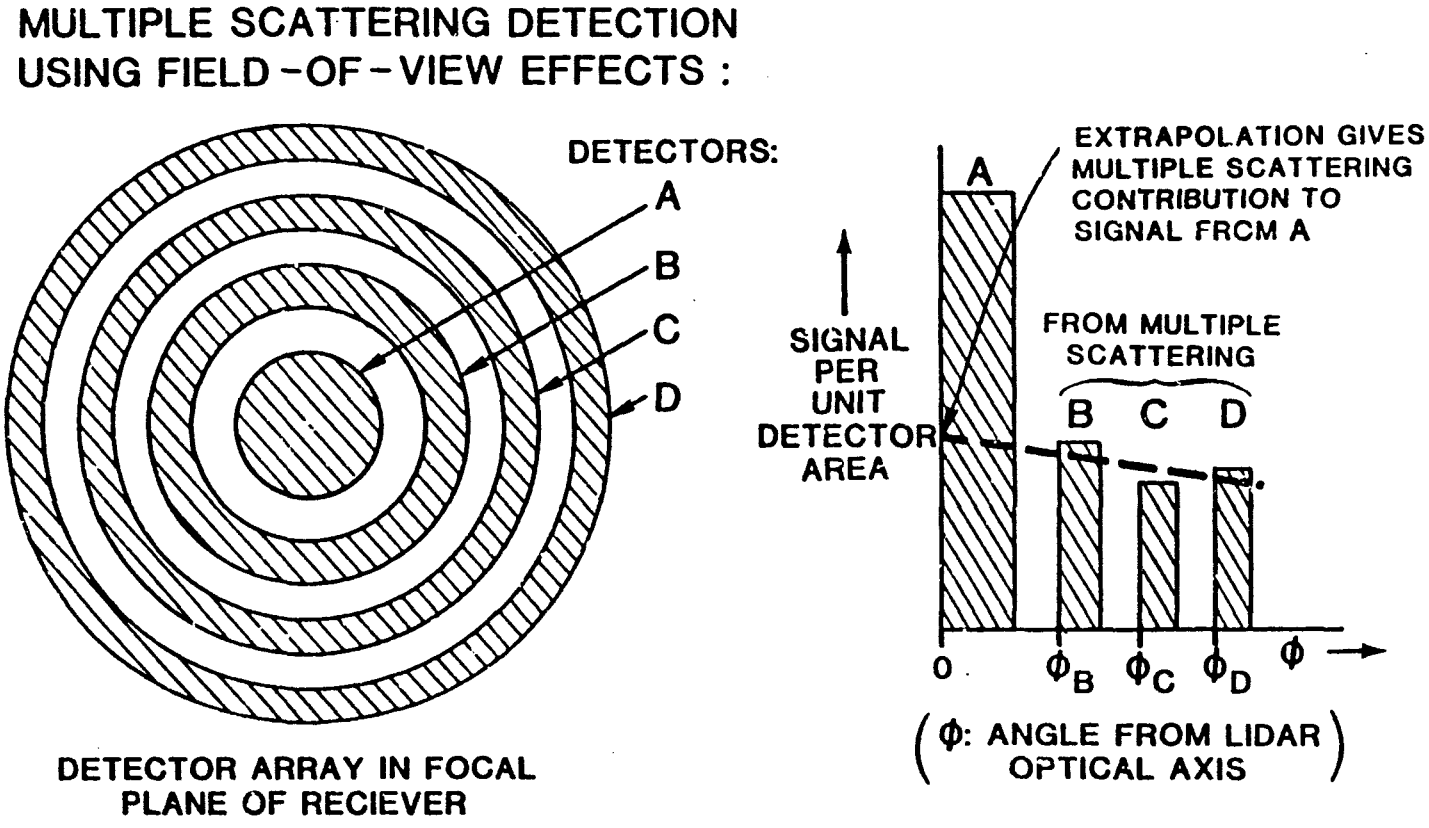

Figure E-1. Multiple scattering detection using field-of-view effects.

ONLY DETECTOR A TO SEE THE SINGLE-SCATTERED RADIATION:

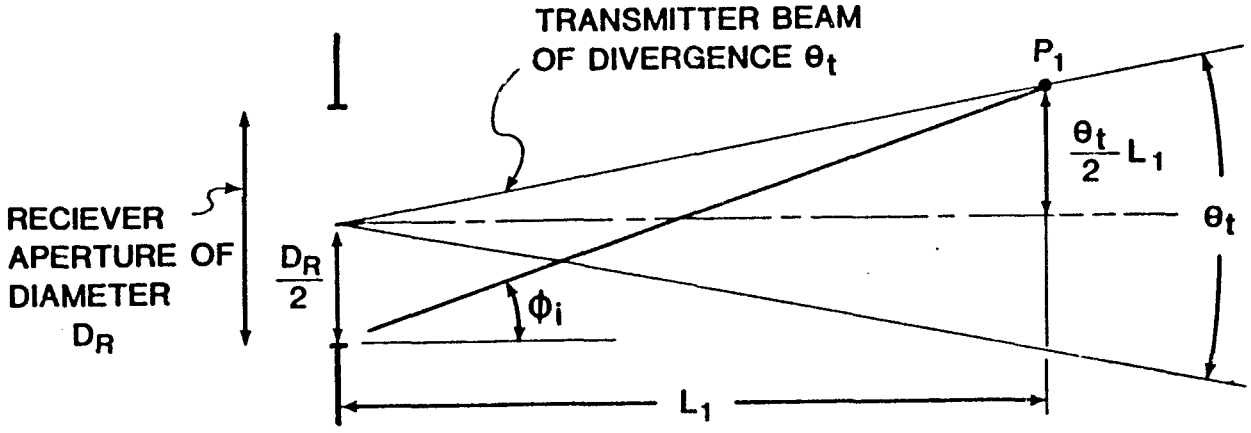

IF NONE OF RADIATION SCATTERED FROM P_1 TO THE APERTURE IS TO BE DETECTED BY B,

① $\phi_B \geq \phi_i = \frac{\theta_t}{2} + \frac{D_R}{2L_1}$. THIS CONSTRAINS MOST AT THE SMALLEST L_1.

Figure E-2. If only detector A to see singly-scattered radiation.

DETECTOR B TO SEE SIGNIFICANT MULTIPLE SCATTERING IF PRESENT:

($\phi_B > \frac{\theta_t}{2}$ by ①)

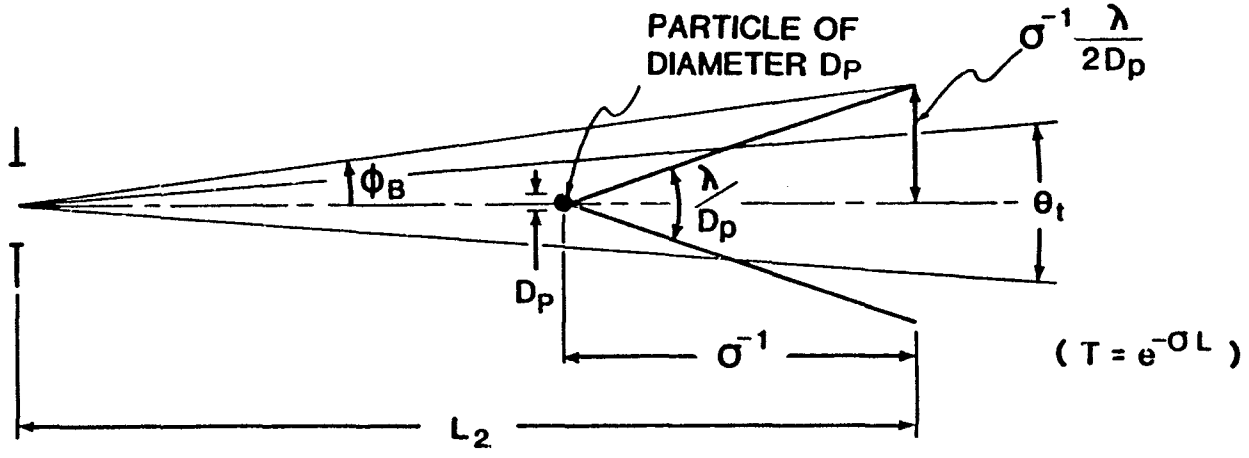

SO

② $\phi_B \leq \frac{\sigma^{-1}\lambda}{2L_2 D_p}$. THIS CONSTRAINS MOST AT THE LARGEST L_2 OBSERVED, AND AT THE SMALLEST σ^{-1} (LARGEST σ) AND LARGER D_P PRESENT.

Figure E-3. If detector B is to see significant multiple scattering if present. (If the particles display two different dimensions as seen from the lidar, the larger must be used for D_p.)

in Table E-1 are the wavelength λ, the lidar transmitter beam divergence θ_t, and the lidar receiver aperture D_R.

It is evident from Table E-1, even at 10 μm lidar wavelength where conditions are most favorable, that detector roles will probably have to be a function of range. This is because optically contributing particles as large as 20 μm can be found in man-made obscurants; for dusts the sizes are even larger--how large depending on how close to the dus creating event the lidar diagnosis is being done.

TABLE E-I

MAXIMUM PARTICLE SIZES FOR MULTIPLE SCATTERING DETECTION USING FIELD-OF-VIEW EFFECTS WITH FIXED DETECTOR ROLES

$\lambda(\mu m)$	θ_t(mr)	D_R(m)	Maximum Allowable Dimension of Optically Contributing Particles (μm)
0.5	1	.1	0.7
		.3	0.3
		.6	0.14
	5	.1	0.4
		.3	0.2
		.6	0.12
1.0	1	.1	1.3
		.3	0.5
		.6	0.3
	5	.1	0.7
		.3	0.4
		.6	0.2
10.0	1	.1	14.
		.3	5.
		.6	3.
	5	.1	7.
		.3	4.
		.6	2.4

APPENDIX F

AVERAGING OF STRUCTURE IN OPTICAL SMOKE/OBSCURANT PROPERTIES OVER OPTICAL PENCIL CROSS SECTIONS

INTRODUCTION

Consider an area on a target as seen by a sensor looking at (or toward) the target at some instant through a smoke/obscurant cloud. Trace all direct rays leaving this area of the target which enter the sensor aperture. These rays form an optical pencil.

The following questions are addressed here: Considering in turn, attenuation, and scattering and emission by the cloud, for what size of area on the target, more specifically, for what size of pencil cross section is the effect, on the sensor, of cloud structures in a pencil independent of their distribution across each cross section along the pencil? For what size of optical pencil cross section can an effective attenuation coefficient in the pencil be defined which is a function of length along the pencil only, i.e. so that Beer's law can be applied to the direct radiation in the pencil, as a whole, rather than to each individual direct ray in the pencil?

STRUCTURES IN THE ATTENUATION COEFFICIENT

We consider here the effect of structures in the local attenuation coefficient of the smoke/obscurant cloud, attenuation coefficient structures which might vary significantly across a pencil. These structures affect the attenuation of the rays from the target (or from the background if another pencil) and the scattered and cloud-emitted rays.

Consider two cases with the same amount of cloud inside each pencil cross section in each case. The first is a pencil in which the attenuating

cloud particles are distributed uniformly and the transmittance is just below the threshold for the sensor on the end of the pencil, so the sensor does not perform. In the second case consider the same cloud particles confined to a much smaller pencil which is inside the original pencil and running parallel to it. The transmittance on paths within and along the inside pencil will be very small, but the transmittance along paths within the original pencil but outside the inside pencil will be 1 . Since the inside pencil is small, most of the paths, and therefore most of the radiation, inside and along the original pencil will have a transmittance of 1 and the sensor will perform, the flux incident on it from the pencil as a whole being well above threshold. We see in these two cases that the local average of the attenuation coefficient across the pencil width, $\sigma(L)$, which is the same in both cases, is not a significant, useable parameter! The parameter $\sigma(L)$ is, of course, the common attenuation coefficient for a beam of radiation and the one which would be measured by lidar. [It is denoted here as $\sigma(L)$ to indicate that it is a function of distance along the pencil, L, only, and that structural effects across the pencil have been averaged out.] Note that with both of these cases occurring, Beer's law

$$T = e^{-\int \sigma(L')\,dL'}$$

will not apply to radiation in the pencil as a whole. (There is, of course, not a single application of transmittance that does not apply Beer's law to a pencil or a beam of radiation.) Things look pretty grim at this point of the discussion.

Note, however, that there were two conditions, and both of these had to be met, for the effective transmittance along the original pencil to vary significantly between the two cases. The first is that the σ correlation lengths in the cross-pencil directions had to be the order of or smaller than the respective cross-sectional dimensions of the pencil. (The smaller pencil width had to be smaller than the original pencil width because if σ varied little across the original pencil width there would be little difference between the two cases.) In real smoke/obscurants the attenuation coefficient σ, as indicated by the concentration, C, appears to be well-correlated over typical pencil cross-sectional sizes at distances from the source typical of Smoke Week instrumentation. In particular, two identical, calibrated concentration measurement devices with a cross-wind separation of 2 meters (within a trailor) correlate very well in the Smoke Week smoke/obscurant tests (Dietz, 1984).

The second condition, required for the second of the two cases of the example to differ significantly from the first, is that the correlation in σ extend along L for distances that are not small compared to the difference in σ^{-1} of the dense portion and σ^{-1} of the thin portion of the pencil cross section. (The small pencil had to remain straight--rather than corkscrew around inside the original pencil--over distances in which the transmittance through the small pencil decreased significantly compared to the decrease of the transmittance on a path inside the original pencil but outside of the small pencil and parallel to it.) There is little information specifically concerning this type of correlation in real smoke/obscurants.

There is, however, a test of sorts as to whether the behavior of the example occurs in real smoke/obscurants in pencils of 1 meter cross section. It may be made by comparing the data giving $-\ln T$ ($= \int \sigma dL$) for two parallel

lines of sight ("center row" and "elevated row") separated vertically by 3.5 meters in Smoke Week II. (One expects and observes the most differentiation with vertical separation, yet almost all the features in the data from one line of sight are obviously common to the data from the other--i.e., the lines of sight are close enough for linear interpolation.) Using linear interpolation on the difference between -ln T on the two lines of sight as a function of time, and interpolating from 3.5 m separation to 0.5 m separation (more characteristic of a 1 m pencil width), gave dual plots of -ln T where the disagreement between -ln T values was small compared to the fluctuations in -ln T, the desirable result. (See the section discussing the desirable data accuracy.) In a few trials the agreement was good at the full 3.5 meters separation. The types of obscurants included fog oil, HC, dust and WP. The lowest line-of-sight elevation was 2 meters. (We expect more vertical differentiation to occur the closer the line of sight to the ground.)

So in these obscurants, at this elevation and at typical Smoke Week instrumentation distances from the source, it appears that the effect of structures in the attenuation coefficient in optical pencils (i.e., in beams, or in resolution elements in fields of view) of cross-sectional size 1 meter and down can be averaged over the cross section of the pencil. [Apparently the attenuation coefficient does not vary much over such distances.] So, in such pencils, the effective attenuation coefficient $\sigma(L)$ is only a function of length along the pencil, L, and Beer's law holds in its usual form.

STRUCTURES IN SCATTERING AND EMITTING PROPERTIES

We consider the unattenuated effect of structures in the local scattering and/or emitting properties of the smoke/obscurant cloud, structures which might vary significantly across a pencil. The effect of these structures within a pencil is to generate direct rays, either by last scattering or emission, which are detected by the sensor.

AVERAGABLE CROSS-SECTION SIZES AS SET BY THE SENSORS. Consider a pencil whose size at the target is the minimum area resolvable by the sensor at the target location under the very best of contrast conditions. Differing points of origin of generated rays which begin in a cross section of this pencil and enter the sensor aperture (but which are not part of an overlapping pencil of different propagation direction) cannot be distinguished by the sensor. This is because for each such generated ray belonging to the pencil there is a direct ray which begins somewhere at the target location on the minimum resolvable area of the same pencil and which is coincident with the generated ray from its point of origin to the sensor. (This is the definition of "belonging to a pencil".) Just as these direct rays from the minimum resolvable area cannot be resolved by the sensor even under the best of conditions, neither can the generated rays coincident with them be resolved. Thus the distributions of emitting and scattering cloud structures may be averaged over the cross sections of such minimum resolution pencils; their effect is independent of their distribution in a cross section.

The angular size of minimum resolution pencils, as seen from the sensor, can be no less than the diffraction angle (diffraction limit) which is approximately λ/D, set by the sensor wavelength λ and sensor aperture diameter D. Good optics are found on the battlefield. Good optics, regardless of wavelength, approach the diffraction limit in their angular resolution and

so their angular resolution, the angular size of the minimum resolution pencils as seen from the sensor, is not much larger than λ/D. These angular resolution sizes will range from around 3 milliradians (mm-wave with 30 cm aperture), to .3 to .7 milliradian (bare eye in daylight), to 0.1 milliradians (10 μm wavelength with 10 cm aperture), to about 0.01 milliradians (binoculars in the visible).

At one kilometer distance from the sensor therefore, except for mm wave sensors, the cross-sectional dimensions of the pencils over which emitting and scattering structures in clouds may be averaged, as obtained from the best possible sensor performance alone, range below 1 meter to as little as 1 centimeter in size.

If the scattering and emitting structures of a cloud are of low contrast as seen by the sensor, these maximum sizes may increase.

AVERAGABLE CROSS-SECTION SIZES AS SET BY THE CLOUD STRUCTURE (WITH ASSUMPTIONS). If the local structure in the scattering or emitting properties of a smoke/obscurant cloud has correlation lengths, or scale sizes of appreciable property change which are larger than the sizes of the pencil cross sections determined from the sensor resolution alone, then the pencils over whose cross section these properties may be averaged without affecting sensor performance prediction may have cross-sectional dimensions approaching this larger scale size. Published data concerning the scale sizes in the cloud for scattering and emission, as such, appears to be lacking. A report by Rice and others of OptiMetrics which might give a lead in this matter (through the scale size of emission- and scatter-induced clutter) was not yet available through the contract sponsor.

If one assumes that the emissive and scattering properties of the cloud will be closely coupled (at least locally, over a region of a few meters in extent) to the concentration in the cloud so that the correlation lengths for the cloud emissive and scattering properties will be the same as for the concentration, then the above discussion [see the subsection on structures in the attenuation coefficient], concerning observed concentration correlation over 2 meters horizontal separation at Smoke Week source distances, can be applied to horizontal emissive and scattering property correlation.

If one assumes that the emissive and scattering properties of the cloud will be closely coupled to the attenuation coefficient in the cloud (either directly, or via close coupling with the concentration with local proportionality between the concentration and the attenuation coefficient [a locally constant α]), and if one assumes the above approximate equality of $\int\sigma dL$ on parallel lines of sight separated by 0.5 to 1 meter is due to equality of the σ's at each distance L (rather than there being a random difference which averages to zero in the path integration), then the above discussion concerning the observed path-integrated attenuation ($\int\sigma dL$) correlation can be applied to obtain the statement that the structure in the local cloud emissive and scattering properties can be averaged over optical pencil cross sections of about 1 meter in extent without changing the performance of sensors, at least at typical smoke week distances from the source, at 2 meters height and for the obscurants mentioned. The requirement that one go beyond the observed equality of $\int\sigma dL$ on nearby parallel rays to assume this arises from the equality of the σ at adjoining points on the rays comes from the difference in the role played by the cloud attenuation coefficient on a ray traversing

a cloud and the role played by the cloud emissive or scattering properties on a ray being generated, or contributed to by those processes.

CONCLUSIONS

STRUCTURES IN THE ATTENUATION COEFFICIENT. From some data from Smoke Week II it appears that the effect of structures in the attenuation coefficient may be averaged over the cross sections of optical pencils of 1 meter cross-sectional dimension and less--at least in HC, WP, fog oil and dust, 2 meters off the ground and at typical Smoke Week distances from the source. Closer to the source, closer to the ground, on longer, downwind rather than crosswind paths,and, perhaps, in other obscurants, the pencil dimension may have to be reduced.

STRUCTURES IN CLOUD SCATTERING AND EMISSIVE PROPERTIES. When assumptions are applied to the just-mentioned data from Smoke Week II the conclusion may be reached that the scattering and emissive properties may also be averaged over the cross sections of optical pencils of 1 meter cross-sectional dimension and less--at least under the conditions just cited. This conclusion is not only restricted, as is the above, but it is also tentative.

REFERENCES

Barrett, E. W., and O. Ben-Dov, 1967, Application of the Lidar to Air Pollution Measurements. J. Appl. Meteor., 6, 500-515.

Best, A. C., 1950, The Size Distribution of Raindrops, Q. J. Roy. Met. Soc. 76, 16-36.

Brinkworth, B. J., 1971, Calculation of Attenuation and Backscattering in Cloud and Fog, Atmo. Environ. 5, 605-611.

Brinkworth, B. J., 1973, Pulsed-Lidar Reflectance of Clouds, Appl. Opt. 12, 427.

Campani, John, 1984, LeCroy, personal communication.

Carrier, L. W., G. A. Cato and K. J. von Essen, 1967, The Backscattering and Extinction of Visible and Infrared Radiation by Selected Major Cloud Models, Appl. Opt. 6, 1209-1215.

Carswell, A. I. and S. R. Pal, 1980, Polarization Anisotropy in Lidar Multiple Scattering from Clouds, Appl. Opt. 19, 4123-4126.

Collis, R. T. H., W. Viezee, E. E. Uthe and J. Oblanas, 1970, Visibility Measurement for Aircraft Landing Operations, AFCRL-70-0598, Air Force Cambridge Research Laboratories, Bedford, Massachusetts [NTIS No. AD 716 483].

Crawford, Ian D., 1984, Analog Modules Inc., personal communication.

Dabberdt, Walt and Warren Johnson, ~ 1971, Atmospheric Effects on Laser Eye Safety: Part II (Contract F41609-69-C-0001 with Brooks AFB), SRI International.

Davis, P. A., 1969, The Analysis of Lidar Signatures of Cirrus Clouds, Appl. Opt., 8, 2099-2102.

de Leeuw, G., 1982, Mie Calculations on Particle Size Distributions: Influence of Size Limits and Complex Refractive Indices on the Calculated Extinction and Backscatter Coefficients, PHL 1982-50, Physics Laboratory, National Defense Research Organization, The Netherlands.

Department of the Army, 1984, TB MED 524, Control of Hazards to Health from Laser Radiation (to be distributed shortly).

Dietz, Kathryn Krist, 1984, University of Tennessee Space Institute, personal communication.

Douglas, C. A. and R. L. Booker, 1977, Visual Range: Concepts, Instrumental Determination, and Aviation Applications, FAA-RD-77-8, Systems Research and Development Service, Federal Aviation Administration, Washington, D.C.

Eloranta, E. W. and S. T. Shipley, 1982, A Solution for Multiple Scattering, in Adarsh Deepak (Ed.), Atmospheric Aerosols: Their Formation, Optical Properties and Effects, Spectrum Press, Hampton, Virginia.

Evans, B. T. N., 1984, DREV, Canada, personal communication.

Evans, B. T. N., E. Cerny and P. Gagné, 1983, Computerized Lidar Displays of IR Obscuring Aerosols, Paper A-12 of the Unclassified Section of the Proceedings of the Smoke/Obscurants Symposium VII, DRCPM-SMK-T-001-83, Project Manager Smoke/Obscurants, Aberdeen Proving Ground, Maryland.

Farmer, W. Michael, 1984, STC Corporation, personal communication.

Farmer, W. M., et al, 1981, Smoke Week III Electro-Optical System Performance in Characterized, Obscured Environments at Eglin Air Force Base, Florida, August 1980, DRCPM-SMK-TR-81-29, Project Manager Smoke/Obscurants, Aberdeen, Maryland (Confidential).

Ferguson, Jerry A. and Donald H. Stephens, 1983, Algorithm for Inverting Lidar Returns, Appl. Optics 22, 3673-3675.

Fernald, Frederick G., Benjamin Herman and John A. Reagan, 1972, Determination of Aerosol Height Distributions by Lidar, J. of Appl. Meteor. 11, 482-489.

Giglio, D. A., B. J. Rod and H. M. Smalley, 1974, Nephelometer for Mapping of Backscatter and Attenuation Coefficients of Clouds, HDL TR-1660, Harry Diamond Laboratories, Washington, D.C

Hanël, G., and K. Bullrich, 1978, Physico-Chemical Property Models of Tropospheric Aerosol Particles, Beitr. Phys. Atmos. 51, 129-138.

Hanna, Steven R., 1984a, The Exponential PDF and Concentration Fluctuations in Smoke Plumes, in Lecture Notes--IFAORS Short Course No. 480, Institute for Atmospheric Optics and Remote Sensing, Hampton, Virginia.

Hanna, Steven R., 1984b, Environmental Research and Technology, Inc., personal communication.

Hanna, Steven R., Gary A. Briggs, and Rayford P. Hosker, Jr., 1982, Handbook on Atmospheric Diffusion, DOE/TIC-11223, Technical Information Center, US Department of Energy, available as DE82002045 from the National Technical Information Service.

Herrmann, H., F. Köpp and C. Werner, 1981, Remote Measurements of Plume Dispersion Over Sea Surface Using the DFVLR Minilidar, Opt. Eng. 20, 759-764.

Hitschfeld, W., and J. Bordan, 1954, Errors Inherent in the Radar Measurement of Rainfall at Attenuating Wavelengths, J. Meteor., 11, 58-67.

Johnson, Warren, William E. Evans and Edward E. Uthe, 1970, Atmospheric Effects Upon Laser Eye Safety: Part I, AD 875549 (Contract F41609-69-C-0001 with Brooks AFB), SRI International.

Johnson, Warren B., 1983, Meteorological Tracer Techniques for Parameterizing Atmospheric Dispersion, Journal of Climate and Appl. Meteor. 22, 931-946.

Kiech, Earl, 1984, Calspan Inc., Arnold Engineering Development Center, personal communication.

Killinger, D. K. and A. Morradian, 1983, Eds., Optical and Laser Remote Sensing, Springer-Verlag, New York.

Klett, J. D., 1984, Stable Analytical Inversion Solution for Processing Lidar Returns, Appl. Opt. 20, 211-220.

Kohl, R. H., 1978, Discussion of the Interpretation Problem Encountered in Single-Wavelength Lidar Transmissometers, J. of Appl. Meteor. 17, 1034-1038.

Kohl, R. H., 1983, The Extinction Coefficient: The Concept, the Significance and the Status of the Measured Values, Paper B-9, Proceedings of Smoke/Obscurant Symposium VII, held at Harry Diamond Laboratories, 26-28 April 1983.

Kohl, Ronald H., 1984, Lidar as a Diagnostic of Smoke/Obscurant Clouds, Paper A-20, Proceedings of the Smoke/Obscurants Symposium VIII, Project Manager, Smoke/Obscurants, Aberdeen Proving Ground, Maryland (to be published).

Lamberts, C. W., and Ir. H. Dekker, 1975, Raman Lidar: A Feasibility Study, PHL 1975-49, National Defense Research Organization TNO (Physics Laboratory), The Hague, The Netherlands (available from NTIS as N76 3181 H2/E).

Lentz, W. J., 1982, The Visioceilometer: A Portable Visibility and Cloud Ceiling Height Lidar, ASL-TR-0105, Atmospheric Sciences Laboratory, White Sands Missile Range, New Mexico.

Marshall, Wes, 1984, telephone communication, Laser Microwave Division, US Army Environmental Hygiene Agency.

Measure, E. M., 1984, personal communication.

Measure, E. M., J. D. Lindberg and W. J. Lentz, 1983, The Use of Lidar as a Quantitative Remote Sensor of Aerosol Extinction, ASL-TR-0136, Atmospheric Sciences Laboratory, White Sands Missile Range, New Mexico.

Melfi, S. H., 1970, Raman Backscatter of Laser Radiation in the Earth's Atmosphere, Ph.D. Dissertation, College of William and Mary, Williamsburg, Virginia.

Moninger, William R., 1983, Environmental Research Laboratory--NOAA, response to survey.

Moninger, W. R. and R. A. Kropfli, 1982, Radar Observations of a Plume from an Elevated Continuous Point Source, Journal of Applied Meterology 21, 1685-1697.

Montgomery, W. W., and R. H. Kohl, 1980, Opposition Effect Experimentation, Optics Letters 5, 546-48.

Pasquill, F., 1974, Atmospheric Diffusion, John Wiley and Sons, New York.

Petheram, John C., 1981, Differential Backscatter from the Atmospheric Aerosol: The Implications for IR Differential Absorption Lidar, Applied Optics 22, 3941-3946.

Pinnick, R. G., S. G. Jennings, P. Chylek, C. Ham and W. T. Grandy, Jr., 1983, Backscatter and Extinction in Water Clouds, J. Geophys. Res. 88, 6787-6796.

Reagan, John A., Dale M. Byrne and Benjamin Herman, 1982, Bistatic Lidar: A Tool for Characterizing Atmospheric Particulates: Part I--The Remote Sensing Problem, IEEE Trans. Geosci. & Remote Sensing 20, 229-235; Part II--The Inverse Problem, IEEE Trans. Geosci. & Remote Sensing 20, 236-243.

Reagan, J. A., D. M. Byrne, M. D. King, J. D. Spinhirne, and B. M. Herman, 1980, Determination of Complex Refractive Index and Size Distribution of Atmospheric Particulates from Bistatic-Monostatic Lidar and Solar Radiometer Measurements, J. of Geophys. Res. 85, 1591-1599.

Rubio, R., E. M. Measure and D. C. Knauss, 1983, Lidar Determination of Smoke Concentrations and Linear Extinction Coefficient, Paper A-11 of the Unclassified Section of the Proceedings of the Smoke/Obscurants Symposium VII, DRCPM-SMK-T-001-83, Project Manager Smoke/Obscurants, Aberdeen Proving Ground, Maryland.

Shipley, S. T., 1978, The Measurement of Rainfall by Lidar, Ph.D. Thesis, University of Wisconsin-Madison.

Shipley, S. T., D. H. Tracy, E. W. Eloranta, J. T. Trauger, J. T. Sroga, F. L. Roesler, and J. A. Weinman, 1983, High Spectral Resolution Lidar to Measure Optical Scattering Properties of Atmospheric Aerosols, 1: Theory and Instrumentation, Appl. Optics 22, 3716-3724.

Sliney, David and Myron L. Wolbarsht, 1981, Safety with Lasers and Other Optical Sources: A Comprehensive Handbook, Plenum Publishing Co., New York, New York.

Smalley, Howard M., 1981, Final Report, Smoke Week III, DPG-FR-80-305, Dugway Proving Ground, Utah, AD B056774L.

Sroga, J. T., E. W. Eloranta, S. T. Shipley, F. L. Roesler, and P. J. Tryon, 1983, High Spectral Resolution Lidar to Measure Optical Scattering Properties of Atmospheric Aerosols, 2: Calibration and Data Analysis, Appl. Optics 22, 3725-3732.

Stapleton, 1972, Unclassified Figure from a Classified Santa Barbara Research Report.

Sztankay, Z. G., D. McGuire, J. Griffin, W. Hattery, G. Martin and G. Wetzel, 1980, Near-IR Extinction, Backscatter and Depolarization of Smoke Week III Aerosols, Draft Paper, Harry Diamond Laboratories. (Probably in the Proceedings of Smoke/Obscurants Symposium IV.)

Twomey, S., and H. B. Howell, 1965, The Relative Merit of White and Monochromatic Light for the Determination of Visibility by Backscattering Measurements, Appl. Opt. 4, 501-506.

Uthe, Edward E., 1983, Lidar Applications for Obscurant Evaluations, Paper A-13 of the Unclassified Section of the Proceedings of the Smoke/Obscurants Symposium VII, DRCPM-SMK-T-001-83, Project Manager Smoke/Obscurants, Aberdeen Proving Ground, Maryland.

Uthe, Edward E., 1984, SRI International, personal communication.

Waggoner, A. P., N. C. Ahlquist and R. J. Charlson, 1972, Measurement of the Aerosol Total Scatter-Backscatter Ratio, Appl. Opt. 11, 2886-2889.

Young, Andrew T., 1980, Rayleigh Scattering, Appl. Optics 20, 533-535.

Young, Andrew T., 1982, Rayleigh Scattering, Physics Today 35, 42-48.

Zalay, A. D., R. H. Kohl and E. W. Coffey, 1979, Utilization of a Laser Doppler Velocimeter System for the Measurement of Battlefield Smoke and Dust Characteristics, LMSC-HREC TM D568919 (Report on Contract DAAK 40-77-A-0010 with USA Missiles Research and Development Command, Redstone Arsenal, Alabama), Lockheed Missiles and Space Company, Huntsville Research and Engineering Center, Huntsville, Alabama.

Zuev, V. E. and I. E. Naats, 1983, Inverse Problems of Lidar Sensing of the Atmosphere, Springer-Verlag, New York.

SUPPLEMENTARY

INFORMATION

AD-A152576

January 10, 1986

Errata for DTIC Report
AD A152576

LIDAR AS A DIAGNOSTIC OF SMOKE/OBSCURANTS:
OVERVIEW AND ASSESSMENT OF THE DEVELOPMENT
WITH RECOMMENDATIONS

by Ronald H. Kohl
3 October 1984

Final Report on Contract DAAD05-83-M-M106
prepared for

Project Manager
Smoke/Obscurants
Attn: DRCPM-SMK-T
Aberdeen Proving Ground, MD 21005

Page	Replace	By
33 (3rd line from bottom)	go toward zero...toward positive infinity.	go toward zero and the determination of $\sigma(L)$ will become highly unstable. As $I(L)$ in the numerator of Equation (13) will go like $T^2(L)$, $\sigma(L)$ will either blow up toward positive infinity or go toward zero depending on the nature of the experimental errors present.
75 (last line)	5 mA	5 mÅ (5-milliAngstroms)
171 (3rd last line)	TB MED 5234	TB MED 524

END

FILMED

3-86

DTIC